Ecophysiology of Brown Ring Disease in the Manila clam *Ruditapes philippinarum*, experimental and modelling approaches.
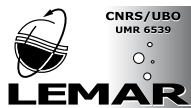
VRIJE UNIVERSITEIT

ECOPHYSIOLOGY OF BROWN RING DISEASE IN THE MANILA CLAM *Ruditapes philippinarum*, EXPERIMENTAL AND MODELLING APPROACHES

ACADEMISCH PROEFSCHRIFT

ter verkrijging van de graad Doctor aan
de Vrije Universiteit Amsterdam,
op gezag van de rector magnificus
prof.dr. L.M. Bouter,
in het openbaar te verdedigen
ten overstaan van de promotiecommissie
van de faculteit der Aard- en Levenswetenschappen
op woensdag 23 januari 2008 om 15.45 uur
in de aula van de universiteit,
De Boelelaan 1105

door

Jonathan Gaston Flye-Sainte-Marie

geboren te Bédarieux, Frankrijk

promotor: prof.dr. S.A.L.M. Kooijman
copromotor: dr. F. Jean

Contents

Chapter 1

Introduction

1.1 The Manila clam

1.1.1 Systematic position and synonymy

The Manila clam, *Ruditapes philippinarum* (Adams & Reeves, 1850), belongs to the *Veneridae* (Rafinseque, 1815) and its systematic position is detailed below. A synonymy list is given in Tab. 1.1.

Phylum   *Mollusca*
     Class   *Bivalvia* (Linné, 1758)
         Order   *Veneroidea* (Adams & Adams, 1857)
            Family   *Veneridae* (Rafinseque, 1815)

1.1.2 Geographic distribution

Fig. 1.1 shows the actual distribution of the Manila clam. The species is native to the Indo–Pacific and its original distribution area ranged from the Kuril islands (52°N, 150°E) in the Northern Pacific ocean to Pakistan (30°N, 65°E) in the Indian ocean (Fig. 1.1). The Manila clam was subsequently introduced to Hawaii in 1929 (Yap, 1977), and ten years later, accidentally to the North-West coast of the United States. Naturally established populations are now present from Oregon to British Columbia.

     Between 1972 and 1975, the species was also introduced in France and at the end of the 70's also in Great Britain (Flassch and Leborgne, 1992) for aquaculture purposes, because of its higher growth rate compared to the European carpet shell, *Ruditapes decussatus*. Since 1988, natural populations have colonised most embayments along the French Atlantic coast. Today, natural populations are found on the South coast of Great Britain (Humphreys et al., 2007), all along the French, and Spanish Atlantic and Mediterranean coasts (mainly in the Adriatic sea) (Laruelle, 1999; Cesari and Pellizzato, 1990). This species has also been reported from different other places in the world: Norway (Mortensen and Strand, 2000), California, Marocco, Tunisia (Cesari and Pellizzato, 1990), Israel and Tahiti (Ponurovsky and Yakolev, 1992).

TAB. 1.1: Synonymy of the Manila clam (from Laruelle, 1999; Kim, 1994)

Genera	Species
Ruditapes	*philippinarum*
	semidecussata
Tapes	*philippinarum*
	semidecussatus
	denticulata
	indica
	grata
	quadriradiata
	violascens
	japonica
	bifurcata
Venerupis	*philippinarum*
	japonica
	semidecussata
Venus	*semidecussatus*
	semidecussata
	japonica
	tesselata
Amygdala	*semidecussata*
	philippinarum
	ducalis
	japonica
Paphia	*bifurcata*
	philippinarum
Protothaca	*bifurcata*

1.1.3   Biology and ecology

The bivalve, *Ruditapes philippinarum*, (Fig. 1.2) is an infaunal filter feeder that mainly lives in shallow embayments and estuaries. It is able to tolerate temporarily freshwater at low tide and the bathymetric distribution of the species ranges from high spring tide levels to a few meters deep into the subtidal zone. This species can be found in various sediments: coarse sand, sand, muddy gravel, mud and in *Zostera noltii* beds. As attested by its wide geographic distribution (Fig. 1.1) the thermal tolerance range of the species is wide and the optimal growth temperature ranges from 20°C to 24°C (Solidoro et al., 2000).

The Manila clam buries a few centimeters into the sediment. Its siphons are attached over most of their length and only detached at few millimeters at their extremities (1.2 B); this characteristic allows to distinguish this species from
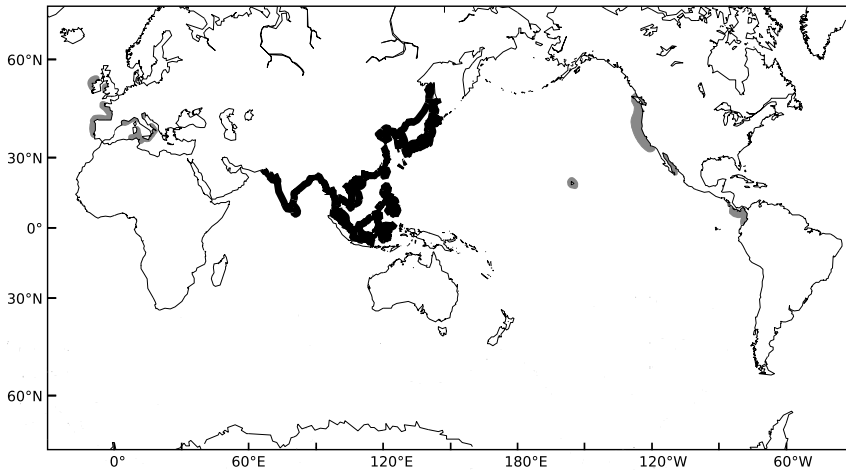
FIG. 1.1: Geographic distribution of *Ruditapes philippinarum* (from Cesari and Pellizzato, 1990; Kim, 1994; Laruelle, 1999). In black the original distribution. In grey areas where introduced population have developed.

the European carpet shell clam, *Ruditapes decussatus* which has unattached siphons. As most infaunal bivalves, the Manila clam filters water at the water–sediment interface, rendering the estimation of its main food source complex (Flye-Sainte-Marie et al., 2007a). This point will be further discussed in section 2.4.

R. philippinarum is a gonochoric species. As in most venerids its gonad is a diffuse organ within the visceral mass. Although exceptions can be found in cold waters (Drummond et al., 2006a), gametogenesis is initiated when water temperature rise over 12°C (Laruelle et al., 1994; Laruelle, 1999; Mann, 1979; Park and Choi, 2004; Ngo and Choi, 2004) and lasts for 2 to 5 month before the first spawning events occur(Laruelle, 1999; Devauchelle, 1990). Spawning periods vary geographically (Devauchelle, 1990). Along the French Atlantic coast, a major spawning event occurs in late August–beginning of September (Robert et al., 1993; Goulletquer, 1989a; Laruelle, 1999) and in this case all individuals of the population spawn synchronously. Depending on the environmental conditions several asynchronous "partial spawning" events can occur between May and the end of August (Laruelle, 1999; Calvez, 2003). During these partial spawning events, only a fraction of the gonad content, corresponding to the mature ovocytes, is released (Laruelle, 1999; Calvez, 2003). These

A   B
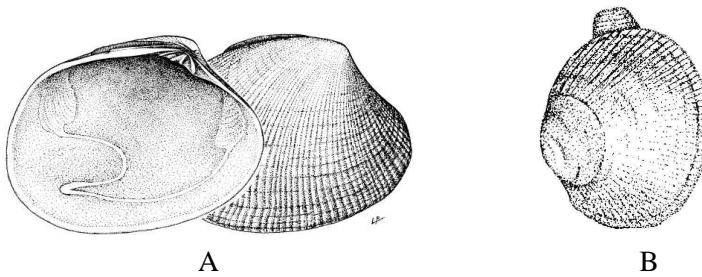
FIG. 1.2: The Manila clam, *Ruditapes philippinarum*, an infaunal bivalve. A: Internal and external shell. B: Note the presence of two attached siphons.

events seem inefficient in terms of recruitment (Calvez, 2003). If environmental conditions are favourable a late spawning event can still occur at the end of the autumn (Goulletquer, 1989a).

The Manila clam, *R. philippinarum*, is meroplanctonic: as in most bivalves, gametes are released in the water column where fertilization and larval development takes place. Fertilized eggs are about $70\,\mu m$ in diameter (Pronnier, 1996), reach the D–larvae stage after 24 to 48 hours (Helm and Pelizzato, 1990; Jones and Sanford, 1993; Calvez, 2003) and start to feed on phytoplancton. Planctonic life lasts for 10 to 15 days (Jones and Sanford, 1993; Calvez, 2003) during wich larvae are passively dispersed in the water (Calvez, 2003). Larval life takes end at the pediveliger larvae stage ($200\,\mu$m, Jones and Sanford, 1993) at which larvae passively sediment and fix to the substrate (Jones and Sanford, 1993). Calvez (2003) showed an active substrate selection process during settlement; in which post-larvae prefer sandy over muddy substrates. For this reason, highest densities of juveniles (8–$12\,mm$) are generally found in sandy areas (personal observation)

Although gonadal tissue can be observed in $15\,mm$–individuals under favourable conditions (personal observation), first gametogenesis generally occurs at $20\,mm$ (Laruelle, 1999). Maximum length (Von Bertalanffy maximum length L_∞) has been estimated between $46\,mm$ and $50\,mm$ on the french Atlantic coast (Robert et al., 1993 and personnal data). Nevertheless $60\,mm$–specimen have been observed in British Columbia (Quayle and Bourne, 1972) and in Norway (Mortensen and Strand, 2000) and I own personally a $67\,mm$ Norwegian specimen. Maximal length of the species can thus be estimated as approaching 70 to $80\,mm$.

1.2 The Brown Ring Disease

1.2.1 History

The high commercial value, its high growth performance and tolerance in terms of sediment quality, salinity and temperature made the Manila clam a target species for aquaculture. After its introduction in France during the 70s (Flassch and Leborgne, 1992), Manila clam culture became increasingly widespread along most of the Atlantic coast embayments: Arcachon bay (Robert and Deltreil, 1990), bay of Marennes–Oléron (Goulletquer, 1989a) and the Aber basin (Finistère) (Flassch and Leborgne, 1992). Between spring and summer 1987, high mortalities occurred in the Aber basin cultured clam beds. At that time, this site was the first production site of France (Paillard et al., 1989; Flassch and Leborgne, 1992). Mortality was associated with a characteristic symptom: a brown deposit on the peripheric inner shells (Paillard et al., 1989; Fig. 1.3) giving to the disease its name: Brown Ring Disease. The occurrence of these symptoms, associated with mass mortality was subsequently reported all along the French Atlantic coast: in the Marennes–Oléron bay in 1988 (Goulletquer et al., 1989a), and in the Arcachon bay in 1989 (Robert and Deltreil, 1990). The mortalities considerably contributed to the decline of venerid culture; an activity which has today disappeared from the Aber basin (Paillard, 2004b).

1.2.2 The pathogen *Vibrio tapetis*

The pathogenic agent causing Brown Ring Disease was first isolated at Landéda (Northern Finistère, France) and was shown to be a bacterium, first named *Vibrio* Predominant 1 (VP1) and subsequently renamed *Vibrio tapetis* (Paillard and Maes, 1990; Borrego et al., 1996b). This bacterium belongs to the family of *Vibrionaceae* and its systematic position is shown below:

Phyllum	*Proteobacteria* (Stackebrandt *et al.*, 1986)
Class	*Gammaproteobacteria*
Order	*Vibrionales*
Family	*Vibrionaceae* (Véron, 1965)

1.2.3 Symptoms and diagnosis

The main symptom of Brown Ring Disease is the brown deposit on the peripheric inner shell which is generally observed between the pallial attachment and the shell edge. It is essentially composed of conchiolin, the organic matrix

secreted by the mantle as a base for the calcification process (Paillard et al., 1989). In the disease, this conchiolin is melanized (Paillard, 1992) and its biochemichal composition seems different from organic normal matrix (Goulletquer et al., 1989a).
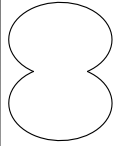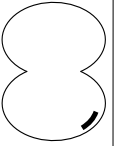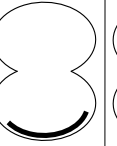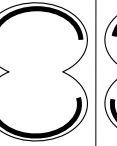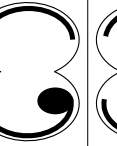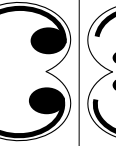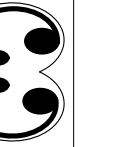
CDS	1	2	3	4	5	6	7
Symptoms							
	microscopic		visible by bare eye				

FIG. 1.3: Illustration of the classification scale of BRD symptoms established by Paillard and Maes (1994). Symptoms can be observed bare eyed at CDS=2 and higher. The brown deposit takes a significant place on the inner shell at CDS=4 and more.

Stages of BRD development and recovery can be assessed by scaling macroscopic symptoms according to the Paillard and Maes (1994) classification system illustrated in Fig. 1.3. This scaling method takes into account the extent, the position and the thickness of the brown deposit. First stages are characterized by the presence of conchiolin spots surrounded by a pale halo adhering to the inner shell. These stages (Conchiolin Deposit Stage; CDS 1 et 2) are nearly invisible to the bare eye (Fig. 1.3). More intense stages are signaled by a macroscopic deposit and its extent increases with disease development. At stage CDS 3 and higher the brown deposit is clearly visible by the bare eye and at stage CDS 4 and higher the brown deposit takes a significant place on the inner shell (Fig. 1.3). When the deposit is thick, the outer fold of the mantle can present some lesions (Paillard, 1992; Paillard et al., 1994). During disease recovery, the clam is able to cover the symptomatic brown deposit by depositing new calcified layers (Paillard, 1992). Four Shell Repair Stages (SRS) have been described (Paillard and Maes, 1994). The brown deposit recalcification process begins by the apposition of calcified concretions (SRS 1). At SRS 2 et 2.5 calcified plates recover partially the brown deposit and repair is complete at SRS 3.
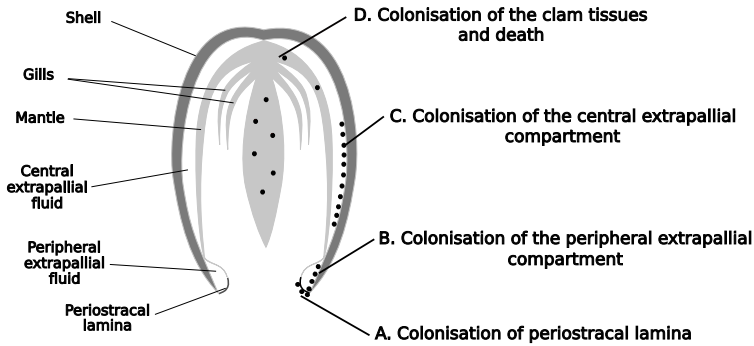
FIG. 1.4: Progression stages of Brown Ring Disease in the clam *R. philippinarum* (modified after Paillard, 2004b).

1.2.4 Progression of the disease

Disease progression has been reviewed in Paillard (2004b) and is illustrated in Fig. 1.4. According to this author, the initial process is the attachment of the pathogen *V. tapetis* to the periostracal lamina (Fig 1.4 A), but disease may develop only after penetration of the pathogen into the extrapallial compartment. Modalities of entry of *V. tapetis* into the fluids are poorly known. Following Paillard (2004b) "In favourable conditions for the pathogen, *V. tapetis* colonisation provokes some alterations and rupture of the periostracal lamina which allows the penetration of bacteria into the extrapallial fluids". This critical point will be further discussed in chapter 5. Peripheral extrapallial fluids are first infected (Fig 1.4 B) and depending on the progress of the disease, central extrapallial fluids can subsequently be colonised (Fig 1.4 C). The interaction between the bacterium and the mantle induce the formation of the brown deposit. At this stage of disease progression, *V. tapetis* can be considered has a microparasite. If tissue lesions occurs, *V. tapetis* can penetrate into the hemolymph and colonise the tissues, provoking the death of the individual by a generalised septicemia (Allam et al., 2002c; Paillard, 2004b).

1.2.5 Impact on the host

The most obvious symptom of BRD is of course the brown deposit (see section " Symptoms and diagnostic"1.2.3) systematically associated with an alteration of the periostracal lamina (Paillard and Maes, 1995a). Also, shell deformations can be observed during disease development (Paillard, 1992). Although tissue

lesions are not systematically observed in the first stages (Paillard et al., 1994), alterations of the digestive diverticula, which presents degeneration signs, can be observed at more advanced stages (Plana and Le Pennec, 1991; Plana, 1995). At these stages, the mantle edge presents some lesions (desquamation and hypertrophia of the mantle epithelium; Paillard, 1992; Paillard et al., 1994; Paillard and Maes, 1995a).

Experimental contamination with *V. tapetis* induces an increase in the number of circulating hemocytes in the hemolymph (Paillard et al., 1994; Allam et al., 2000a, 2006; Paillard, 2004b). This is interpreted as a mobilisation of hemocytes towards the infection site (Paillard et al., 1994). A decrease in phagocytic activity of hemocytes (Allam et al., 2002b; Allam and Ford, 2006) and an increase of the dead cells (hemocyte) percentage (Allam et al., 2000a; Allam and Ford, 2006; Allam et al., 2006) have also been observed. Leucine aminopeptidase activity in the hemolymph is also affected upon an experimental bacterial challenge (Oubella et al., 1993, 1994, 1996). An increase of hemocyte concentrations in extrapallial fluids is observed in naturally infected clams suggesting a mobilisation of immunocompetent cells towards the most infected site (Allam, 1998; Allam and Paillard, 1998; Allam et al., 2000a,b).

Field observations showed that burrowing activity is decreased in highly diseased individuals, which are often found at the sediment surface (Goulletquer et al., 1989a; Paillard, 1992).

In natural conditions disease development is associated with a decrease of the condition index (ratio between total flesh dry weight and shell dry weight) (Goulletquer, 1989a; Paillard, 1992; Paillard et al., 1994). Experimental infections induce a weight loss and a decrease in flesh glycogen concentration (Plana, 1995; Plana et al., 1996), the main energy storage compound in molluscs (see reviews in: Gabbot, 1976, 1983; Lucas, 1993). All these observation suggest that BRD development affects the host's energy balance, a point which will be developed in Part III.

1.2.6   Disease modulation by environmental factors

Although Brown Ring Disease was first observed massively during spring and summer 1987 (Paillard et al., 1989; Paillard, 1992), field and laboratory studies showed the positive effect of low temperature on the development of this disease (Maes, 1992; Paillard et al., 1997, 2004). This disease is subsequently considered as a "cold water disease" (Maes, 1992; Paillard et al., 1994; Allam et al., 2000b; Paillard, 2004a,b). The map in Fig. 1.5 indicates the different locations where the disease has been observed in Manila clam. The locations are distributed along the French Atlantic coast, in Ireland, in Great Britain, in

Spain and in Italy (Paillard et al., 1994; Allam et al., 2000b; Castro et al., 1996; Novoa et al., 1998; Paillard, 2004b; Lassalle et al., 2007; and personal observations). Symptoms have recently also been observed in Norway but have not yet been attributed to *Vibrio tapetis* with certainty (Paillard et al., submitted). The disease was reported in the Northern Adriatic sea (Italy) in 1990, but the disease did not spread and disappeared after the summer months (Paillard et al., 1994). This distribution shows the "Northern character" of Brown Ring Disease. Until recently, BRD had only be reported from the European coast, but has recently also been reported in South Korea, in the original distribution area of the Manila clam (Park et al., 2006b).
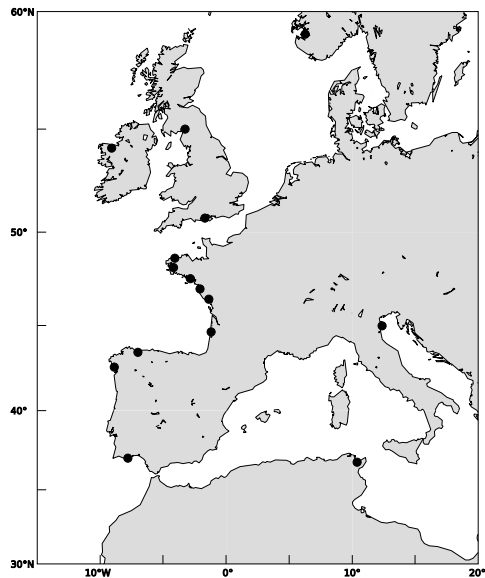
FIG. 1.5: Map of the different locations (●) where Brown Ring Disease symptoms have been reported in the Manila clam, *R. philippinarum* (following Paillard, 2004b; Paillard et al., submitted; Lassalle et al., 2007 and personal observations)

Temperature seems thus to be one of the major environmental factors controlling disease development. The pathogenic agent, *Vibrio tapetis*, has an optimal growth temperature of around 20°C (Maes, 1992; Haberkorn, 2005). High temperatures inhibit *V. tapetis* growth and no growth is observed over 27 - 30°C (Maes, 1992; Haberkorn, 2005). Since temperatures above 27°C can

be lethal for this bacterium, Maes (1992) suggested that exposure of BRD–
affected clams to this temperature could be curative. This author also showed
that between 15 and 21°C the intensity of disease development is inversely
correlated to temperature. The influence of temperature on symptom devel-
opment and on immune parameters has subsequently been studied by Paillard
et al. (2004). These authors suggest that the temperature influences the de-
velopment of Brown Ring Disease by modulating *V. tapetis* growth but also
by modulating the host's immune response and recovery processes. Following
these authors the "optimal temperature" for the development of the disease is
near 14°C.

Annual extreme temperatures seems to explain the geographical repartition
of the disease (Paillard, 2004a). An epidemiological survey along the French
Atlantic coast (from the Aber basin in the North to Noirmoutier in the South)
indicated that the prevalence minima were found on the site where tempera-
tures were lowest in winter (Paillard et al., 1997). Following these authors,
temperatures under 3°C can inhibit *V. tapetis* pathogenicity, and absence of
disease development in the South of France and in the Adriatic sea could be
explained by the higher summer temperatures which rise above 25°C (Paillard
et al., 1994; Paillard, 2004a), temperature being susceptible to reduce growth
and in some extent lethal to *V. tapetis* (Maes, 1992).

In natural populations, a seasonal pattern is not systematically observed,
especially when prevalence and intensity are low (see Chap. 4; Paillard, 2004a).
Nevertheless, the evolution of disease prevalence follows an annual pattern
(Paillard et al., 1997; Paillard, 2004a): generally BRD symptoms increase to-
wards the beginning of the spring and decrease towards the beginning of sum-
mer (Paillard et al., 1997; Paillard, 2004a). Low temperatures during the rising
phase of prevalence have been invoked to explain this pattern (Paillard et al.,
1997, 2004; Paillard, 2004a,b) but an alternative hypothesis will be discussed
in chapter 5.

The effects of salinity on BRD development has poorly been described. A
laboratory study however, showed that low salinities (under 20 ‰) can favour
the development of this pathology and negatively affect defence–related hemo-
cyte parameters (Reid et al., 2003).

Finally, sediment grain–size distribution significantly affects Brown Ring
Disease (Paillard, 2004b). In natural populations disease prevalence is posi-
tively correlated to the abundance of big sediment grains. This point will be
discussed in chapter 5.

1.3   Objectives and thesis outline

Diseases development results from interactions between the environment, the host and the pathogen. The environment might influence transmission of the pathogen to the host as well as pathogen and host physiology. Development of the pathogen within the host may depend on the environmental conditions, but also on the efficiency of the host defence system which is indirectly controlled by the environment through host physiology. The aim of this work is to provide a better understanding of these complex relationships in the case of Brown Ring Disease. The interplay between host energetics and disease development are specially emphasized.

The work originally begun with the development of a model describing the interaction between the environment, the host and the pathogen that provided a synthesis of the state of art about BRD. This model is presented in the first part of the manuscript. Chapter 2 presents the construction, calibration and simulations of an individual growth model of the Manila clam, based on the scope for growth concept. In chapter 3, the development of a model describing the interactions between the environment, the host and the pathogen, based on the model described in chapter 2, is presented.

The second part of the thesis presents field observations performed to better understand the influence of the environment on both the defence–related system of the host and on the development of BRD, and to validate the model. Results of field monitoring of hemocyte parameters, environmental parameters and disease in the Manila clam population of the Gulf of Morbihan are shown and discussed in chapter 4. Chapter 5 presents an hypothesis for the first step of the infection : the entry of *Vibrio tapetis* into the extrapallial compartment. Chapter 6 compares the assumptions of the model described in chapter 3 with the field observations.

In the third part of the thesis, the impact of the BRD development on the energy budget of the Manila clam is studied. Chapter 7 presents the effects of disease development on the filtration activity and the respiration rate of the host. Effects of the disease on maintenance costs of the Manila clam are assessed in chapter 8 by both experiments and a model based on Dynamic Energy Budget (DEB) theory. Chapter 9 will describe data and methods used for the estimation of the parameters of the Manila clam energy budget model presented in chapter 8.

Finally, Chapter 10 discusses the results obtained during this thesis work.

Part I

Everything begins with a model...

Chapter 2

An individual growth model of the Manila clam

Ecophysiological dynamic model of individual growth of *Ruditapes philippinarum*

Jonathan FLYE-SAINTE-MARIE, Fred JEAN, Christine PAILLARD, Susan FORD, Eric POWELL, Eileen HOFMANN and John KLINCK.

Abstract

A bioenergetics model of the Manila clam (*Ruditapes philippinarum*) was built to simulate growth, reproduction and spawning in culture and fishery field sites in Marennes–Oléron Bay (French Atlantic coast). The model is driven by two environmental variables: temperature and food supply. The food supply and the clam's filtration rate determine soft tissue condition index, which in turn drives clam growth and reproduction. The model was calibrated and then validated using two independent data sets.

This paper discusses the difficulty of comparing experimental data and individual model outputs when asynchronous spawning events occur in the studied population. In spite of this difficulty, the simulations reproduce the typical pattern of growth and reproduction of the Manila clam.

Simulations showed that water column chlorophyll *a* concentration is not a perfect estimator of food resources for a near bottom suspension feeder such as the Manila clam and emphasize the lack of knowledge about *Ruditapes philippinarum* nutrition.

The individual growth model presented in this paper will be integrated into a numerical population model describing the host-parasite-environment relationship in Brown Ring Disease, caused by the bacterium *Vibrio tapetis*.

Keywords: Model; Individual growth; Energy balance; Reproduction; Food input; Brown Ring Disease.

2.1   Introduction

The Manila clam (*Ruditapes philippinarum*) was introduced for aquaculture purposes to France between 1972 and 1975 (Flassch and Leborgne, 1992). In France, this venerid culture became increasingly widespread, and since 1988 natural populations have colonized most embayments along the French Atlantic coast, resulting in a fishery of ca 1500 tons in the Gulf of Morbihan at the end of the 1990s. *R. philippinarum* is often affected by high mortalities in late winter, which considerably limit aquaculture and fisheries production. These mortalities were first associated with unfavourable environmental factors such as low trophic resources, cold temperatures and low salinity (Goulletquer, 1989b; Bower, 1992). Later, they were attributed to Brown Ring Disease (BRD), a bacterial disease induced by the pathogen *Vibrio tapetis* (Paillard et al., 1989; Paillard and Maes, 1990), in conjunction with low condition index and low biochemical reserves (Goulletquer, 1989a). BRD progression in clams and *V. tapetis* strategies for infection have been described in depth by Paillard et al. (1994) and Paillard and Maes (1994). Infections may theoretically occur any time of the year, but BRD development may be modulated by environmental conditions (Paillard et al., 2004) and clam's defence system (Allam and Paillard, 1998; Allam et al., 2000b). In addition these authors showed that BRD development is modulated by the energy balance of the clam.

As a first step in developing a numerical model describing the host–pathogen–environment relationships in BRD, this study presents the individual ecophysiological model of growth and reproduction of the Manila clam. The aim is to describe the variability in energy balance for an individual without BRD as a function of the two main environmental factors presumed to control BRD development : the trophic resources (Goulletquer, 1989a) and the temperature (Paillard et al., 2004).

2.2   Materials and methods

2.2.1   Basic concept and state variables

The model is based on a the widely applied (see review in Bayne, 1998) scope for growth (SFG) concept. The SFG concept assumes that energy or matter gained by food acquisition is equal to the energy or matter lost for maintenance, growth and reproduction. SFG can be calculated as follows according to Lucas and Beninger (1985):

$$SFG = Gg + Sg + Sh = Cons - (Pp + Fp + Resp + U)$$

where: Gg is gonadal growth; Sg is somatic growth; Sh is shell growth; $Cons$ is consumption (retained organic matter); Pp is pseudofaeces production; Fp is faeces production; $Resp$ is respiration and U is urea and amino acid excretion.

If $SFG < 0$, energy or matter is mobilized, firstly from gonad, then from somatic tissue, and the clam loses weight while using energy reserves. If $SFG > 0$, energy or matter gained is partitioned into shell, soma, and gonad. Partitioning among those three compartments is controlled both by environmental parameters (quantity and quality of food, temperature, salinity, . . .) and by endogenous factors such as genotype, size and physiological condition (see e.g. Shafee and Lucas, 1982; Lucas, 1993; Goulletquer, 1989a; Pérez Camacho et al., 2003).

The conceptual design is described in Fig. 2.1. The structure and formulation of this model is based on the Hofmann et al. (2006) *Mercenaria mercenaria* growth model. The two state variables are the shell length and the total flesh weight including somatic weight and gonadal weight.

2.2.2   Environmental factors

Three data sets (Fig. 2.2) were extracted from Goulletquer (1989a), a survey of Manila clam aquaculture in the Marennes-Oléron basin (French Atlantic coast, see Fig. 2.3):

1. a time series from Nole station (March 1984 to September 1985) of chlorophyll *a* ($Chla$) concentration was used for calibration. Temperature (T; °C) was obtained from the same study site during a 1986 survey;

2. two time series, one from Nole station and the other from Lilleau station, both extending from March 1985 to May 1986, were used for model validation. Both consisted of $Chla$ concentration and temperature series.

Data from all time series were linearly interpolated to obtain daily values when necessary.

In order to evaluate trophic resources, $Chla$ concentration was converted to ingestible dry organic matter (trophic resource $Food$, g L^{-1}) to take into account the pseudofaeces production step, following the equation:
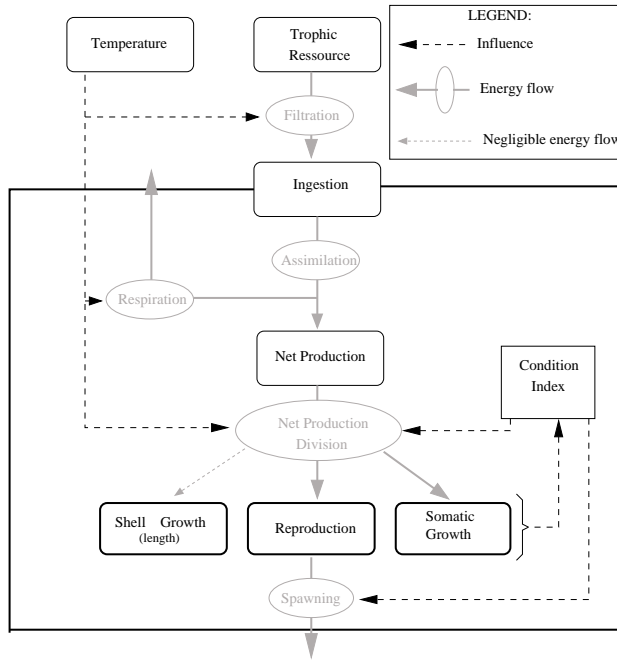
FIG. 2.1: Schematic of the conceptual clam growth model

$$Food = Chla \times FoodCoeff$$

where $FoodCoeff$ in $g\ DW\ \mu g^{-1}\ Chla$ is the coefficient that converts $Chla$ to ingestible dry organic matter.

2.2.3 Physiological mechanisms formulations

Net Production

Net production of dry organic matter ($Pnet$; $g\ day^{-1}$) was calculated with the following equation, which reflects energy gain from assimilation and loss due to respiration:

$$Pnet = Ingest \times Assim - Resp$$

Food acquisition Using data from literature (Goulletquer et al., 1989b; Goulletquer, 1989a), the filtration rate of a 1-$g\ DW$ individual was estimated as a
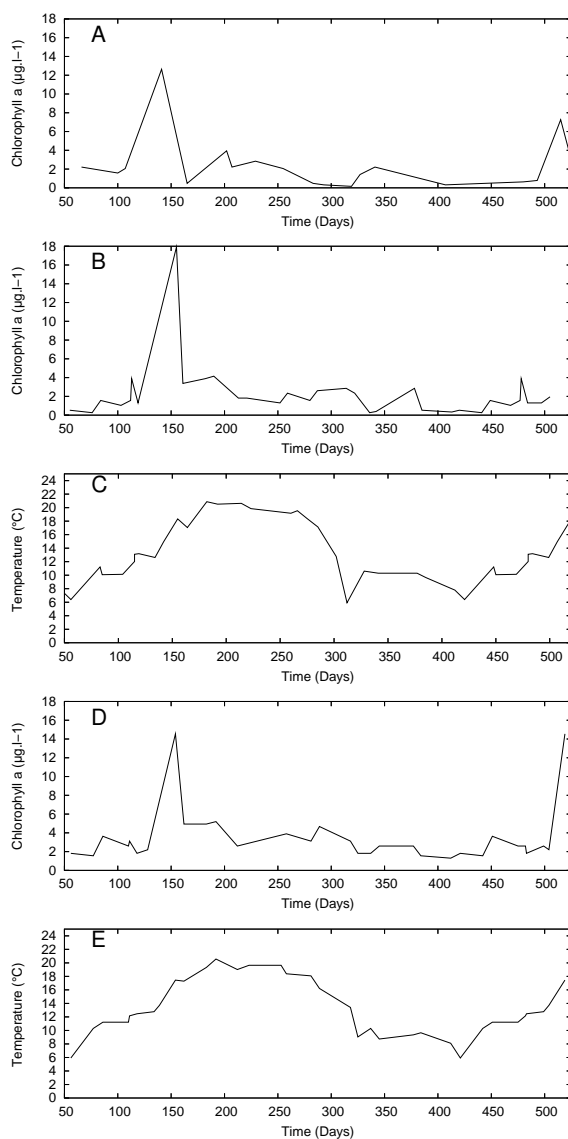
FIG. 2.2: Environmental data sets used for calibration and validation, interpolated from Goulletquer (1989a). Data sets A and B and C were used for the calibration at Nole station. Data sets B and C were used for validation at Nole and data sets D and E were used for validation at Lilleau station.
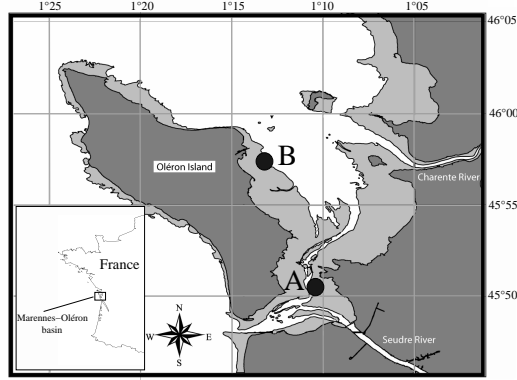
FIG. 2.3: Location of the the two stations studied by Goulletquer (1989a) in Marennes-Oléron basin (Atlantic coast, France). Nole (A), an estuarine station and Lilleau (B), an oceanic station.

function of temperature using the following empirical equation:

$$Filt_T(T) \quad = \quad -5.62\ 10^{-3} \times T^2 + 0.18 \times T - 0.30 \qquad (2.1)$$

$Filt_T$ in $L\ h^{-1}$ reaches its maximum ($Filt_T(16) = 1.16\ L\ h^{-1}$) at 16 °C.

Filtration rate was estimated as a function of dry weight ($Filt_W(W)$ in $mL\ min^{-1}$) following the empirical equation:

$$Filt_W(W) \quad = \quad a_f \times W^{bf} \qquad (2.2)$$

with $a_f = 20.049$ and $bf = 0.257$.

Using equations (2.1) and (2.2), filtration rate was finally expressed as a function of individual weight and temperature ($Filt$; $L\ day^{-1}$) following the equation:

$$Filt(W,T) = a_f \times W^{bf} \times \frac{Filt_T(T)}{Filt_T(16)}) \times 1.44$$

with $a_f = 20.049$ and $bf = 0.257$ being two adjusted allometric parameters.

Ingestion ($Ingest$; $g\ day^{-1}$) of dry organic matter can be then calculated according to the equation:

$$Ingest = Food \times Filt$$

Assimilation Amino acid and urea excretion is very low compared to other parameters and was thus omitted from the model. Therefore, assimilation was considered equal to absorption. Assimilation rate (AE) was estimated as a function of weight according to a Michaelis–Menten formulation:

$$AE = AE_0 + \frac{AE_1 \times W}{K_A + W}$$

where $AE_0 = 0.1$ and $AE_1 = 0.6$ are the minimum and maximum additive assimilation rates respectively, and $K_A = 2.74\ g$ is the half-saturation constant. Assimilation ($Assim$; $g\ day^{-1}$) was then calculated following :

$$Assim = AE \times Food \times Filt$$

Respiration Respiration was also calculated, using data from Goulletquer et al. (1989b) and Goulletquer (1989a), as a function of temperature for a 1-$g\ DW$ individual as

$$Resp_T(T) \quad = \quad -4.75\ 10^{-4} \times T^2 + 2.02\ 10^{-2} \times T + 2.43\ 10^{-2} \quad (2.3)$$

$Resp_T$ ($ml\ O_2\ h^{-1}$) reaches its maximum $Resp_T(21) = 0.24\ ml\ O_2\ h^{-1}$ at 21 °C. Respiration for individual clams was estimated from weight ($Resp_W$ in $Cal\ day^{-1}$) following the empirical equation:

$$Resp_W(W) \quad = \quad a_r \times W^{br} \quad (2.4)$$

where $a_r = 27.88$ and $br = 0.85$.

Using equations (2.3) and (2.4), respiration ($Resp$; $g\ DW\ day^{-1}$) was finally expressed as a function of weight and temperature following the equation:

$$Resp(W, T) = (a_r \times W^{br} \times Resp_T(T)/Resp_T(21)) \times 2.177\ 10^{-3}$$

with $2.177\ 10^{-3}$ being the coefficient to convert calories to $g\ DW$.

Condition index

In bivalve studies, condition index is usually the ratio between shell and dry flesh weights (see review in Lucas and Beninger, 1985). In our model a condition index, based on variation of total flesh weight inside internal shell volume, like that used in oyster studies (Lawrence and Scott, 1982), was calculated as follows:

$$C = \frac{W - W_o}{W_{max} - W_o}$$

where the relationship between the mean flesh weight (W_o) and the shell length (L) is

$$W_o = a_o \times L^{bo}$$

and $a_o = 8.52 \ 10^{-7}$ and $bo = 3.728$. The values were a_o and bo were evaluated using a composite data set (Paillard et al., unpublished data; $n = 921$, $r^2 = 0.904$),

and

$$W_{max} = a_{om} \times L^{bo}$$

where $a_{om} = 1.70 \ 10^{-6}$.

C is related to the shell weight-based condition index (CI) using a linear relationship: $C = 0.0124 \times CI - 1.0562$ ($n = 558$, $r^2 = 0.95$).

Length growth

The organic matrix is only 2 to 3% of shell weight of the Manila clam (Goulletquer and Wolowicz, 1989) and generally accounts for only a small fraction of SFG in bivalves (Thompson, 1984; Dame, 1996; Pouvreau et al., 2000); in the present model, energy allocation to shell growth was thus omitted. Therefore, shell length growth rate $LgrowthRate$ (day^{-1}) is a Michaelis–Menten function of condition index (C) and is saturated as a function of the maximum length (L):

$$LgrowthRate(L, C) = dl_o \times \frac{L_{max} - L}{L_{max}} \times \frac{C - C_S}{K_l + C - C_S}$$

where dl_o is maximum daily growth rate, L is the individual length, L_{max} is the maximum clam length, K_l is the half saturation constant and C_S is the

minimum value of C for $LgrowthRate > 0$. Parameters of the Michaelis–Menten equation were evaluated using a composite data set from (Goulletquer, 1989a) in Marennes–Oléron Bay.

Resources allocation to reproduction

As in most venerids, the gonad of *R. philippinarum* is a diffuse organ in the visceral mass. This is the main reason why rules specifying the priorities for resource partioning by the Manila clam have not been extensively studied (Laruelle, 1999; Laruelle et al., 1994; Calvez, 2003). However, available information was used to make assumptions concerning energy allocation. Most of the information is based on various condition index and histological studies, as well as recent investigations using enzyme-linked immunosorbent assays (ELISA) to quantify egg weight (Park and Choi, 2004; Ngo and Choi, 2004). The gonad is almost never developed in clams less than 20 mm, which is assumed to be the minimum size for reproduction (Laruelle, 1999, Calvez comm. pers). *R. philippinarum* is known to have a reproductive period extending from March-April to October on western European and Korean coasts. This corresponds to a period when water temperature rises above 12°C, which is considered as the minimum temperature allowing gametogenesis (Laruelle et al., 1994; Mann, 1979; Park and Choi, 2004; Ngo and Choi, 2004). Condition index and histological studies showed that most of net production is allocated to reproduction from mid-June to the end of October (Laruelle, 1999; Calvez, 2003). This phenomenon is observed at all stations monitored by those authors along the French Atlantic coast and occurs when condition index is above a threshold value.

Reproductive effort $RepEff$ is the adimensional fraction of net production allocated to gonadal tissues. $RepEff$ becomes positive, and gametogenesis possible, when clam length is above a minimum ($LengthRepMin = 20$ mm; Laruelle, 1999) and temperature is above a minimum ($TempRepMin = 12$ °C; Laruelle, 1999; Park and Choi, 2004; Ngo and Choi, 2004; Mann, 1979). Below those thresholds, $RepEff = 0$. Above the thresholds, reproduction effort is calculated as a function of temperature according to

$$RepEff = RepEff_{Max} \times \frac{1}{2} \times (1 + \tanh(\frac{T - 13.8}{14}))$$

with $RepEff_{Max}$, the maximum fraction of net production allocated to the gonad.

Gamete release

Factors triggering spawning are also not well known or intensively studied in *R. philippinarum*, for the same reasons mentioned for resource allocation. Spawns occur from May to October (Laruelle, 1999; Goulletquer, 1989a; Meneghetti et al., 2004). Spawnings and rapid rematuration after spawning are observed during the whole breeding period. Individuals are well synchronized during the first spring maturation of gametes, which is correlated to temperature increase, but this synchrony may be lost during subsequent spawnings (Laruelle et al., 1994; Toba et al., 1993; Meneghetti et al., 2004). Asynchronous partial spawnings occur from end of May until the end of August. During these partial spawnings events, only a fraction of the gonad content, corresponding to the mature ovocytes, is released. The main spawning is observed in late August or September, when almost all individuals release their entire gonadal content. Under good environmental conditions, late spawning events can occur until end of October (Goulletquer, 1989a; Laruelle, 1999; Calvez, 2003). In the model, partial and major spawning events are distinguished according to the following criteria:

- a clam is ready for a partial spawning event if its condition index and gonado-somatic index (gonad to flesh weight ratio, GSI) reach threshold values ($ParIC$ and $ParGSI$, respectively). After the partial spawning event, the condition index drops to a value ($ParPostIC$) corresponding to the weight lost by gamete release.

- a clam is ready for a major spawning event if its GSI is above the threshold value ($SpawnRatio$) and it has experienced a minimal number of days of gametogenesis, which is evaluated as 119 days from the day the temperature definitively rises above 12°C.

Threshold values for spawning events were estimated using data sets from Calvez (2003) for the Gulf of Morbihan.

2.2.4   Parameter evaluation and model adjustment to experimental data

Most of the parameters of the model were first estimated from published values for individuals without BRD symptoms (Table 2.1), however, some of the parameters could not be evaluated this way and were evaluated by adjusting the model to experimental data (calibration data set at Nole).

2.2.5 Validation

Once parameters were evaluated, the model was then validated using one data set from Nole station and one from the Lilleau station. Chlorophyll *a* and temperature time series are shown in Fig. 2.2. Both data sets are from Goulletquer (1989a) (see section 2.2).

For both calibration and validation, the fit between experimental and modeled results was ascertained using a linear regression through the origin for each state variable (length, weight and condition index). The slope of regression line of modeled *vs* experimental values was compared to 1 (*t*-test) and the coefficient of determination was calculated.

2.3 Results

2.3.1 Model evaluation

Results of a simulation after adjustment of the model to experimental field data are shown in Fig. 2.4. This simulation was obtained using the parameter values in Table 2.1. For all state variables, the slopes of the regression lines between observed and simulated values were not significantly different from 1 (*t*-test, *p-value* > 0.05).

The simulated length trajectory of a standard individual followed that of the average length observed in the field (Fig. 2.4A). Length growth was almost completely explained by the model ($r^2 = 0.98$). Simulated dry weight (Fig. 2.4B) and condition index (Fig. 2.4C) were also close to field observations, even though coefficients of determination were lower ($r^2 = 0.77$ and $r^2 = 0.66$, respectively). These lower values can be attributed to the simulated spawning pattern: the model simulated partial spawning events at days 140 and 153 (end of May and begining of June respectively). Spawning at this time was not noted by Goulletquer (1989a), who collected the data set used to calibrate and validate the model, but they are in accordance with observed spawning patterns on the French Atlantic coast (Laruelle, 1999; Calvez, 2003). A major spawning was simulated at day 230 (late August) at the date where this gamete release was observed in the field by Goulletquer (1989a).

2.3.2 Model validation

Nole

Validation simulations at Nole station are shown in Fig. 2.5. For length and weight, the slopes of the regression lines between observed and simulated val-

TAB. 2.1: Optimum values of the parameters of the model.

Parameter	Explanation	Value	Unit	Evaluated from
$Filt_T(16)$	Maximum of the $FT(T)$ function (at 16°C)	1.16	$L\ h^{-1}$	Goulletquer et al. (1989b); Goulletquer (1989a)
a_f	Allometric coeff. of the eq. relating filtration rate to DW	20.049	no unit	Goulletquer et al. (1989b); Goulletquer (1989a)
bf	Allometric exponent of the eq. relating filtration rate to DW	0.257	no unit	Goulletquer et al. (1989b); Goulletquer (1989a)
AE_0	Minimum additive assimilation rate	0.1	no unit	Goulletquer et al. (1989b)
AE_1	Maximum additive assimilation rate	0.6	no unit	Goulletquer et al. (1989b)
K_A	Half-sat. const. of the M.-M. eq. relating assim. rate to DW	2.74	g	this study
$Resp_T(21)$	Maximum of the $RT(T)$ function (at 21°C)	0.24	$ml\ O_2\ h^{-1}$	Goulletquer et al. (1989b); Goulletquer (1989a)
a_r	Allometric coeff. of the eq. relating respiration rate to DW	27.88	no unit	Powell and Stanton (1985)
br	Allometric exponent of the eq. relating respiration rate to DW	0.85	no unit	Powell and Stanton (1985)
a_o	Allometric coeff. of the eq. relating average DW (W_0) to length	$851.88\ 10^{-9}$	no unit	Paillard (unpublished data)
bo	Allometric exponent of the eq. relating average DW (W_0) to length	3.728	no unit	Paillard (unpublished data)
a_{om}	Allometric coeff. of the eq. relating max. DW (W_{max}) to length	$1703.76\ 10^{-9}$	no unit	Paillard (unpublished data)
L_{max}	Maximum clam length	60	mm	Mortensen and Strand (2000)
dl_o	Maximum length growth rate	0.0045	day^{-1}	Goulletquer (1989a)
K_l	Half-sat. const. of the M.-M. eq. relating C to length growth rate	0.123	no unit	Goulletquer (1989a)
C_S	Minimum value of C for $R_{L,C} > 0$	-0.45 (49)	no unit	Goulletquer (1989a)
$LengthRepMin$	Minimum clam length for reproduction	20	mm	Laruelle (1999), Calvez (unpublished data)
$TempRepMin$	Minimum temperature for reproduction	12	°C	Laruelle (1999)
$ParGSI$	GSI threshold value for partial spawning	0.30	no unit	this study
$ParIC$	Condition index threshold value for partial spawning	0.50 (125)	no unit	Calvez (2003)
$ParPostIC$	condition index value after a partial spawning event	0.23 (104)	no unit	Calvez (2003)
$SpawnRatio$	GSI threshold value for principal spawning	0.42	no unit	Park and Choi (2004)
$C2F$	$Chla$ to dry ingestible org. mat. conversion coeff. at Nole station	0.2552	$g\ DW\ \mu g^{-1}$	this study
$C2F$	$Chla$ to dry ingestible org. mat. conversion coeff. at Lilleau station	0.3432	$g\ DW\ \mu g^{-1}$	this study

Condition index values are expresed in the model condition index (C) experimental equivalent values (CI) are shown in parenthesis.
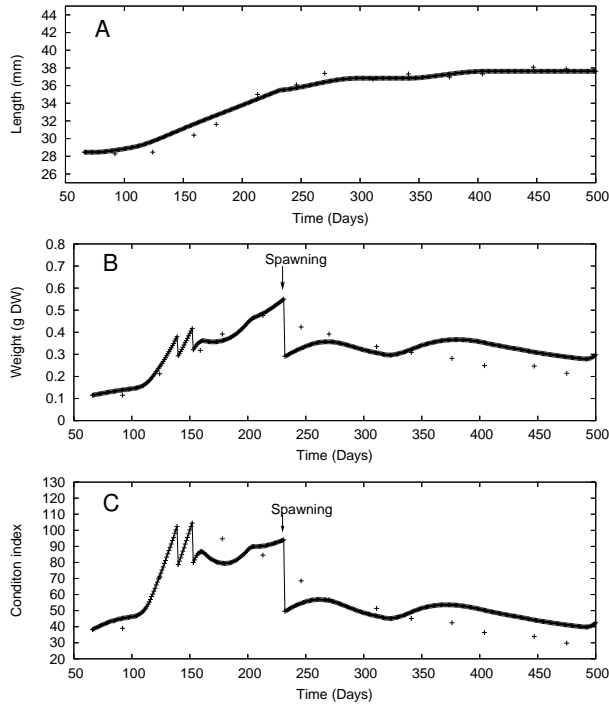
FIG. 2.4: Results of the adjustment of the model to experimental data of Goulletquer (1989a) for (A) length (mm); (B) weight (g DW) and (C) condition index. Continuous lines: model output. Crosses (+): observed data points. The arrow indicates the date where spawning was observed by Goulletquer (1989a). Time (days) is counted from the 1st of January 1984.

ues were not significantly different from 1 (*t*-test, *p-value* > 0.05). The simulated length trajectory (Fig. 2.5A) was close to observed data and the coefficient of determination was very high ($r^2 = 0.95$). Simulated trajectories for weight (Fig. 2.5B) and condition index (Fig. 2.5C) were also near the observed data; two partial spawnings were simulated at days 154 and 187. Laruelle (1999) and Calvez (2003) showed that partial spawnings induced asynchrony of gonadal state, resulting in increased variability of flesh weight within a cohort. The two large standard deviations for weight in the field data between days 154 and day 187 tend to confirm the occurrence of such spawnings.

During the whole gamete release period, from day 150 (late May) to day
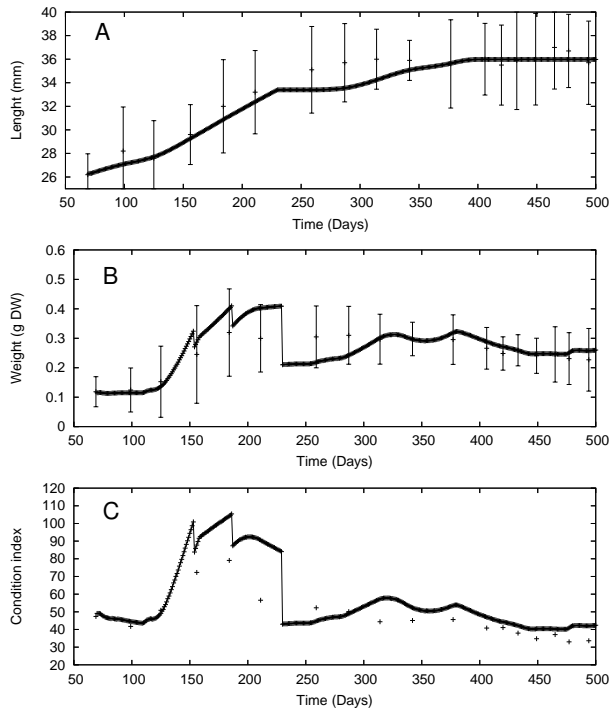
FIG. 2.5: Results of the validation of the model using temperature and *Chla* times series at the Nole Sation for length (A), weight (B) and condition index (C). Continuous lines: model output; crosses (+): observed data points; errorbars indicate standard deviation for field data (Goulletquer, 1989a). Standard deviations for condition index were not available. Time (days) is counted from the 1st of January 1985.

240 (begining of September), the simulated trajectory diverged from observed data because of spawnings. The importance of the principal spawning in the fall induced a divergence of the model compared to observed data. These divergences induced lower coefficients of determination between simulation and field data for weight ($r^2 = 0.63$) and condition index ($r^2 = 0.78$). For condition index, slope of the regression line between experimental and modeled data was 0.84 and significantly different from 1 (*t*-test, *p-value* < 0.05). Nevertheless, for both weight and length, simulations were within the observed standard deviation range.

Lilleau
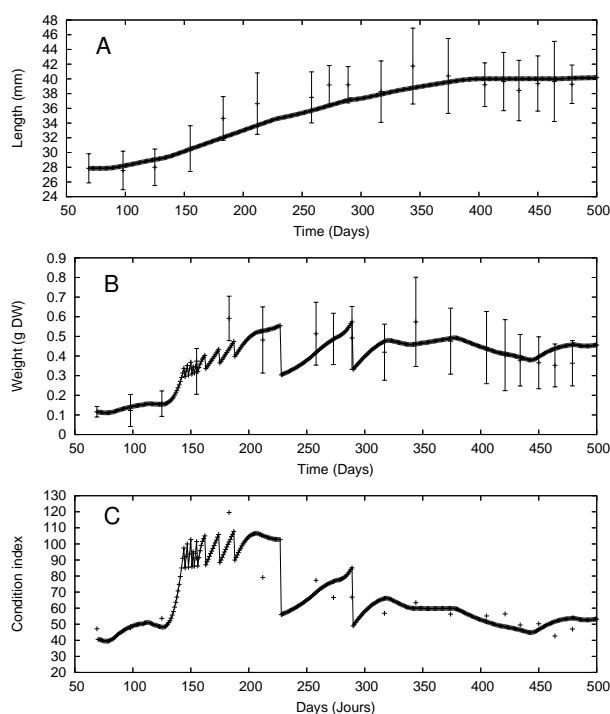
FIG. 2.6: Results of the validation of the model at Lilleau for length (A), weight (B) and condition index (C). Continuous lines show model output, crosses (+) show observed data points and errorbars indicate standard deviation for field data (Goulletquer, 1989a). Standard deviations for condition index were not available. Time (days) is counted from the 1st of January 1985.

Validation simulations for the Lilleau site are shown in Fig. 2.6. For all state variables, the slopes of the regression lines between observed and simulated values were not significantly different from 1 (*t*-test, *p-value* > 0.05). The simulated length trajectory followed closely the observed values at Lilleau ($r^2 = 0.89$) and lay within standard deviation range (Fig. 2.6 A). Condition index was well explained by the model ($r^2 = 0.72$) and the weight simulation was better explained than in the Nole validation simulation ($r^2 = 0.77$). Like the Nole simulation, the first gamete emissions were simulated at the end of the spring (day 144, late May) and continued during the summer. The simulated

principal spawning occured at day 227 (mid August), which was consistent with the observation of Laruelle (1999) and Calvez (2003) for the coast of Brittany, France. In early summer, many (8) partial spawnings are simulated which are not described in the field dataset of Goulletquer (1989a), thus resulting in underestimates of both weight and length growth. Dates of these partial spawnings are in accordance with Laruelle (1999) and Calvez (2003) observations. A simulated late spawning event occured at day 285 (mid October). This gamete release event was noted in the field data set of Goulletquer (1989a) who emphasized that at Lilleau station the reproduction effort was higher than at Nole, which is consistent with the model simulation.

2.4 Discussion

Shell growth

An important and original aspect of this model, which is derived from the Hofmann et al. (2006) hard clam growth model, compared to other individual growth models based on the Scope For Growth concept (e.g. Barillé et al., 1997; Grant and Bacher, 1998; Pouvreau et al., 2000; Hawkins et al., 2002; Gangnery et al., 2003; Fréchette et al., 2005), is that condition index drives both net production division and length growth. In most scope for growth models of bivalves, length is calculated from weight through an allometric equation. In present study weight and length are two state variables independently calculated. Such a formulation for the Manila clam allowed uncoupling of length growth increments and weight growth increments. This is in agreement with observations of Lewis and Cerrato (1997) on *Mya arenaria*, which showed that shell growth could be uncoupled from somatic growth. Simulations were in a very good agreement with field data as the coefficient of correlation values were very high ($r^2 = 0.89$ at Lilleau and $r^2 = 0.95$ at Nole). This formulation also allowed our model to simulate post-spawning shell growth stops, which were shown by Garcia (1993) in *R. decussatus*.

Weight, condition index and reproductive patterns

For both Nole and Lilleau sites, the simulated reproductive pattern deviated somewhat from field observations. The aim of most studies on growth of *R. philippinarum* is to assess the best cultivation strategy for maximizing growth. Most often, authors monitor the evolution of biological variables (length, weight and condition index are among the most common) of a set of homogeneously sized individuals (i.e. a cohort – Maître-Allain, 1982; Bodoy et al., 1980;

Goulletquer et al., 1987; Goulletquer, 1989a; Robert et al., 1993). On each sampling occasion, all individuals in the sample are sacrified to assess those variables and an average length, weight or condition index is calculated. Using such a method, one obtains the trajectory of the average weight, length and condition index of a cohort through time. It is often said to be the trajectory of an "average individual" (i.e. an individual that has average physiological features), although no real individual trajectories are involved in such a data set.

The occurrence of asynchronous events, like partial spawnings, may induce a difference between the trajectory of an "average individual" and the trajectory of the average of a cohort. In order to explain this difference, two theoretical cases are hypothesized both of which lead to the same average–cohort–weight time series (Fig. 2.7).
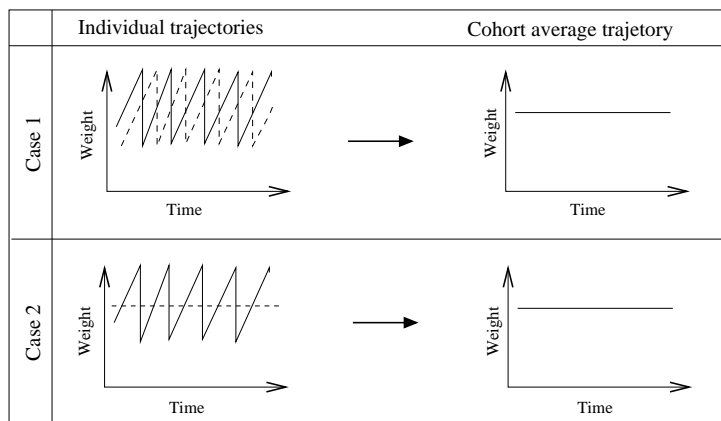
FIG. 2.7: Two hypothetical cases of the inter-individual variability of spawning strategy in a cohort. Case 1: the cohort is composed of individuals presenting similar spawning efforts, with each individual spawning four times, but not simultaneously. The individual trajectories graph shows the evolution of weights of two individuals (continuous and dotted lines). Case 2 : the cohort is composed of individuals presenting different spawning strategies. One class of individuals spawns four times (continuous line in individual trajectories) and the other doesn't spawn at all (dotted lines in individual trajectories). In both cases, because of the asynchronous spawnings, the average weight of the cohort may remain constant.

- Case 1 is a situation where all individuals of the cohort have the same spawning behaviour: each individual spawns with a high frequency, as shown by the individual weight trajectories. If these spawnings don't occur simultaneously in all the individuals of the cohort, the average weight of the cohort may remain constant.

- Case 2 is a situation where the cohort is composed of two kinds of individuals: some of them spawn with a high frequency and the other ones don't spawn at all. As in case 1, if spawnings, when they occur, are not synchronous, the average weight of the cohort may also remain constant.

In both cases, one may obtain the same evolution of average weight; however, the weight variance will be higher in case 1. It is impossible, however, to make assumptions about the behavior of individuals and to distinguish between the two cases just by examining the mean and variance of the weight of the cohort. Processes of reproduction in bivalves are much more complex than these two examples; however, these two theoretical cases illustrate that if asynchronous events occur in a cohort, the average trajectory of the cohort doesn't allow any assumption about individual behavior.

Consequently, simulations of individual variables cannot easily be compared to observed data when asynchronous events occur within a cohort. Trying to fit a model simulating the evolution of mean weight of the cohort when asynchronous partial spawning events occur would not include these events thus resulting in a large underestimate of the reproductive output because it does not take into account the peak reproductive output of individuals clams. In such a case, a high value of the coefficient of correlation (i.e. tending toward 1) between simulated and field data may actually reveal a poor representation of individual behavior. This points out (1) the difficulty of comparing modeled to observed data during the reproductive season and (2) the difficulty of evaluating quantitatively the reproductive output of an "average individual".

For all these reasons, deviations of the model from observed weight and condition index values during the gamete-emission season appear relevant: they explain the lower values of the coefficients of determination obtained for weight and condition index in the validation simulations at Nole ($r^2 = 0.64$ and 0.77, respectively) and at Lilleau ($r^2 = 0.77$ and 0.71, respectively); they also explain the weak value of the slope of regression line between observed and modeled condition index at Nole. During the spawning season, goodness of fit of the simulated weight and condition index can't be validated: poor fit could be attributed to both (1) high variability among individual weights and condition indexes or (2) poor model representation of the individual energy

balance. Thus the model should be validated outside of the reproductive season. When excluding the main spawning season (i.e. from mid May to mid September), simulations of both variables were very close to the observed data; coefficients of determination calculated for weight were higher ($r^2 = 0.86$ at Nole and 0.84 at Lilleau) and the slopes of the regression lines between observed and simulated values were not significantly different from 1 (*t*-test, *p-value* > 0.05) for all state variables. This indicates that our model properly estimates the Manila clam energy balance under forcing by temperature and trophic resource.

Several population dynamics models have been built for bivalves, which use bioenergetic equations to simulate bivalves standing stock transfers among size classes (Powell et al., 1992; Hofmann et al., 1992). They are not individually based. This strategy allows a direct comparison between the model outputs and the experimental data means. Nevertheless, the present study clearly shows that observation at the cohort (or the population) scale may hide some individual–scale processes. As individuals can be considered the basic entity of populations (Kooijman, 1995), the individual–scale processes influence populations processes. This problem of scale transfer was emphasized by Kooijman (1995). The Manila clam model has been developed in order to build a population dynamics, individual-based model following that developed by Hofmann et al. (2006) for *Mercenaria mercenaria*. This strategy permits accounting for the influence of individual–scale processes at the population level.

Trophic resource

The problem of estimating food resources available to suspension feeding bivalves is well known and recognized as a major problem in modelling bivalve energetics (see e.g. Bayne, 1998; Grant and Bacher, 1998). The Manila clam uses food resources available at the sediment-water interface, and may have a very complex diet : it is known for filtering prey items as diverse as bacteria, picocyanobacteria (Nakamura, 2001) and diatoms, as well as detritic particulate organic matter and small rotifers (Sorokin and Giovanardi, 1995) from the water column and the sediment surface. The Manila clam has also been described as ingesting toxic and non toxic dinoflagellates by Li and Wang (2001). Moreover, growth of microphytobenthos is very effective on the Marennes–Oléron mudflats (Guarini et al., 2000), and was shown to be an important food source for oysters *Crassostrea gigas* (Riera and Richard, 1996) once resuspended by tidal currents (Blanchard et al., 1998, 2001). In such mudflats, we can hypothesize that microphytobenthos is an important food source for near-

bottom suspension-feeding bivalves such as *R. philippinarum*. Fegley et al. (1992) have shown that short-term variability in the quantity and nutritional quality of food items available to intertidal near-bottom suspension feeders like *R. philippinarum* may be of particular importance for assessing their growth and reproduction.

Insufficient information is available concerning these diverse potential food sources and the associated variability of feeding rate for them to be considered in our study. We used a classical and simple proxy ($Chla$), which represents a rough estimate of the food input ($Chla \times C2F$) for clams exhibiting such a complex diet. Following Grant and Bacher (1998) with *Mytilus edulis*, our simulations demonstrate that simple formulation of food and feeding may suffice in predicting Manila clam energetics. A careful study of the clam diet, using carbon and nitrogen isotope ratios (Kasai et al., 2004) and pigment analysis of bottom interface water POM, should improve our knowledge.

2.5   Conclusion

Despite the difficulty of comparing field–averaged data sets to model outputs, simulation of growth and reproduction for an "average" individual clam under natural food and temperature gave realistic results. The model can be used to predict length and weight growth as well as gamete production of Manila clams in temperate ecosystems. Further work will focus on modelling interactions between environment, host and pathogen using our results, which provide the environment–clam coupling.

Acknowledgements

Chapter 3

A model of interactions between environment, host and pathogen

Abstract

The aim of this chapter is to describe briefly the construction of a model describing the environment-host-pathogen relationships in Brown Ring Disease and to show few simulations.

The host part of the model has been described in the previous chapter (Chap. 2, Flye-Sainte-Marie et al., 2007a) and allows to simulate evolution of length, weight and condition index over time under forcing of temperature and trophic resource. The *Vibrio* population is represented by an exponential growth model where growth and mortality rates are controlled by temperature. Its presence induces the development of symptoms. All host defence processes against the pathogen are positively controlled by temperature, the main environmental factor controlling BRD development, and under control of condition index, which allows to link host and pathogen models. This linkage results from the assumption that the energy status may control both disease susceptibility and recovery ability. The defence system against the pathogen comprises two variables: (1) the hemocyte concentration and its phagocytosis activity, which is positively related to the condition index and is negatively related to the *Vibrio* concentration, and (2) the recalcification processes that allow the recovery from the symptomatic brown deposit and is also positively related to the condition index. The presence of *Vibrio* induces the development of symptoms.

The individual environment-host-pathogen model was used as a base for the construction of a population model. By varying values of key parameters (assimilation rate, phagocytosis rate and recalcification rate) it was possible to simulate individuals that differ phenotypically in their capacity to recover from the disease. A combination of three specific parameters was attributed to each individual following a theoretical distribution. Thus, rather than tracking a 'standard' host this model simulates host-parasite interactions for individuals with different phenotypes.

Individual simulations showed that individuals with high values for the

three considered phenotypes fully recover after developing few symptoms, whereas individuals with low values do not recover. Thus phenotypic variability for these three functions can provide a potential explanation for the observed variability in disease susceptibility and recovery capacity. Nevertheless, the model seems to underestimate the speed of the dynamics of the disease development and of the recovery process.

Although calibration of the model needs more refinement, the population model simulation reproduces reasonably well the observed seasonal pattern of BRD intensity in the Gulf of Morbihan: an increase of symptom intensity in autumn and a decrease during the spring to reach a minimum in September.

Avant-propos

Le travail présenté dans ce chapitre est le fruit d'une collaboration ayant eu lieu dans le cadre d'un projet de coopération CNRS/NSF impliquant les auteurs suivants : Christine PAILLARD, Susan FORD, Eric POWELL, Jonathan FLYE-SAINTE-MARIE, Frédéric JEAN, John KLINCK et Eileen HOFMANN. L'article ci-dessous, en préparation, détaille précisément la construction et la formulation de de ce modèle.

A theoretical individual based model of Brown Ring Disease in Manila clams, *Ruditapes philippinarum*.

Ce chapitre ne vise en aucun cas à présenter de façon exhaustive la formulation de ce modèle, il a pour objectif de présenter les concepts sous–jasent et les grandes lignes de sa construction. Il présentera et discutera quelques simulations obtenues à partir de ce modèle.

3.1   Introduction

Dans les années 1990, plusieurs modèles décrivant les interactions hôte-parasite chez des bivalves marins ont été proposés. Un modèle d'interaction entre l'huître *Crassotrea virginica* et le protozoaire pathogène *Perkinus marinus* a été publié (Powell *et al.*, 1994; Hofmann *et al.*, 1995; Powell *et al.*, 1996). Plus récemment, des approches en modélisation ont été proposées afin de décrire l'infection par le protozoaire *Haplosporidium nelsoni* chez l'huître *C. virginica* (Ford *et al.*, 1999; Paraso *et al.*, 1999; Powell *et al.*, 1999; Hofmann *et al.*, 2001). Ces deux protozoaires parasites se développent au sein des tissus

de l'hôte, l'infection pouvant atteindre un stade létal. Par contre, la bactérie *V. tapetis*, agent pathogène de la Maladie de l'Anneau Brun, est un pathogène externe qui adhère à la lame périostracale puis pénètre dans les compartiments extrapalléaux dans lesquels il prolifère (Paillard et Maes, 1995a).

Le modèle individuel de croissance de la palourde détaillé dans le chapitre précédent (Flye-Sainte-Marie *et al.*, 2007a) a été utilisé afin de formuler la partie hôte d'un modèle d'interaction environnement–hôte–pathogène. Bien que certains des concepts de base des modèles précédents aient été appliqués à la construction de ce modèle, il diffère de ces derniers en plusieurs points. À la différence des modèles cités précédemment, celui-ci simule les interactions hôte–pathogène pour des individus variables d'un point de vue phénotypique. Par ailleurs, l'intensité de la maladie n'est ici pas mesurée en termes de charge parasitaire, mais par le développement et l'intensité du symptôme majeur : le dépôt brun (Paillard *et al.*, 1994). Enfin, une des originalités de ce modèle est qu'il explicite en tant que variables d'état la population et l'activité de phagocytose des hémocytes qui semblent jouer un rôle majeur dans l'élimination du pathogène (Allam *et al.*, 2001).

3.1.1   Développement de MAB et variabilité inter–individuelle

Les principales étapes du développement de la Maladie de l'Anneau Brun ont été développées dans la section 1.2. *Vibrio tapetis* colonise dans un premier temps la lame périostracale (Paillard et Maes, 1995a). S'il y a rupture de la lame périostracale, il pénètre dans les sinus extrapalléaux dans lesquels il prolifère (Allam, 1998). Sa présence perturbe la formation de la lame périostracale, induisant de ce fait une déposition de conchioline sur la face interne de la coquille (Paillard *et al.*, 1994). La présence du dépôt brun n'est pas considérée comme étant une cause de mortalité hormis dans les stades (CDS) les plus avancés. Il semble que les mortalités soient généralement associées à une septicémie ; celle–ci pourrait avoir lieu si *V. tapetis* pénètre dans le compartiment extrapalléal central (Paillard, 2004a) ou lorsqu'il pénètre dans les tissus et y prolifère (Allam *et al.*, 2002c).

Deux processus permettant la guérison des palourdes ont été décrits. Le premier est un contrôle de la prolifération de *V. tapetis* qui met en jeu les hémocytes, capables de phagocyter la bactérie, et les enzymes antibactérien tels que le lysozyme, qui sont à la fois présents dans les fluides extrapalléaux et dans l'hémolymphe (Allam et Paillard, 1998; Allam *et al.*, 2000b). Une activité de phagocytose plus élevée a été associée à une résistance aux contaminations expérimentales (Allam *et al.*, 2001). Le second processus est une déposition de carbonate de calcium sur les couches symptomatiques de conchioline, qui

séquestrerait les bactéries sous les couches coquillères néoformées (Paillard et Maes, 1994).

Le diagramme présenté dans la Fig. 3.1 présente une approche conceptuelle synthétique du développement de la MAB au niveau individuel. Ce diagramme montre les trajectoires individuelles plausibles dans le plan stade de réparation / stade de maladie. Dans un premier temps, *V. tapetis* colonise la lame périostracale puis il pénètre dans le compartiment extrapalléal externe. Il s'ensuit un développement des symptômes conjointement à une prolifération de la bactérie. C'est alors qu'a lieu une compétition entre la croissance du pathogène et les capacités de défense de l'hôte : les individus capables de lutter efficacement contre la bactérie répareront avant un développement important des symptômes, alors que les individus contrôlant moins efficacement la croissance du pathogène développeront des symptômes plus intenses aboutissant à leur mort. Cette approche sur la variabilité de la capacité à lutter contre le pathogène, permet de fournir une explication au fait que la relation entre la charge en *V. tapetis* dans les fluides extrapalléaux et les symptômes, bien que positive en moyenne, soit hautement variable (Paillard, 2004a).
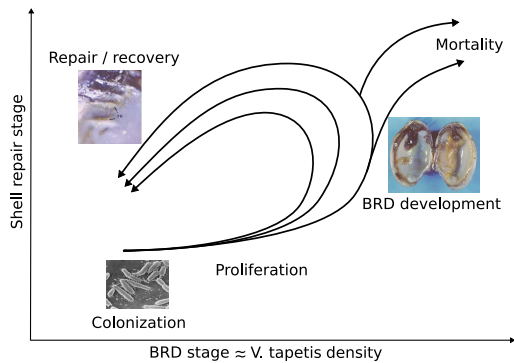
FIG. 3.1: Approche conceptuelle du développement de la Maladie de l'Anneau Brun à l'échelle individuelle. Ce diagramme présente les différentes trajectoires individuelles plausibles dans un plan stade de réparation / stade de maladie.

3.1.2 Objectifs

En synthétisant les données acquises au cours des vingt dernières années de recherche sur la Maladie de l'Anneau Brun, ce modèle a pour but d'une part de proposer une explication à la variabilité de la susceptibilité et de la capacité

à réparer observée chez l'hôte, et d'autre part de comprendre l'influence de l'environnement sur l'interaction *Vibrio*–palourde.

3.2 Fonctionnement du modèle individuel environnement–hôte–pathogène

Le fonctionnement du modèle individuel d'interactions entre l'hôte, son pathogène et l'environnement est illustré par le schéma conceptuel présenté en Fig. 3.2. L'ensemble des équations, non détaillé ici, est issu d'ajustements empiriques dans les données disponibles issues d'études en laboratoire et sur le terrain. Cette démarche permet de calibrer le modèle pour un "individu moyen".
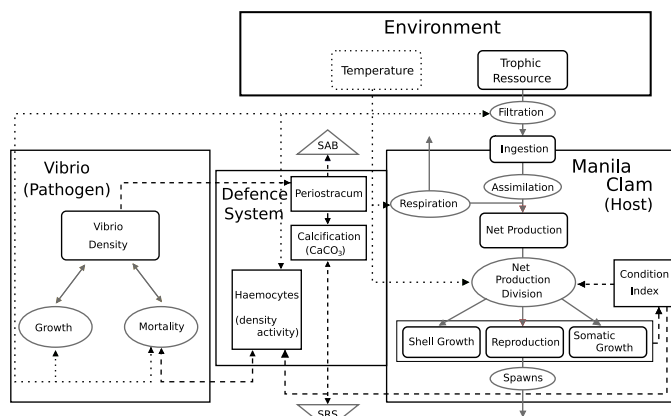
FIG. 3.2: Schéma conceptuel du modèle individuel environnement–palourde–vibrio

Modèle hôte On reconnaît aisément dans la Fig. 3.2 la partie hôte du modèle décrite dans le chapitre précédent (Flye-Sainte-Marie *et al.*, 2007a). Ce modèle vise à simuler la croissance et la reproduction de l'hôte, ainsi que les variations de son indice de condition, attestant de son statut énergétique ; cette variable joue un rôle majeur dans le couplage avec le système immunitaire.

Développement des symptômes et système de défense contre la maladie
La déposition de périostracum est explicite et permet de représenter le déve-

loppement des symptômes (CDS). Le taux de déposition du périostracum est positivement relié à la concentration en *Vibrio*.

L'ensemble des processus de lutte contre la maladie sont sous dépendance de l'indice de condition : en effet Paillard (1992) a observé que les palourdes symptomatiques ont un indice de condition plus faible que les palourdes saines, ce qui peut laisser penser que l'indice de condition contrôle la susceptibilité et la capacité à lutter contre la maladie. Le système de défense contre la maladie comprend deux variables :

1. La concentration hémocytaire, celle–ci est positivement reliée à l'indice de condition et négativement reliée à la concentration en *Vibrio*, car la bactérie est capable de détruire les hémocytes (Allam *et al.*, 2000a). Les variations de l'activité de phagocytose des hémocytes sont aussi prises en compte et sont positivement reliée à la température.

2. La recalcification, représentant la déposition de carbonate de calcium sur le dépôt brun et permettant de représenter les stades de réparation coquillère (SRS). Le taux de recalcification est positivement contrôlé par la quantité de périostracum déposée (CDS) et l'indice de condition.

Le pathogène   La multiplication du pathogène est représenté simplement par un modèle de croissance exponentielle classiquement utilisé pour représenter la croissance des micro–organismes. Le taux de croissance de *Vibrio* est contrôlé par la température : il croît avec la température tant celle-ci est en dessous de l'optimum thermique (25°C) et décroît lorsque ce dernier est dépassé. La croissance de la population bactérienne est contrôlée par un taux de mortalité associé à la concentration en hémocytes et à leur activité de phagocytose. Les températures supérieures à 27°C étant létales pour le *Vibrio* (Maes, 1992), un terme de mortalité thermique a été rajouté et contrôle la croissance de la population bactérienne.

Forçage environnemental   Comme nous l'avons vu dans le chapitre précédent, la ressource trophique disponible influe sur le taux d'ingestion de l'hôte. De même, dans le modèle hôte, la température influence le taux de filtration, le taux de respiration, l'allocation de la production nette ainsi que les pontes. La température contrôle l'activité de phagocytose des hémocytes, ce qui permet d'introduire dans le modèle une dépendance directe entre la capacité à lutter contre le pathogène et la température, comme il a été montré en milieu expérimental (Paillard *et al.*, 2004). Enfin, la température influence le taux de croissance et le taux de mortalité de *V. tapetis*.

3.3   De l'individu à la population : des phénotypes variables

Une population à partir d'un modèle individuel...   Nous venons de voir les relations majeures du modèle pour un "individu moyen", et comment celles-ci sont forcées par l'environnement. La stratégie adoptée pour passer à l'échelle de la population est illustrée dans la Fig. 3.3. Le modèle individuel environnement–hôte–pathogène moyen, permettant de simuler un individu présentant des caractéristiques physiologiques moyennes, a été calibré à partir de relations moyennes issues des données disponibles. Néanmoins, les paramètres sont variables au niveau inter–individuel. En se basant sur une distribution théorique des paramètres d'intérêt, il est possible de construire des modèles individuels dont les valeurs des paramètres sont différentes de celles du modèle individuel moyen, et de représenter ainsi une population dont les individus diffèrent d'un point de vue phénotypique.
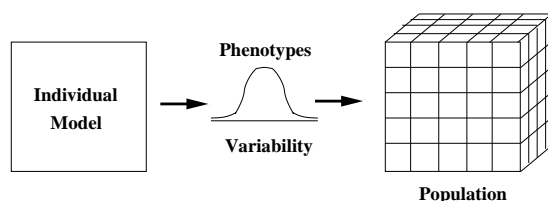
FIG. 3.3: A partir du modèle individuel moyen, différents individus sont individus sont simulés, on attribue à chacun d'entre eux des valeurs de paramètres propres, cette démarche permet de simuler une populations dont les individus diffèrent d'un point de vue phénotypique.

Des phénotypes variables   Ainsi représentée, la variabilité phénotypique a été introduite dans le modèle pour les paramètres susceptibles d'influencer le développement de la maladie :

– Le taux d'assimilation qui contrôle les acquisitions d'énergie et donc indirectement l'indice de condition qui, comme nous l'avons vu, joue un rôle majeur dans le couplage entre le bilan énergétique de l'hôte et son système de défense contre le pathogène.

– Le taux de phagocytose qui contrôle la capacité de l'hôte à éliminer le pathogène.

   – Le taux de recalcification, processus impliqué dans la couverture du dépôt brun symptomatique et qui contrôle par conséquent la capacité de l'individu à récupérer de la maladie.

Pour chaque individu, un coefficient multiplicateur variant de 0.2 à 1.8 est attribué à chacune des valeurs moyennes de ces trois paramètres, permettant ainsi de générer des individus dont les caractéristiques phénotypiques varient entre 20% et 180% par rapport à la valeur moyenne du paramètre considéré. Cette démarche est essentiellement théorique puisque les ordres de grandeur observés de variabilité de ces paramètres n'ont pas été respectés. Par souci de simplification, la distribution des coefficients multiplicateurs a été discrétisée en 9 valeurs comprises entre 0.2 à 1.8. Le modèle peut donc générer $9 \times 9 \times 9 = 729$ individus différents. Dans la population, la distribution de fréquence pour chacun des phénotypes suit une gaussienne, comme indiqué en Fig. 3.4.
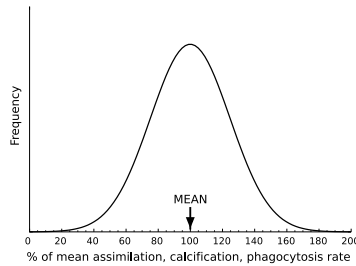
FIG. 3.4: Distribution théorique des phénotypes dans la population modélisée : les phénotypes varient entre 20% et 180% de la valeur moyenne du paramètre considéré (Taux d'assimilation, taux de phagocytose, taux de calcification). La fréquence des phénotypes est distribuée selon une gaussienne.

La Fig. 3.5 illustre cette variabilité pour deux phénotypes considérés dans le modèle et leurs conséquences. La Fig. 3.5 (A) montre la relation entre le temps de demi–vie du *Vibrio* et l'indice de condition pour des individus dont le taux de phagocytose varie. Lorsque l'indice de condition est faible, le temps d'élimination du *Vibrio* par les hémocytes est long (le temps de demi–vie du *Vibrio* augmente) lorsque le phénotype "phagocytose" est faible (LOW) ; inversement si le phénotype "phagocytose" est élevé (HIGH) le *Vibrio* est éliminé plus rapidement. Aux forts indices de condition, la différence entre phénotypes faible et fort est moindre. La Fig. 3.5 (B) montre l'influence de la variabilité du taux de calcification sur la relation entre calcification et la couverture en

périostracum symptomatique. Sans surprise, lorsque le phénotype "calcification" est élevé, la déposition de carbonate de calcium sur le dépôt brun est plus rapide et inversement.
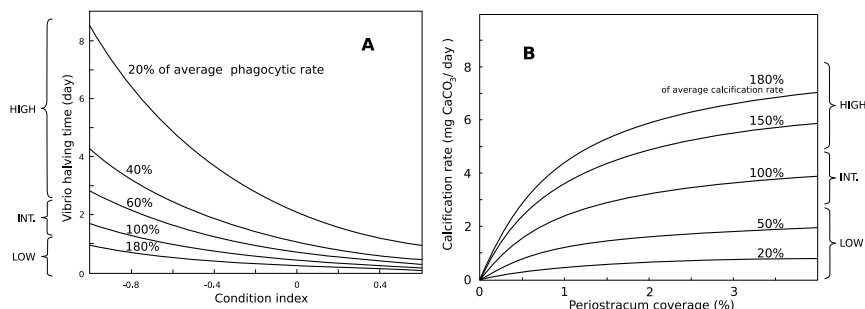
FIG. 3.5: Deux exemples de variabilité phénotypique et de leurs conséquences. A : Influence de la variabilité du taux de phagocytose sur la relation entre la vitesse d'élimination de *V. tapetis* et l'indice de condition. L'indice de condition présenté ici n'est pas l'indice de condition classiquement calculé mais l'indice de condition du modèle présenté dans le chapitre précédent (Chap. 2, section 2.2.3). B. Influence de la variabilité du taux de calcification sur la relation entre la couverture en périostracum et le taux de calcification.

3.4   Simulations

3.4.1   Exemple de conséquences de la variabilité des phénotypes sur le développement de la maldie

La Fig. 3.6 montre des simulations de la relation entre stade de maladie (CDS) et stade de réparation (SRS) pour des individus présentant des caractéristiques phénotypiques variables, au cours d'une période de 5 ans. L'infection n'a lieu que lors de la deuxième année de simulation afin d'éviter pour éviter les artefacts liés aux conditions initiales des variables d'état. Pour un individu présentant des caractéristiques moyennes pour les trois phénotypes considérés (taux d'assimilation, de phagocytose et de recalcification), le modèle simule une réparation complète (SRS=3) après un développement modéré des symptômes dont le stade (CDS) n'excède pas 5 (Fig. 3.6 B). Plusieurs cycles de développement/réparation de la maladie sont simulés. Pour un individu présentant des caractéristiques élevées pour les trois phénotypes considérés, le

modèle simule une réparation après un fable développement des symptômes qui n'excèdent pas le stade 3 (Fig. 3.6 A), plusieurs cycles de développement et réparation sont aussi simulés et la simulation se termine par une réparation complète. Par contre, pour un individu présentant des caractéristiques faibles pour les trois phénotypes considérés, aucune réparation des symptômes n'est simulée et le modèle simule un développement sévère des symptômes qui dépassent le stade 6 au cours de la cinquième année de simulation (Fig. 3.6 C).

Ces différentes simulations (Fig. 3.6) des trajectoires individuelles dans le plan stade de maladie/stade de réparation peuvent être mises en parallèle avec l'approche conceptuelle présentée dans la Fig. 3.1. Cette approche indique que la variabilité inter-individuelle des fonctions supposées critiques pour le développement de la maladies permet de fournir une explication potentielle à la variabilité observée dans le développement et la réparation de la maladie.

Néanmoins, il semble que la dynamique temporelle simulée du développement de la maladie et de la réparation soit peu réaliste. En effet, pour un individu présentant des caractéristiques phénotypiques moyennes, le modèle ne simule un cycle de développement et de réparation complète de la maladie qu'à partir de la troisième année, soit deux ans après le début de l'infection. L'individu simulé présentant des caractéristiques phénotypiques faibles ne dépasse le stade CDS 6 qu'après la quatrième année de simulation, soit trois ans après le début de l'infection. Peu de données sont disponibles concernant la dynamique de la maladie à l'échelle individuelle, néanmoins les infections expérimentales réalisée par Paillard *et al.* (2004) montrent qu'une réparation complète peut avoir lieu en un mois dans des condition favorables de température (21°C) suggérant une dynamique plus rapide que celle simulée par le modèle.

3.4.2   Simulation de la variabilité saisonnière de l'intensité de la maladie

La Fig. 3.7 (A) montre l'évolution saisonnière de l'intensité des symptômes chez les palourdes symptomatiques dans un semis expérimental effectué sur l'île de Bailleron en 1998 (Golfe du Morbihan, France). Au cours de cette expérimentation, deux maxima d'intensité de la maladie ont été observés : le premier en période hivernale et au début du printemps et le second en fin d'automne et en période hivernale. La décroissance de l'intensité des symptômes entre le premier maximum hivernal et le minimum estival peut être associé à la fois à une guérison de la maladie et à une mortalité des palourdes les plus affectées. La Fig. 3.7 B montre que le modèle simule une augmentation de l'intensité des symptômes au cours de l'automne et simule un maximum hivernal.
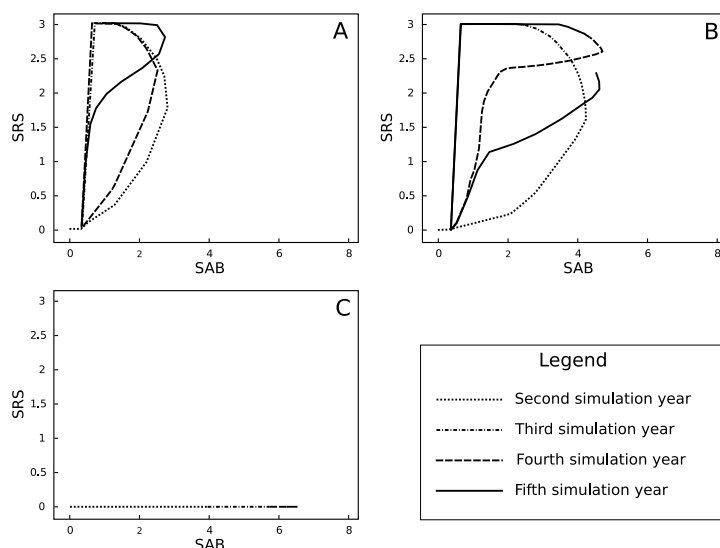
FIG. 3.6: Simulations de la relation entre stade de réparation (SRS) et stade de maladie pour des phénotypes variables, au cours d'une période de 5 ans. Le départ de l'infection par *Vibrio* n'est simulée qu'au début de la 2ème année, la 1ère année n'est donc pas visible sur les graphes. Les données environnementales (température et chlorophylle *a*) proviennent de la Rade de Brest en 1998 (Données SOMLIT). A : Simulation pour un individus présentant des caractéristiques élevées (180%) pour chacun des phénotypes. B : Simulation pour un individus présentant des caractéristiques moyennes (10%) pour chacun des phénotypes. C : Simulation pour un individus présentant des caractéristiques faibles (20%) pour chacun des phénotypes.

Il simule aussi un minimum estival légèrement décalé par rapport aux observations. Le modèle reproduit donc de façon raisonnable l'évolution saisonnière observée de l'intensité de la maladie ; néanmoins au cours de la période estivale le modèle surestime la proportion de palourde présentant des stades de développement intenses des symptômes.

3.5 Conclusion

Le développement du modèle présenté dans ce chapitre a permis de faire une synthèse des connaissances acquises sur les relation entre l'environnement,

la physiologie de l'hôte et l'infection par *V. tapetis*. Comme dans tout modèle, un certain nombre d'hypothèses de fonctionnement ont été faites, la principale étant de lier le développement et la susceptibilité de la maladie à l'état énergétique de l'hôte au travers de l'indice de condition. Ce modèle permet de simuler une population composée d'individus présentant des caractéristiques phénotypiques variables pour des processus supposés critiques (assimilation, phagocytose et recalcification) dans le développement de la maladie. Les simulations individuelles montrent que la variabilité de ces fonctions peut fournir une explication potentielle à la variabilité inter-individuelle observée du développement de la maladie. Ce modèle reproduit aussi de façon raisonnable l'évolution saisonnière observée de l'intensité des symptômes. Ce travail montre aussi le besoin de mieux comprendre la dynamique de la maladie à l'échelle individuelle. Par ailleurs certaines hypothèses formulées lors de la construction de ce modèle doivent être validées par des observations en milieu naturel. C'est précisément dans cet objectif qu'a été mené le travail de terrain exposé dans la partie II.
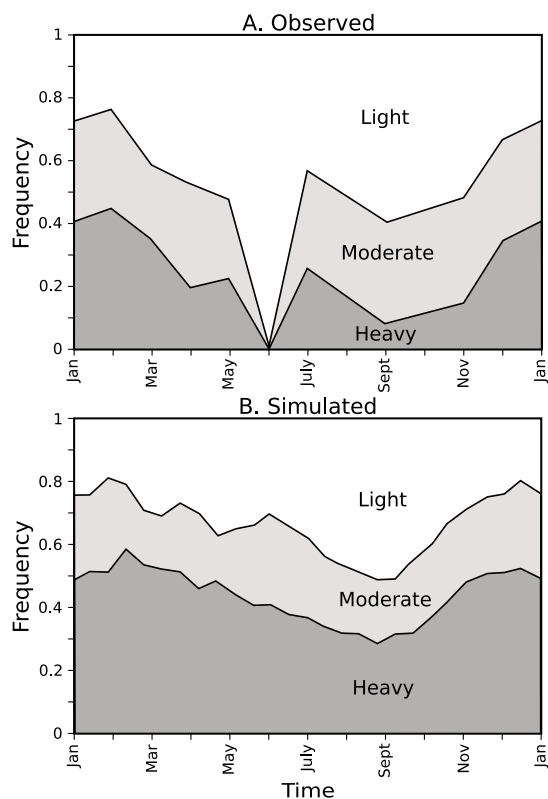
FIG. 3.7: Evolution saisonnière de l'intensité des symptômes de la MAB observée (A) et simulée (B) chez les palourdes symptomatiques uniquement. Ligh : CDS 1 & 2, Moderate : CDS 3 et Heavy : CDS4–7. Les données de terrain proviennent d'un semis effectué dans le Golfe du Morbihan en 1998. Les données environnementales utilisées pour la simulation (température et chlorophylle *a*) proviennent de la Rade de Brest en 1998 (Données SOMLIT).

Part II

What is going on in the field?

Chapter 4

Seasonal variations of hemocyte parameters in the field

Variability of the hemocyte parameters of *Ruditapes philippinarum* in the field during an annual cycle.

in prep.

Jonathan FLYE-SAINTE-MARIE, Philippe SOUDANT, Christophe LAMBERT, Nelly LE GOIC, Madeleine GONÇALVEZ, Marie–Agnès TRAVERS, Christine PAILLARD, Fred JEAN.

Abstract

Field monitoring of hemocyte parameters of the Manila clam, *Ruditapes philippinarum*, was conduced in the Gulf of Morbihan (Brittany, France), a site moderately affected by Brown Ring Disease and perkinsosis. The aims of this study were (1) to assess factors controlling the hemocyte parameters of the Manila clam and (2) to assess their relative contribution to the overall variability of these parameters. From July 2004 to September 2005, sixty clams ranging from 20 to 50 mm in length were sampled monthly. On each individual, Total Hemocyte Count (THC), granulocyte and hyalinocyte counts, phagocytosis, phenoloxidase activity, length, flesh dry weight, and condition index were measured. *Perkinus olseni* infection and Brown Ring Disease symptoms were also monitored as well as temperature and the trophic resource.

All hemocyte parameters significantly varied according to the sampling date. Results indicate that temperature controls granulocyte count and subsequently THC. The effect of salinity was unclear and the trophic resource had no direct influence on the measured hemocyte parameters. Almost all parameters measured were significantly affected by size/age. Independently of season, all hemocyte counts were lowly, but significantly, related to the condition index. For both pathologies there was no clear seasonal pattern, prevalence was moderated (<50% for perkinsosis, and <10% for BRD) and highly correlated to size. There were poor relationships between pathologies and hemocyte parameters presumably because of low infection intensities. Nevertheless, high *P.*

olseni infection intensity significantly increased total and granulocyte counts and decreased phagocytosis.

An interesting result of this study is that the measured biotic and abiotic factors poorly contribute to the explanation of the total variability of hemocyte parameters. Granulocyte concentration was the best explained parameter. However, only 16.4% of its variance was explained by cumulating temperature, length, condition index and *P. olseni* infection effects. This study emphasizes the need for a better understanding of hemocyte functions and the factors modulating these functions.

Keywords: Hemocyte parameters; Environmental factors; Variability; Manila clam; Brown Ring Disease; *Perkinsus* .

4.1   Introduction

The Manila clam *Ruditapes* (=*Tapes*, =*Venerupis*) *philippinarum* is one of the most extensively cultivated bivalve molluscs. This species was originally endemic to Indo-Pacific waters and its high adaptive capacity to various rearing environments made of it a target species for aquaculture. In Europe, this species was first introduced in France between 1972 and 1975 for aquaculture purposes and later in England, Spain and Italy (Flassch and Leborgne, 1992). In the late 1980s, natural populations have developed in Italy (Marin et al., 2003), and England (Jensen et al., 2004; Humphreys et al., 2007) as well as in most embayments along the French Atlantic coast, resulting in a fishery of ca. 1500 tons in the Gulf of Morbihan at the end of the 1990s. This species is mainly affected by two pathologies: Brown Ring Disease (BRD) and Perkinsosis (see *e.g.* Paillard, 2004b; Villalba et al., 2004). Brown ring disease is caused by the bacterium *Vibrio tapetis* (Paillard and Maes, 1990; Borrego et al., 1996b) which disrupts the production of the periostracal lamina and causes an anomalous deposition of periostracum on the inner shell (Paillard and Maes, 1995a,b). Perkinsosis is induced by the protozoan parasite *P. olseni* and can affect both *Ruditapes decussatus* and *R. philippinarum* (see Villalba et al., 2004, for a review). Both pathologies can interfere with the host energy balance (Ngo and Choi, 2004; Park et al., 2006a; Leite et al., 2004; Flye-Sainte-Marie et al., 2007b) and can be responsible for mass mortalities (see *e.g.* Paillard et al., 1989; Castro et al., 1992; Paillard, 1992, 2004b; Villalba et al., 2005, 2004). Epidemiological surveys also indicated that both pathologies are influenced by environment factors (Paillard et al., 1997; Villalba et al., 2005). Different laboratory experiments have been performed to assess the effect of environmental

factors (temperature and salinity) on cellular-defence related parameters (Reid et al., 2003; Paillard et al., 2004) linked with pathologies and few field studies assessed the seasonal variation of these parameters (Matozzo et al., 2003; Soudant et al., 2004). Collection of field data is needed to better understand the relationships between environmental factors, defence–related parameters physiological status and disease development.

Mainly as a result of aquaculture and fisheries industry and associated disease events, the hemocyte system, thought to be involved in immune response of bivalves, was extensively studied during the past 30 years. More recently appeared the interest in using bivalve hemocyte parameters as biomarkers for environmental perturbations. Numbers of studies allowed to show that hemocyte parameters are controlled by numerous factors either environmental (temperature and salinity), parasitic and internal (reproduction; see review in Chu, 2000). These factors may contribute to explain the high degree of variability of the hemocyte response and activities which has been reported only in few studies (see *e.g.* Ashton-Alcox and Ford, 1998; Ford and Paillard, 2007). To better understand the linkage between environment, host physiology and disease development, the relative contribution of biotic and abiotic factors to the overall variability of hemocyte parameters in the field is a key question and remains poorly known.

A multiparametric study was designed to assess the relative effect of environmental and internal factors and diseases on hemocyte parameters in the field. The Gulf of Morbihan is one of the largest Manila clam fisheries of Brittany. Information on the physiology and reproduction of the Manila clam of Gulf of Morbihan is available (Calvez, 2003; Laruelle et al., 1994; Laruelle, 1999). Manila clam population from this site is known to be moderately affected by both BRD and perkinsosis (Paillard et al., 1997; Paillard, 2004a,b; Lassalle et al., 2007). Seasonal variations were taken in account by monthly sampling over a one year period. Flow cytometry methods were applied to determine hemocyte counts, viability and phagocytosis activity.

4.2 Materials and methods

4.2.1 Clam sampling

From July 2004 to September 2005, 60 *R. philippinarum* ranging from 20 mm to 50 mm were monthly sampled at low tide from the natural clam bed of Bailleron island in Gulf of Morbihan in southern Brittany, France (Fig. 5.1). Clams were stored in an isolated container until processing in the laboratory. During this period, a total of 1020 individuals was sampled from 17 sampling
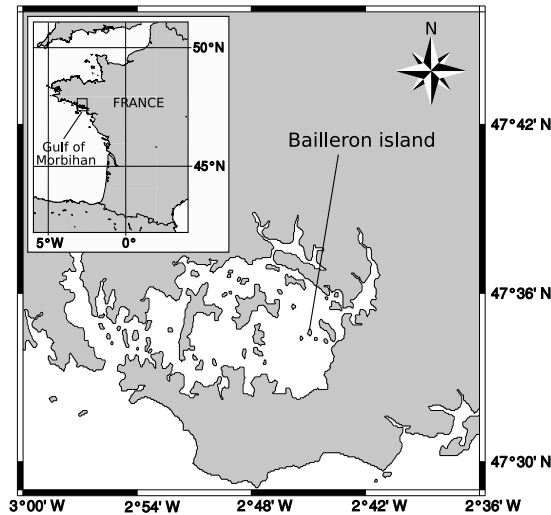
FIG. 4.1: Location of Bailleron island in Gulf of Morbihan, Southern Brittany, France.

dates. At each sampling date, the 60 clams were processed individually according to the protocol that follows.

4.2.2   Analysis of hemocyte parameters by flow cytometry

Hemolymph sampling

A minimum of $450\,\mu$L of hemolymph was withdrawn from the adductor muscle of each clam using a 1 mL plastic syringe fitted to a 25-gauge needle and observed under the microscope to control the sample quality. Hemolymph was filtered through a $80\,\mu m$ mesh in order to eliminate large debris and stored individually in 1.5 mL micro–tubes kept on ice.

Instrumentation

Analysis of hemocyte parameters was performed using a FACScalibur flow cytometer (Becton-Dickinson, San Diego, CA, USA) equipped with a 488 nm argon laser. The light scattered by particles indicated (1) their size through the FSC sensor (Forward SCatter height) and (2) their internal complexity through

the SSC sensor (Side SCatter height). The flow cytometer is equipped with three specific fluorescence sensors: FL1 (green, 500-530 nm), FL2 (orange, 550-600 nm) and FL3 (red, >630 nm) allowing the detection of autofluorescence or fluorescent dyes.

Hemocyte viability, Total and Differential Hemocyte Counts (THC and DHC)

These parameters were measured following the protocol developed by Delaporte et al. (2003). Briefly, $100\,\mu$L of hemolymph from each individual was added to a tube containing $200\,\mu$L of anti-aggregant solution for bivalves (AASH; Auffret and Oubella, 1994) and $100\,\mu$L of filtered sterile seawater (FSSW). Samples were incubated 2 h at 18°C in the dark with $4\,\mu$L of SYBR Green working solution (obtained by diluting 10 x the commercial solution; Molecular probes, Oregon, USA) and propidium iodide (PI, Sigma) at a final concentration of $10\,\mu$g mL^{-1}. Live and dead cells are stained by SYBR Green; whereas, dead cells are only stained by PI. SYBR Green fluorescence is detected by the FL1 detector, and PI fluorescence by the FL3 detector. By using a density plot visualisation of FL1 vs FL3, it was possible to estimate precisely the percentage of dead cells in each sample.

A density plot visualisation of SSC vs FL1 allowed differentiation and gating of hemocytes stained by SYBR green from other particles in the hemolymph. This allowed to calculate THC by taking into account the flow rate of the cytometer calculated according to the method of (Marie et al., 1999).

Similarly to Allam et al. (2002a), two distinct sub-populations could be identified on a FSC vs SSC density plot: granulocytes (high SSC and high FSC), hyalinocytes (low SSC and high FSC). Results of THC, granulocyte and hyalinocyte counts are expressed as number of cells per mL of hemolymph.

Phagocytosis assays

Phagocytic activity of hemocytes was measured following the protocol described in Delaporte et al. (2003) using 2 μm diameter latex fluorescent beads (fluoresbrite microspheres YG 2.0 microns, polysciences, Eppelheim, Germany). A 150 μL sub-sample of hemolymph, diluted with 150 μL of FSSW, was brought in contact with 30 μL of the working solution of fluorescent beads (obtained by diluting 50 x the commercial solution) in micro–tubes. Tubes were incubated for 2 h at 18°C in the dark. Analysis by flow cytometry allowed to detect hemocytes containing fluorescent beads. The phagocytic activity of hemocytes was calculated as the percentage of hemocytes that have ingested

three fluorescent beads or more.

Phenoloxidase activity

Ninety-six-well plates containing 100 μL hemolymph samples were thawed and phenoloxidase activity measured as described by Reid et al. (2003). Briefly, 50 μL of Tris–HCl buffer (0.2 M, pH = 8) with 100 μL of L–DOPA (20 mM, L-3,4-dihydrophenyl-alanine, Sigma D9628) were added to each well. The microplate was rapidly mixed for 10 s. The reaction was then measured at ambient temperature with colour change recorded every 5 min, at 492 nm, over a period of 1 h. The microplate was mixed again prior to each measurement. Controls, without hemolymph, but containing L–DOPA and Tris–SDS buffer, were run in parallel and the values subtracted from test values to correct for possible auto-oxidation of L-DOPA. Total soluble protein concentration was measured following the protocol described in Ford and Paillard (2007). Briefly, thawed 5-mL hemolymph samples were placed in ninety-six-well microtiter plates, one clam per well. Total soluble protein was measured spectrophotometrically at 595 nm using the method of Bradford (1976), modified for small volumes (micromethod of BioRad, Hercules, CA, USA) and standardized against bovine serum albumin (BSA).

Results of the specific PO activity were expressed as arbitrary units : 1 A.U. = Δ DO$_{490\,nm}$ min^{-1} mg protein^{-1}.

4.2.3 Diseases

Detection and quantification of <u>Perkinsus olseni</u> infection

Detection and quantification of *P. olseni* were performed in gills since Choi et al. (2002) showed that the total number of *P. olseni* cells in the whole clams is linearly correlated with the number of *Perkinsus* cells in the gill tissue. After hemolymph sampling, clams were opened using a scalpel, gills were dissected and wet weighted. *P. olseni* presence and infection intensity in the gills were assessed according to the quantitative method of Ray (1966) and modified by Choi et al. (1989). Gills of individual clams incubated in 10 mL of fluid thioglycollate medium (FTM, Difco) supplemented with 67 μg of streptomycin (Sigma) and 32 μg of penicilin G (Sigma) dissolved in 100 μL in distilled water to limit bacterial growth. Vials were incubated at room temperature over one week in the dark. *Perkinsus* cells were counted after dissolving the FTM cultivated clam gills with 2 M NaOH according to Choi et al. (1989).

Characterisation and classification of Brown Ring Disease (BRD) syndrome

BRD symptoms were monitored on the inner surface of the clams shells according to the description of Paillard and Maes (1994): conchiolin deposit stage (CDS) range from microscopic brown spots on the inner face of the shell in the earliest stage (CDS 1), to a thick brown deposit covering most of the inner shell in the most advanced stage (CDS 7).

4.2.4 Biometric measurements

After gill dissection, remaining flesh was removed from the shell and placed in pre-weighted aluminium capsules. Capsules were then freeze-dried for 48 h and dry flesh were weighted. As gills were removed for *P. olseni* diagnosis, total flesh dry weight was calculated by adding dry flesh weight and gills dry weight. Gills dry weight was estimated from wet gill weight using the coefficient 0.153 g dry g wet estimated from clams collected in Bailleron island (additional samples, n = 25; S.D. = 0.008).

Shells were air dried and weighted. Length following the maximal length axis was measured using an electronic caliper and shells were stored until BRD diagnosis.

Condition index was calculated using the following formula:

$$CI = \frac{Flesh\ Dry\ Weight}{Shell\ Dry\ Weight} \times 100$$

4.2.5 Environmental factors

Temperature and salinity *In situ* sediment temperature was measured using an autonomous temperature data logger (EBI-85A, Ebro, Germany) embedded under 5 cm of sediment, the depth at which Manila clam are usually found. The probe measured temperature every 20 min. A daily average was calculated. Salinity data were provided by the IFREMER laboratory of La Trinité-sur-Mer (LER-MPL) and were measured using a Micrel probe in Fort Espagnol were salinity variation are supposed to be similar to those at Bailleron island.

Trophic resource Trophic resource monitoring begun in September 2004. Water samples were collected weekly at 50 cm above the sediment, and stored in a freezer (-18°C) until further analysis. For each water sample, six subsamples were filtered through pre-weighted GF/F filters (25 mm) and freeze-dried to constant weight. These filters allowed to measure total suspended

particulate matter (TPM). Three of the six filters were burnt (4h, 450°C) and allowed to measure suspended particulate inorganic matter (PIM). Particulate organic matter (POM, $mg\,L^{-1}$) was calculated by subtracting TPM and PIM. Burnt and unburnt filters were analysed for total carbon and nitrogen on a CE Instruments NC2500 elemental analyser (CE Elantech, USA). Particulate organic carbon (POC, $mg\,L^{-1}$) and nitrogen (PON, $mg\,L^{-1}$) were then calculated by subtracting particulate carbon from unburnt and burnt filters. The choice of characterisation of suspended organic matter quantity (POM) and quality (POC and PON) rather than chlorophyll *a* to estimate the trophic resource for the Manila clam was motivated by a modelling study that emphasized that chlorophyll *a* was not a good estimator of the trophic resource for the Manila clam (Flye-Sainte-Marie et al., 2007a).

4.2.6   Statistical analysis

Statistical analysis were performed using the R software (R Development Core Team, 2006). Differences in hemocyte parameters among sampling dates were tested using the Kruskal–Wallis test. Differences in prevalence of both diseases among sampling dates were tested using a χ^2 test. Relationships between environmental factors and hemocyte parameters were assessed by the mean of linear models.

When seasonal effect on a biological variable was significant (*i.e.* hemocyte parameters and condition index), it was removed to test the relationships between those variables and between hemocyte parameters and length or sex. Seasonal trends were considered to be represented by the variations of the mean of the considered biological variable in healthy individuals (*i.e.* BRD-asymptomatic and null *P. olseni* clams), as along sampling dates. The season detrended value of the variable was calculated for each individual as:

$$D_s \ = \ X_{tn} - \bar{X}_{tH}$$

Where D_s is the season detrended residual, X_{tn} is the original value of the variable on sampling date t for individual n and $\bar{X}_{tH}$ is the mean of the variable on sampling date t calculated for healthy clams.

Clams length had a significant effect on the THC, the concentration of both granulocytes and hyalinocytes, and the proportion dead cells in healthy f clams. Clam size also had a significant effect on prevalence for both pathologies. In order to test for the effect of pathologies independently of size, a linear model was used to calculate the effect of length on each of those variables among healthy clams; residuals of these models were used in further calculations for

testing the potential effect pathologies on those hemocyte parameters and on prevalence.

To assess effect of categorical factors (*i.e.* infected *versus* non infected), *t*–tests were used for normal–distributed data. The Fisher test for homogeneity of variance was performed. If variances were significantly different, a Welsch approximation to the degrees of freedom was used. A Wilcoxon test was used for non–normal data. Effect of continuous factors (*i.e.* length) on hemocyte parameters were assessed using linear models.

4.3 Results

4.3.1 Environmental factors

Average daily temperature in the sediment varied between 6 and 23°C (Fig. 4.2 A) during the sampling period. Temperature and salinity profiles were highly correlated (Fig. 4.2 A; Pearson $r = 0.66$, p–value $= 6\,10^{-3}$). Particulate organic matter (POM, Fig. 4.2 B) was highly correlated to total particulate organic matter (POM), particulate organic carbon (POC) and particulate organic nitrogen (PON) (Pearson $r > 0.94$, p–value$< 10^{-3}$).

4.3.2 Influence of environmental factors on hemocyte parameters

Evolution of hemocyte counts (total hemocyte, granulocyte and hyalinocyte counts) are shown in Fig. 4.3. All hemocyte parameters significantly varied during the sampling period (Kruskal–Wallis test; p-values < 0.005). Nevertheless, there were few significant relationships between hemocyte parameters and measured environmental factors (Tab. 4.1). Temperature significantly and positively affected all hemocyte counts (THC, granulocyte and hyalinocyte counts, Tab. 4.1). The significance was higher for the granulocyte concentration as the correlation coefficient of the linear model was high ($r^2 = 0.62$) and the correlation is clearly visible on Fig. 4.3. Salinity only affected the granulocyte concentration (Tab. 4.1). Neverthless, salinity and temperature were correlated, thus only the effect of temperature was tested against hemocyte parameters (Tab. 4.1) because temperature was more correlated to THC and granulocytes than salinity. Food quantity (POM) and quality (POC and PON) had no significant effects on hemocyte parameters (Tab. 4.1). Hyalinocyte concentration, number of aggregates, percentage of dead cells, percentage of phagocytosis and PO activity were not correlated to any of the measured environmental factors (Tab. 4.1).

TAB. 4.1: Relationships between environmental factors and hemocyte parameters tested using linear models. POM: particulate organic matter, POC particulate organic carbon, PON, particulate organic nitrogen.

Hemocyte parameter	Temperature (°C)		Salinity (‰)		Trophic resource					
					POM (mg L^{-1})		POC (mg L^{-1})		PON (mg L^{-1})	
	slope	p–value	slope	p–value	slope	p–value	slope	p–value	slope	p–value
THC (cell mL^{-1})	$1.7\,10^4$	*	$4.5\,10^4$	NS	$-4.2\,10^4$	NS	$-3.9\,10^4$	NS	$-2.9\,10^5$	NS
Granulocytes (cell mL^{-1})	$1.7\,10^4$	**	$4.6\,10^4$	*	$-1.7\,10^4$	NS	$3.0\,10^3$	NS	$6.1\,10^4$	NS
Hyalinocytes (cell mL^{-1})	$-1.2\,10^3$	NS	$-3.9\,10^3$	NS	$-2.2\,10^4$	NS	$-3.8\,10^4$	NS	$-3.2\,10^5$	NS
Aggregates (nb mL^{-1})	$1.3\,10^3$	*	$2.4\,10^3$	NS	$-2.9\,10^3$	NS	$-3.8\,10^3$	NS	$-3.0\,10^4$	NS
Dead cells (%)	-0.03	NS	-0.23	NS	-0.07	NS	-0.45	NS	-4.01	NS
Phagocytosis (%)	-0.78	NS	-1.3	NS	-0.44	NS	0.96	NS	8.6	NS
PO activity (A.U.)	$7.7\,10^{-5}$	NS	$1.9\,10^{-4}$	NS	$1.2\,10^{-5}$	NS	$-6.4\,10^{-6}$	NS	$-2.5\,10^{-4}$	NS

A.U. = arbitrary units ($\Delta\,DO_{490\,nm}\,min^{-1}\,mg\,protein^{-1}$)

Significance of the slope of the linear model:

NS: not significant (p–value > 0.05); *: p–value < 0.05; ** p–value < 0.01
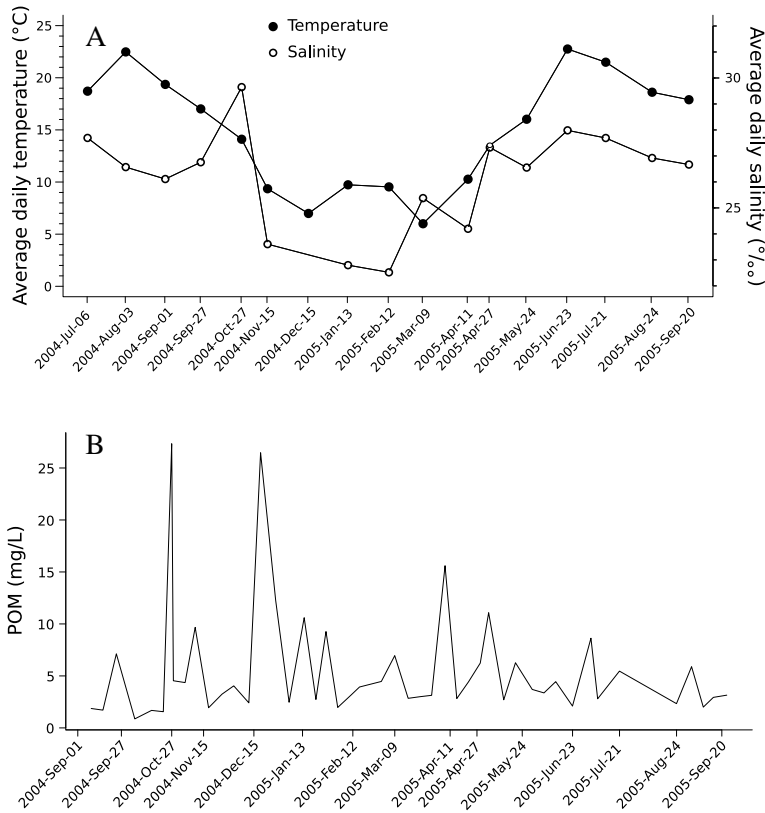
FIG. 4.2: Evolution of environmental factors during the studied period. A: daily average temperature in the sediment and salinity at the sampling dates. B: evolution of particulate organic matter (POM).

4.3.3 Influence of endogenous factors on hemocyte parameters

Effect of size/age Relationships between size/age (length) and hemocyte parameters were tested using linear models only in uninfected individuals (neither BRD–symptomatic nor *Perkinsus* affected clams) to avoid effects of disease (Tab. 4.2). Although r^2 were low, all hemocyte counts (THC, granulocyte and hyalinocyte concentrations) significantly increased with size/age. The percentage of dead cells and the PO activity significantly decreased with size/age (Tab. 4.2).
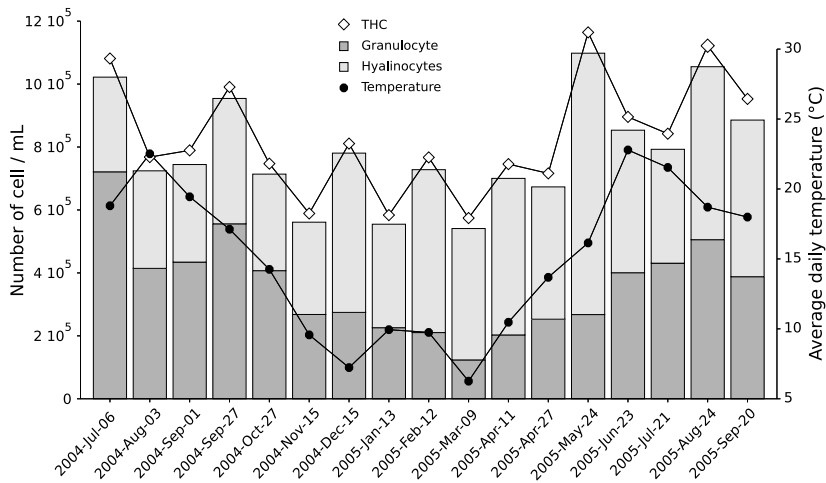
FIG. 4.3: Evolution of Total Hemocyte Count (THC), granulocyte and hyalinocyte concentrations and temperature during the study period.

Effect of sex and reproduction   Effect of sex was tested during the reproduction period (end of April to end of September) when sex determination was possible. There were no significant differences between males and females in any of the hemocyte parameters (*t*–test and Wilcoxon test ; *p*–values > 0.05). Massive spawning generally occurs at mid August/beginning of September in the Gulf of Morbihan and result in a decrease of the condition index (Laruelle et al., 1994; Laruelle, 1999; Calvez, 2003). The decrease in the granulocyte concentration in the 2004-Aug-03 and 2004-Sep-03 samples (Fig. 4.3) coincide with this period. Although condition index indicated that clams had spawned at the 16th sample (2005-Aug-24) a decrease of granulocyte count was not observed.

Condition index residuals   In order to test if the energetic status could be linked to hemocyte parameters independently of seasonal variations, the relationships between condition index residuals and hemocyte parameters were tested using linear models (Tab. 4.2). There were significant positive relations between condition index residuals and all hemocyte counts but r^2 were very low (<0.01).

TAB. 4.2: Relationships between length and hemocyte parameters residuals in uninfected individuals and between condition index residuals and hemocyte parameters residuals (in uninfected and infected clams) tested using linear models.

Hemocyte parameter residuals	Length (uninfected clams)			Condition index residuals (all clams)		
	slope	r^2	p–value	slope	r^2	p–value
THC (cells mL^{-1})	$1.9\,10^4$	0.034	**	$4.2\,10^4$	0.009	*
Granulocytes (cells mL^{-1})	$1.2\,10^4$	0.052	**	$1.9\,10^4$	0.006	*
Hyalinocytes (cells mL^{-1})	$6.9\,10^3$	0.010	**	$2.4\,10^4$	0.008	*
Aggregates (nb mL^{-1})	$-1.5\,10^2$	0.000	NS	$-1.2\,10^3$	0.004	NS
Dead cells (%)	-0.07	0.017	**	-0.03	0.000	NS
Phagocytosis (%)	-0.08	0.001	NS	-0.74	0.004	NS
PO activity (A.U.)	$-1.4\,10^{-4}$	0.023	**	$-1.4\,10^{-4}$	0.002	NS

A.U. = arbitrary units ($\Delta\,DO_{490\,nm}\,min^{-1}\,mg\,protein^{-1}$)
Significance of the slope of the linear model:
NS: p–value > 0.05; *: p–value < 0.05; ** p–value < 0.01

4.3.4 Diseases

Prevalences of BRD symptoms and perkinsosis

BRD prevalence was low (Fig. 4.4 A.; average prevalence: 9.7%) and showed no significant variation during the sampling period ($\chi^2 = 12.96$, $df = 16$, p-value = 0.675). The disease intensity was also low: 90% of the symptomatic clams had a CDS lower than 4 on a scale going from 0 to 7.

Perkinsosis prevalence was moderated (Fig. 4.4 A.; 20–50% average prevalence: 38.2%). Although variations in prevalence during the sampling period were significant ($\chi^2 = 37.79$; $df = 16$; p–value = 2.10^{-3}) no clear seasonal patterns appeared. *P. olseni* infection intensity ranged between 0 and $1.63\,10^6$ cells/g gill WW, with a mean of $1.96\,10^4$. *P. olseni* prevalence and infection intensity were not correlated to temperature (linear models, p–value = 0.902 and 0.979 for prevalence and infection intensity, respectively).

There were significant positive correlations between size and both BRD (Fig. 4.4 B.) and perkinsosis prevalences (Fig. 4.4 C.)

4.3.5 Influence of disease on hemocyte parameters

There were no difference in any measured hemocyte parameter residuals between BRD–asymptomatic clams and symptomatic clams (p–values > 0.05), neither between BRD–asymptomatic clams and clams with CDS = 3 and higher
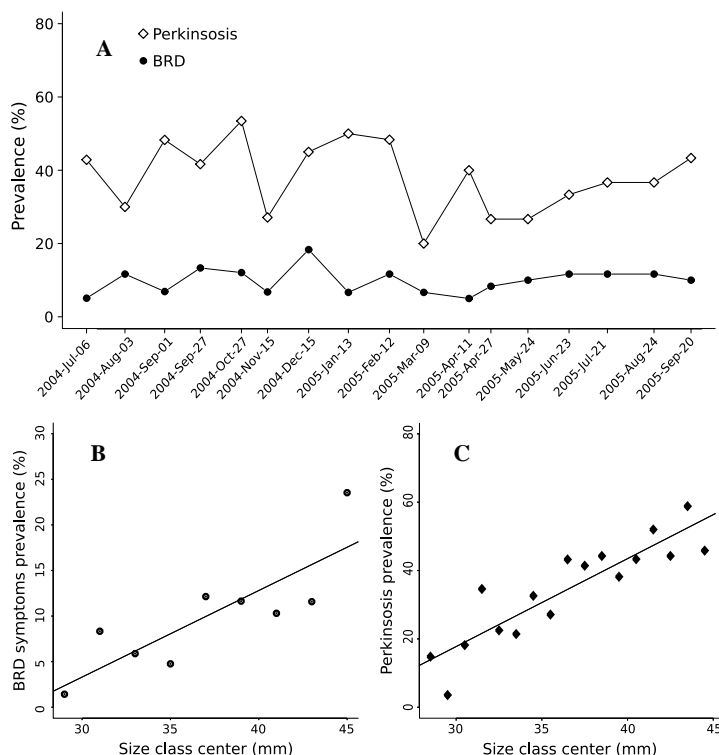
FIG. 4.4: A: Evolution of prevalence of perkinsosis and BRD during the sampling period; B: Relationship between center of the size classes and BRD symptom prevalence ($y = 0.94\,x - 0.25$; $r^2 = 0.52$; p-value $= 0.005$); C: Relationship between center of the size classes and perkinsosis prevalence ($y = 2.57\,x - 59$; $r^2 = 0.77$; p-value $= 1.83\,10^{-6}$)

(p–values > 0.05). Also, no significant relationship between condition index residuals and BRD stage could be found (linear model, p–value $= 0.211$).

The effect of perkinsosis could only be detected (Fig. 4.5) when uninfected clams were compared with highly infected clams ($>100\,000$ *P. olseni* cell/g gill WW). *P. olseni* significantly increased granulocyte concentration and THC and significantly decreased the phagocytosis percentage (Fig. 4.5). No effect of *P. olseni* infection was observed on hyalinocyte concentration, number of aggregates (*t*–test, *p*value > 0.05), dead cells percentage (*t*–test, *p*value > 0.05) and PO activity (Wilcoxon Test, p–value > 0.05).
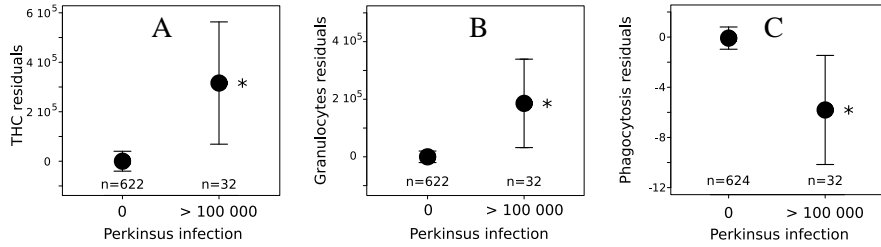
FIG. 4.5: Comparisons of A: total hemocyte count, B: Granulocyte count, C: Phagocytosis percentage between uninfected individuals (0 *P. olseni* cell/g gill WW; *i.e.* under the detection threshold) and highly infected individuals (> 100 000 *P. olseni* cell/g gill WW). Results are expressed as mean ±95% confidence interval. The star (*) indicates significant differences (*p*–value < 0.05).

4.3.6   Overall variability of hemocyte parameters

Contributions of the environmental condition, internal factors and disease to overall variability of four hemocyte parameters (THC, granulocyte and hyalinocyte concentration, phagocytosis) were investigated using MANOVA (Tab. 4.3), only factors that had a significant effect on these hemocyte parameters were considered. Results indicate that the most explained hemocyte parameter was the granulocyte concentration (Tab. 4.3) for which only 16.4% of the variability was explained by temperature (11.3%), length (4.1%), *P. olseni* infection (0.6%) and condition index residuals (0.4%). Only 10% of the THC variability was explained by these factors. Factors explaining most of the variance of the hemocyte parameters were temperature and length. *P. olseni* explained only very little of the overall variability of the hemocyte system : its effects are significant when comparing uninfected to heavily infected clams (Fig. 4.5) but no significant trend could be detected when using a continuous linear model of THC or phagocytosis against concentration of *P. olseni*.

4.4   Discussion

The aim of this study was to better understand the relative effect of environmental and internal factors as well as diseases on hemocyte parameters in the field. Independent effects of each factor on the hemocyte parameters will be

TAB. 4.3: Summary of the weights of environmental (temperature) and internal factors (size/age and condition index residuals) and *P. olseni* infection on the total variability of THC, granulocyte concentration (cell mL^{-1}), hyalinocyte concentration (cell mL^{-1}) and phagocytosis percentages calculated from a MANOVA. Factors that had no significant effect were not included in the computations. Partial r^2 values indicate the weight of each factor on the total variability of each parameter, r^2 indicates the weight of all included factors on the total variability of each parameter.

Factor	THC		Granulocyte conc.		Hyalinocyte conc.		Phagocytosis	
	partial r^2	*p*–value	partial r^2	*p*–value	partial r^2	*p*–value	partial r^2	*p*–value
Temperature	0.033	**	0.113	**	NI		NI	
Length	0.055	**	0.041	**	0.030	**	0.028	**
CI residuals	0.009	**	0.004	*	0.009	**	NI	
P. olseni	0.003	NS	0.006	**	NI		2.4 10^{-5}	NS
	r^2	*p*–value	r^2	*p*–value	r^2	*p*–value	r^2	*p*–value
All factors	0.100	**	0.164	**	0.039	**	0.028	**

CI: condition index

NI: not included in MANOVA

NS: not significant (*p*–value > 0.05); *: *p*–value < 0.05; ** *p*–value < 0.01

discussed first. Subsequently, the combined effect of the measured factors to the overall variability of hemocyte will be discussed.

Effect of environmental factors on hemocyte parameters

Temperature was the major environmental factor modulating hemocyte parameters. There was a positive correlation between temperature and both granulocyte and total hemocyte counts. Since the slopes of the linear models relating temperature with granulocyte concentration and THC are equal (Tab. 4.1) it can be concluded that the increase in THC simply reflects the augmentation of the granulocyte concentration. Several laboratory experiments emphasized the positive effect of temperature on hemocyte concentration in hemolymph in various bivalve and crustacean species (see *e.g.* Truscott and White, 1990; Chu and La Peyre, 1993; Fisher et al., 1996; Chu, 1998; Liu et al., 2004; Paillard et al., 2004; Monari et al., 2007). Only few studies however showed the occurrence of this pattern in the field (Fisher et al., 1996; Carballal et al., 1998; Soudant et al., 2004). The increase of circulating hemocyte counts is generally considered as a consequence of proliferation or movement of cells from tissue into the hemolymph (Pipe and Coles, 1995). Thus an increase of the hemocyte proliferation with temperature could explain the observed pattern. The number of hemocyte aggregates was also positively correlated to temperature. Hemocyte aggregation is presumed to be involved in hemostasis and wound healing (Chen and Bayne, 1995) but also in defence mechanisms (Tiscar and Mosca, 2004). Formation of hemocyte aggregates is the result of the adhesion activity of the hemocytes (Chen and Bayne, 1995; Auffret and Oubella, 1997). Since bivalves are poikilotherms, hemocyte activity may scale with temperature, explaining the correlation between aggregate concentration and temperature.

Extreme (high and low) salinities have been shown to induce variations of total hemocyte counts in several bivalve species (Chu and La Peyre, 1991; Reid et al., 2003; Matozzo et al., 2007), but generally variation of salinity within the life range of the species does not affect hemocyte counts (Matozzo et al., 2007). This tends to confirm that, in this study, the observed correlation between salinity and granulocyte concentration is only attributable to the correlation between temperature and salinity.

Although phagocytosis significantly varied during the studied period, this parameter does not seem to be affected by any of the measured environmental factors. This appears in contradiction with laboratory experiments which showed that phagocytosis varied with temperature (Chu and La Peyre, 1993; Allam et al., 2002b; Monari et al., 2007) and salinity (Reid et al., 2003). The reasons for this discrepancy remains unclear but emphasizes the difficulty in

extending laboratory results to the field.

Low food levels and starvation have been shown to reduce THC in oysters (Delaporte et al., 2006; Butt et al., 2007). However, in an earlier study, Ashton-Alcox and Ford (1998) showed that a 4-week starvation did not affect hemocyte counts in oysters. This result suggest that this time lapse is not long enough to induce a starvation stress. In our study, indicators of food quantity (POM) and quality (POC, PON) did not appear to affect any of the measured hemocyte parameters, suggesting that in such natural conditions food level and quality are not low enough to induce any modification of hemocyte parameters during the studied period.

The poor relationship between other environmental factors and hemocyte parameters emphasizes the difficulty to assess the environmental control of hemocyte system in the field.

Effect of endogenous variables

Size/age   Variability of hemocyte parameters with size/age have been little studied (Carballal et al., 1997; Lopez et al., 1997; Carballal et al., 1998; Barracco et al., 1999) and a clear effect of size on the hemocyte parameters was rarely found. Only Carballal et al. (1998) found a significant increase in the number of circulating granulocytes with age in *Mytilus galloprovincialis* for one of their two samples. In most of the above studies, the size ranges were smaller than in our study (this study: 200% of difference between the smallest and the largest individuals and 127%, to 150% in Lopez et al., 1997; Carballal et al., 1998; Barracco et al., 1999, studies). Furthermore, the large number of individuals sampled in our study allowed to distinguish the effect of size/age within the large variability of the hemocyte parameters. Our study emphasizes that, in the Manila clam, total hemocyte, granulocyte and hyalinocyte counts are significantly positively correlated to size while percentages of phagocytosis and dead cells are negatively correlated to size.

Sex and reproduction   Links between gender and the hemocyte system are poorly known (Barracco et al., 1999; Gagné et al., 2007). In both studies, as in the present, results tend to show that hemocyte parameters are independent of gender. Such relationships were unexpected since the hemocyte system plays an important role in maintaining organism homeostasis which requirements should not vary with gender.

However, the gonadal cycle can influence the hemocyte system (see Oliver and Fisher, 1999, for a review), in a laboratory experiment. Delaporte et al.

(2006) observed a decrease in THC during gametogenesis in the oyster *Crassotrea gigas*. Field studies also showed that THC decrease during spawning period (Pipe et al., 1995; Fisher et al., 1996) presumably because of hemocyte infiltration in the gonadal tissue. In our study, the condition index profile indicated that clams had already spawned on the 2004-sep-01 and 2005-aug-24. These events could not be associated to a decrease in THC or any other of the measured parameter.

Condition index residuals Condition index residuals provide a rough information about the energetic status independently of seasonal variation (*i.e.* is the individual more or less fat for the season?). Our study shows that there is small positive, but nonetheless significant, effect condition index residuals on hemocyte counts. This tends to confirm the hypothesis of Ashton-Alcox and Ford (1998) that suggested that molluscan hemocyte parameters variability could be linked to the amount of stored energy reserves explaining the high observed inter–individual variations. This relationship could be explained by the involvement of hemocytes in nutrient mobilisation (Cheng, 1996). Nevertheless the relationship only explains little of the total variability of hemocyte parameters.

Diseases

Prevalence and intensity of perkinsosis and BRD Prevalence of *P. olseni* infection was moderated and ranged between 20 and 50% (average 38.2%) which is comparable to the values of 32.9% obtained by Ngo and Choi (2004) in natural *R. philippinarum* beds of Jeju (Korea) and values reported by Leite et al. (2004) in various *R. decussatus* beds from Portugal. These prevalences are lower than those reported by Park and Choi (2001) in various places of Korea where prevalence reached 100% in some locations and by Villalba et al. (2005) in natural *R. decussatus* beds of Galicia (Spain; 45 to 100%). Although perkinsosis prevalence showed significant variation during the study period, no clear annual pattern appeared. Epizootiology studies showed that *Perkinsus marinus* infection in the oyster *Crassostrea virginica* prevalence is closely related to temperature and salinity (see review in Villalba et al., 2004) which results in an increased prevalence in summer. A 5–year survey of *P. olseni* infection in a *Ruditapes decussatus* bed from Galica (Spain) showed an annual pattern with an increase of prevalence in spring and autumn (Villalba et al., 2005). In Jeju island (Korea), Ngo and Choi (2004) found higher prevalences of *P. olseni* infection in *R. philippinarum* during spring. These studies contrast with our results. Nevertheless, Leite et al. (2004) did not found any annual

patterns of *P. olseni* in *R. decussatus* along the Portuguese coasts during their
2–year survey which showed that seasonal patterns are not always observed in
P. olseni infection prevalence.

Estimation of *P. olseni* burden in gill (cells/g gill WW) provide an over–
estimation of the total body burden (cells/g flesh WW) (Choi et al., 2002). In
our study *P. olseni* infection intensity was low (average: $2\,10^4$ cells/g gill WW)
and our values are consistent with the values obtained by Lassalle et al. (2007)
in the Gulf of Morbihan. Higher values have been reported in more southern
locations along the French Atlantic coast : more than $8\,10^4$ cells/g gill WW in
Arcachon bay (Lassalle et al., 2007). Higher values were also reported in Ko-
rea (up to $8.7\,10^6$ cells/g flesh WW; Park and Choi, 2001), in Japan ($2.25\,10^6$
cells/g flesh WW; Ishaya bay; Choi et al., 2002) and in Spain ($\simeq 5\,10^4$ cells /
g flesh WW in *R. decussatus* from Galicia; Villalba et al., 2005).

Average prevalence of BRD symptoms during the study period (9.7%) was
low in comparison to the prevalences observed in aquaculture clams beds of
Northern Brittanny (Brouennou, Finistère, France) that ranged between 33 and
100% (Paillard, 1992; Paillard et al., 1997; Paillard, 2004a). Our results are in
accordance with previous studies performed in natural populations of the Gulf
of Morbihan (Paillard, 2004a; Lassalle et al., 2007) that found prevalences be-
tween 4 and 30%. However, no annual pattern in BRD prevalence was found
and this contrasts with the field surveys of Paillard et al. (1997) and Paillard
(2004a). These studies showed that symptomatic clams are found all around
the year, but generally BRD symptoms increase toward the beginning of spring
and decrease towards the beginning of the summer. Low temperatures during
the rising phase of prevalence have been invoked to explain this pattern (Pail-
lard et al., 1997, 2004; Paillard, 2004a,b). The lack of a pattern observed in
our study may be explained by the low prevalence and intensity of BRD during
the period studied. BRD symptom intensity was low during the survey: 80%
of symptomatic clams had a CDS of 3 or less, stage at which the extend of the
brown deposit is localised to small areas on the inner shell (Paillard and Maes,
1994).

Size-prevalence relationships   The positive relationships between size and
prevalence for both disease correspond to the general pattern observed for most
parasites in filter feeder bivalves (Guralnick et al., 2004). This pattern has al-
ready been shown for the *P. marinus*/*C. virginica* (Andrews and Hewatt, 1957)
and *P. olseni*/*R. decussatus* interactions (Villalba et al., 2005). The explanation
of such a pattern lies in both an increased filtration rate in biggest individuals
and an accumulation of the parasite during life span, these processes leading

to an increase of prevalence and infection intensity with size (Andrews and Hewatt, 1957; Guralnick et al., 2004; Villalba et al., 2005). Nevertheless, a recent study also linked grain-size of the sediment and prevalence suggesting another interpretation for the size–BRD prevalence relationship: increased body surface area with size could lead to higher probability of contact with big sediment grains that may induce disruptions and subsequently a potential entry for the pathogen *V. tapetis* (Flye-Sainte-Marie et al., unpublished data).

Relations between hemocyte parameters and disease   *P. olseni* infection effects on hemocyte parameters could only be found in highly infected individuals (> 100 000 *P. olseni* cells/g gill WW). High *P. olseni* infection significantly increased granulocyte concentration and consequently THC. This result is contradictory to those of Ordás et al. (2000) who found a decrease of THC in *R. decussatus* infected by *P. olseni*. Nevertheless, augmentation of circulating hemocytes has been widely documented in *C. virginica* heavily infected by *P. marinus* (see *e.g.* Anderson et al., 1992; Chu and La Peyre, 1993; Anderson et al., 1995; La Peyre et al., 1995; Anderson et al., 1996). These authors suggest that this increase reflects a mobilisation/production of hemocytes to counteract *Perkinsus* sp. development. In our study, high *P. olseni* infection also significantly reduced hemocyte phagocytosis percentage which is in accordance with previous studies who showed an inability of *R. decussatus* hemocytes to phagocyte *P. olseni* zoospores (Lopez et al., 1997) and a decrease in the percentage of phagocytosis in *P. olseni*-infected *R. decussatus* Ordás et al. (2000). Muñoz et al. (2006) found an increase in the PO activity in *R. decussatus* lowly and moderately infected by *P. olseni*. Although the low and moderate *P. olseni* infection intensity observed in our samples, no significant effect could be found with our data.

   In this study, BRD had no significant influence on any of the hemocyte parameters. These results contrast with previous experimental studies which showed that (1) *V. tapetis* inoculation induces an increase in THC (Paillard et al., 1994; Allam et al., 2000a, 2006; Paillard, 2004b), (2) a decrease in phagocytic activity (Allam et al., 2002b; Allam and Ford, 2006), and (3) an increase of the dead cell percentage (Allam et al., 2000a; Allam and Ford, 2006; Allam et al., 2006). Symptoms of BRD results of the interaction between the bacteria and the clam over time. Experimental infection may uncouple bacterial burden and symptoms (brown deposit). In these conditions, the effect on the hemocyte system may be detected before apparition of symptoms. Thus, the discrepancy between the above experimental observations and our results may be explained by the low natural infection intensity, presumably associated

to a low *V. tapetis* burden. Consistently with our study, Reid et al. (2003) failed to find any significant effect of BRD on PO activity.

Allam et al. (2001) suggested that higher granulocyte concentrations may be related to a higher resistance to BRD. Interestingly, in our study, granulocyte concentrations significantly varied but BRD prevalence was not lower when granulocyte concentration was high. Granulocyte concentration significantly increased with size/age but prevalence and size were also correlated. Thus, it was not possible to link a high granulocyte concentration with any variation of BRD prevalence. This observation is consistent with Reid et al. (2003) who indicated that increased hemocyte populations did not appear to have a direct role in reducing BRD levels. This suggest that association of resistance to BRD and hemocyte parameters is not straightforward.

Disease and condition index   Low infection intensities of both disease observed during the study period explains that condition index was not affected in infected individuals. These results are consistent with previous studies indicating that both disease are susceptible to interfere with the energy balance and to affect the condition index (Leite et al., 2004; Park et al., 2006a; Flye-Sainte-Marie et al., 2007b) only at high infection intensities.

Variability of hemocyte parameters in the field

Consistently with previous studies, this multiparametric field study emphasizes that part of the variability of the hemocyte system of bivalves is attributable to environmental and internal factors as well as disease. Temperature was the only environmental factor explaining seasonal variations of some of the hemocyte parameters and contributed to 10% of the variability of granulocyte concentrations. Effect of size/age on hemocyte parameters have been poorly described in literature (Carballal et al., 1997; Lopez et al., 1997; Carballal et al., 1998; Barracco et al., 1999). It was nevertheless the factor both affecting most of the measured hemocyte parameters and significantly contributing to the explanation of the variability of hemocyte system. Interestingly, although links between disease and hemocyte system have been extensively described in the literature these links were little established in our study. In accordance with Adamo (2004), this study emphasizes that the measures of hemocyte parameters cannot directly be interpreted as measurement of immunocompetence (*i.e.* capacity of defence against a pathogen).

Although this study identified factors that significantly affect the hemocyte system, these factors only explain little of the overall variability of the hemocyte parameters. For the mostly explained parameters (granulocyte concentra-

tion) only 16.4% of the variance could be explained from the measured factors. Part of the unexplained variability can be attributed to unexplained month to month variations, suggesting that other environmental factors than temperature, salinity or trophic resource may modulate the hemocyte system. Effect of contaminants and toxic algae on the hemocyte system of bivalves have also been documented in literature (see *e.g.* Oliver et al., 2001; Auffret et al., 2004, 2006; Hégaret and Wikfors, 2005b,a; Hégaret et al., 2007) and could in part explain these month to month variations. Most of the variability of the hemocyte system could be attributed to inter–individual differences and thus could not be associated with any parameter that we measured. Ashton-Alcox and Ford (1998) suggested that variability in molluscan hemocytes could be more immediately linked to individuals metabolic condition than to an inability to buffer hemolymph against external ambient conditions. In the past 30 years, many authors have studied the link between hemocyte system and disease and thus tend to reduce the role of hemocyte system to immune functions. Nevertheless, although poorly documented, there is evidence of implication of the hemocyte system in various other functions such as nutrition, inflammation, wound repair (Fisher, 1986; Cheng, 1996) and shell repair and mineralization (Fisher, 1986, 2004; Mount et al., 2004). This study emphasize the need for a better understanding of the various functions of the hemocyte system and the way these functions control the hemocyte system. Such a knowledge is necessary to better understand the linkages between environment, bivalve metabolic status, hemocyte system and disease development, and for the use of bivalve hemocyte parameters as environmental biomarkers.

Acknowledgements

Chapter 5

A portal of entry for *Vibrio tapetis* ?

Jonathan FLYE-SAINTE-MARIE, Fred JEAN, Susan E. FORD, Christine PAILLARD.

Abstract

Brown ring disase (BRD) in the Manila clam is induced by the bacterium *Vibrio tapetis*. During the infection process, the pathogen enters the extrapallial compartment of the Manila clam and induces the formation of a characteristic brown deposit that gives the disease its name. Although post-infection processes have been widely described for this disease, the mechanisms of entry of the bacteria into the extrapallial compartment remains unclear. From relationships between clam size and BRD prevalence, and between grain–size distribution in natural habitats and prevalence, we propose a simple explanation for this step: *V. tapetis* benefits from mechanical disruptions of the periostracal lamina or valve margins to colonize the extrapallial compartment. Such disruptions may be induced by the presence of large sediment grains in natural habitats, which become lodged in the shell opening. This hypothesis suggest that limiting handling of clams may help to limit development of BRD in cultured clam beds.

Keywords: Manila clam ; Brown Ring Disease ; BRD ; *Vibrio tapetis* ; prevalence ; size ; grain–size.

5.1   Introduction

The Manila clam, *Ruditapes philippinarum*, was introduced in France for aqua-
culture purposes between 1972 and 1975 (Flassch and Leborgne, 1992). In
France, this venerid culture became increasingly widespread, and since 1988
natural populations have colonized most embayments along the French At-
lantic coast, resulting in important fisheries.

   Brown ring disease (BRD) in this species is a bacterial disease induced by
the pathogen *Vibrio tapetis*. It was first observed in 1987 in northern Brittany
(France) and has rapidly been reported along the French Atlantic coast (Pail-
lard, 1992). The disease is now observed along the entire European Atlantic
coast, from Norway to southern Spain, and in Italy (Paillard, 2004b; Paillard,
unpublished data). The disease, which causes mass mortalities in cultured
clam beds, has severely affected venerid culture in northern Brittany but has a
lower impact in natural beds, where maximum prevalence reaches only 30%
(Paillard, 2004b).

   During the infection process, the pathogen proliferates within the extrapal-
lial compartment and disrupts the normal production of periostracal lamina,
inducing the formation of a brown conchiolin deposit on the inner shell; this
characteristic clinical sign gave the disease its name (Paillard, 1992). BRD
progression has been described in depth in Paillard et al. (1994) and Paillard
(2004b). The following steps for the disease progression have been proposed
by Paillard (2004b) : (1) adherence of the pathogen, *V. tapetis*, to the periostra-
cal lamina; (2) penetration and colonization of the extrapallial compartment;
and (3) formation of the anomalous brown conchiolin deposit, in which the
pathogen becomes embedded. Although post–infection processes (i.e. after
penetration into extrapallial compartment) have been widely described (see
Paillard, 2004b, for a review), mechanisms of entry of *V. tapetis* into the ex-
trapallial fluids remain poorly understood. Paillard (2004b) stated that "in
favourable conditions for the pathogen, *V. tapetis* colonization provokes some
alteration and rupture of the periostracal lamina which allows the penetration
of the bacteria into the extrapallial fluids". By revisiting three unpublished data
sets, we propose a simple hypothesis to explain the entry of *V. tapetis* into the
extrapallial compartment.

5.2   Methods

All three data sets were collected from intertidal natural populations in the Gulf
of Morbihan (southern Brittany, France) between 1999 and 2006 (Fig. 5.1).
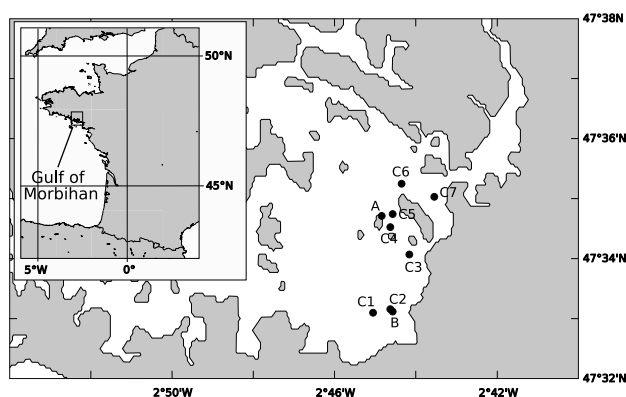
FIG. 5.1: Map of the sampling sites of the data sets used for this study. A: Ile de Bailleron; B: Ile aux Oiseaux. C1–C7: Sampling sites of the third data set.

For all data sets, BRD signs in the clams were monitored on the inner surface of the clam shells according to the criteria of Paillard and Maes (1994) in which conchiolin deposits stages (CDS) range from microscopic brown spots on the inner face of the shell in the earliest stage (CDS 1), to a thick brown deposit covering most of the inner shell in the most advanced stage (CDS 7).

The first data set came from a monthly monitoring of haemocyte parameters of Manila clams at Ile de Bailleron (Fig. 5.1, site A) (Flye–Sainte–Marie et al., unpublished data). During this survey, a total of 17 samples of 60 clams each was collected between the 6th of July 2004 and the 20th of September 2005 (total : 1020 individuals). This survey included individuals from a wide size range: from 26 mm to 55 mm along the maximum length axis. The prevalence of BRD was low (mean = 9.7%, SD=3.5%) and showed no significant variation during the sampling period ($\chi^2 = 12.96$, $df = 16$, $p = 0.675$), allowing pooling of the whole data set in order to extract a size–prevalence relationship. In this data set, disease intensity was also low: 80% of the affected clams had a CDS of 3 or less.

The second data set was collected on the 29th of March 2006 in Ile aux Oiseaux (Fig. 5.1, site B). A total of 530 individuals was collected and the size ranged from 11 mm to 42 mm (maximum length axis). In this data set, disease prevalence and intensity were also low: average prevalence was 4.1% and 80% of the affected clams presented a CDS of 3 or less.

For these two data sets, individuals were distributed into 2–mm size classes;
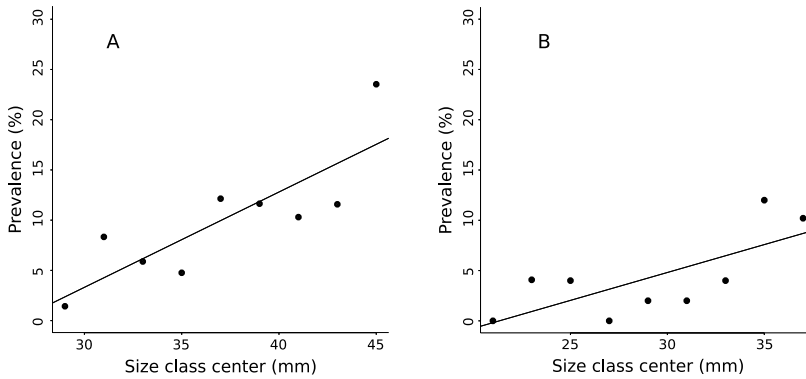
FIG. 5.2: Relationship between center of the size classes and prevalence in the data set from (A) Ile de Bailleron ($y = 0.94\,x - 0.25$; $r^2 = 0.52$; $p = 0.005$) and the data set from (B) Ile aux Oiseaux ($y = 0.55\,x - 0.12$; $r^2 = 0.66$; $p = 0.028$)

prevalence (percentage of affected individuals) was calculated for each size class. Size classes with fewer than 40 individuals (left and right tails of the size distributions) were excluded from computations. Relationships between clam size and prevalence were analysed using linear models, the *p*–value corresponds to the significance of the linear model (*i.e.* probability of the difference between the value of the slope and 0).

The third data set came from a survey of Manila clam density, BRD prevalence and *Vibrio tapetis* abundance in the sediment, as estimated by an ELISA test (Allam et al., 2002c) in the Gulf of Morbihan during 1999 (Paillard, unpublished data). During this study, sediment cores were collected at some of the sampling stations. Grain–size distribution in sediment cores was measured following Weiss and Frock (1976). For seven stations (Fig. 5.1, sites C1-C7) both BRD prevalence and grain–size distribution were available, which allowed analysis of the relationship between those two parameters. For this purpose, the relationship between the grain size of the upper 5% fractile of the sediment and prevalence was analysed using a linear model.

5.3   Results and discussion

Figure 5.2 illustrates the relationships between clam size and BRD prevalence for the data sets from Ile de Bailleron (Fig. 5.2 A) and from Ile aux Oiseaux (Fig. 5.2 B). For both data sets, correlation coefficients were high ($r^2 > 0.50$)
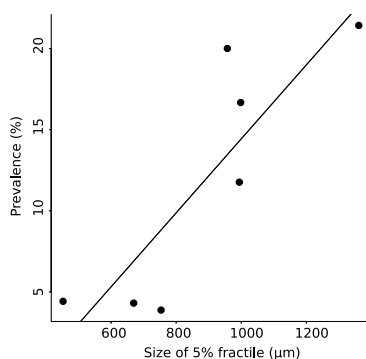
FIG. 5.3: Relationship between grain size of the upper 5% fractile of the sediment and BRD prevalence in the sampling stations of the third data set from Gulf of Morbihan (see Fig. 5.1, sites C1-C7); ($y = 0.0228\,x - 8.37$; $r^2 = 0.74$; $p = 0.013$).

and slopes were significant ($p < 0.05$), clearly indicating a positive relationship between clam size and BRD prevalence in natural populations. Such a pattern has been widely described for parasitic disease of filter feeding bivalves and is attributed to the greater probability that a larger (and presumably older) individual (1) has been exposed to potential infections longer and (2) has a higher filtration capacity and resulting higher probability of encountering parasites, compared to a small clam (see e.g. Andrews and Hewatt, 1957; Guralnick et al., 2004; Villalba et al., 2005).

Figure 5.3 shows the relationship between the grain size of the upper 5% fractile of the sediment in localized habitats (Fig. 5.1, sites C1–C7) and the BRD prevalence. For this relationship, the correlation coefficient was high ($r^2 = 0.74$) and slope was significant ($p = 0.013$), indicating a significant positive correlation of prevalence with the abundance of large particles in the sediment. This relationship suggests an increased probability of infection linked to the abundance of large particles in the sediment.

From these relationships, it can be hypothesized that a factor contributing to the initiation of the infection (i.e. the entry of *V. tapetis* into the Manila clam extrapallial compartment) is a mechanical rupture of the periostracal lamina or chipping of the valve margins induced by mechanical impact with large sediment particles. In the sediment, when a clam is active, its siphons are extended out of the shell and in direct contact with the sediment; when the siphons retract, sediment particles adherent in siphon mucus, may be trapped between
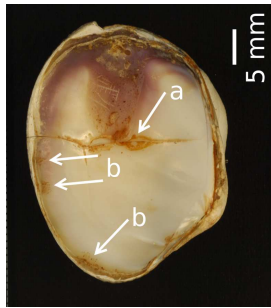
FIG. 5.4: Photograph of cracked shell, with the symptomatic brown deposit around the crack (arrow a) suggesting that shell breakage is a potential portal of entry for *V. tapetis*. Arrows b show the symptomatic brown deposit around the valve margins. (Photographs: E. Amice/LEMAR)

the valve margins. Moreover, sediment particles may be trapped within the shell aperture. When the clam closes its valves, these particles may disrupt the periostracal lamina or chip the shell edge, thereby opening a portal of entry for the pathogen *V. tapetis*. This hypothesis is supported by figure 5.4, which shows a cracked Manila clam shell. Around the crack the characteristic brown deposit is visible, suggesting that a shell rupture is a potential point entry for *V. tapetis*. Since siphon surface area and shell aperture length are directly related to clam size, the probability of trapping a potentially deleterious sediment particle may increase with size, which providing an additional potential explanation for the size/BRD relationship in natural populations. This hypothesis may also explain why early clinical signs are frequently observed in the siphonal area (Goulletquer et al., 1989a; Paillard, 1992; Paillard et al., 1994; Paillard and Maes, 1994).

Seasonal variations in BRD are not always observed, especially when average prevalence is low (first data set; Paillard, 2004a). Epidemiological surveys of BRD showed that affected clams are found throughout the year, but generally, the prevalence of BRD signs increases toward the beginning of the spring and decreases toward the beginning of the summer (Paillard et al., 1997; Paillard, 2004a). Low temperatures during the rising phase of prevalence have been suggested to explain this pattern (Paillard et al., 1997, 2004; Paillard, 2004a,b). However, this period also coincides with the beginning of the growth season (Goulletquer, 1989a); the newly calcified layer on the valve margins may be more susceptible to mechanical disruption. Therefore, disruptions of

the periostracal lamina and valve margins may occur more frequently during this period. Thus, seasonality of BRD development could be explained both by low temperatures and weakness of the valve margins.

5.4 Conclusion

This study suggest that the pathogen *V. tapetis* may benefit from mechanical disruption of the periostracal lamina or the valve margins to colonize the Manila clam extrapallial compartment. These disruptions may be induced by the presence of large sediment grains. This simple hypothesis provides a valuable explanation for some of the observed BRD development patterns. In cultured clam beds, limiting rough handling of clams, especially at the beginning of the growth season (spring), may help to limit development of BRD.

Acknowledgments

Chapter 6

Comparison of field data with the model hypothesis

Abstract

The construction of a model describing the relationship between the environment, the host and the pathogen in Brown Ring Disease has been described in part I. It describes the development of BRD symptoms under forcing of two environmental variables: temperature and trophic resource. It allowed to summarize the knowledge about the disease development. The assumptions made during the model's construction, developed in chapter 3, needed to be validated. Most of the model relationships were calibrated using laboratory experiments, and needed to be validated by field studies. The field study presented in chapter 4 was originally designed to build a data set in order to validate the model by field study. The purpose of this chapter is to compare data with the assumptions of the model.

In the model, the temperature controls the defense system against the pathogen, and subsequently the development of disease. The field study confirmed that temperature controls some hemocyte parameters: granulocyte concentration and total circulating hemocytes concentration. Nevertheless, during the study period prevalence of disease did not show significant variations. It was also not possible to link variations of hemocyte parameters with the disease development, suggesting that the relation between hemocytes and disease development is more complex than described by the model.

A strong hypothesis of the model was the link of disease development to the energetic status via the condition index. Although field studies indicated a significant relationship between condition index and hemocyte parameters, it was not possible to show any significant relationship between symptoms and condition index. This shows that the condition index may not explain disease susceptibility. The observations tend to invalidate this assumption of the model. The relation between condition index and presence of symptoms observed by Paillard (1992) in highly diseased individuals suggest that BRD affects the energy balance of the host. This point will be studied in part III of this thesis.

6.1   Introduction

Dans la partie I, nous avons décrit la construction d'un modèle d'interaction entre l'environnement, l'hôte et le pathogène visant à étudier le développement de la Maladie de l'Anneau Brun dans des populations naturelles de palourde japonaise en fonction de deux paramètres environnementaux : la température et la ressource trophique disponible. Ce modèle prenant en compte une variabilité interindividuelle des phénotypes permet à la fois de fournir une explication potentielle à la variabilité interindividuelle observée dans le développement de la MAB et de simuler les variations saisonnières de l'intensité des symptômes. L'un des intérêts majeurs de ce modèle a été l'élaboration d'une synthèse des connaissances disponibles concernant la MAB. Comme pour la plupart des modèles, l'élaboration de celui-ci a nécessité la formulation d'hypothèses, qui ont été évoquées dans le chapitre 3. L'une des hypothèses fortes était de lier les variations de l'activité du système immunitaire aux variations de l'état énergétique de l'hôte au travers de l'indice de condition, l'ensemble du couplage entre le modèle hôte et le développement du pathogène reposant sur cette hypothèse.

Le modèle a essentiellement été calibré à partir de données provenant d'expérimentations en laboratoire. Le suivi simultané des conditions environnementales, des paramètres hémocytaire et des maladies présenté dans le chapitre 4 avait pour objectif de valider ou d'infirmer par des observations en milieu naturel les hypothèses formulées lors de la construction du modèle.

Sans être exhaustif, ce chapitre a pour objectif de confronter les observations effectuées en milieu naturel avec certaines des hypothèses formulées lors de la construction du modèle.

6.2   Forçage par l'environnement

Dans le modèle l'effet de la température est pris en compte a plusieurs niveaux : au niveau du bilan énergétique de l'hôte, de la croissance du *Vibrio* et du système immunitaire. Les observations de terrain ont permis de montrer que la température était le facteur environnemental expliquant la plus grande part de la variabilité expliquée des paramètres hémocytaires. Les variations saisonnières de la concentration en granulocytes et du nombre total d'hémocytes circulant sont en effet significativement positivement corrélées à la température (*cf* Tab. 4.1 p. 60), ce qui tend à confirmer cette relation du modèle. Par contre ce n'est pas le cas du pourcentage de phagocytose, qui ne présente pas de corrélation significative avec la température (*cf* Tab. 4.1 p. 60). Ce pour-

centage de phagocytose est mesuré en comptant le nombre d'hémocytes ayant phagocyté trois billes de latex et plus, les incubations des hémocytes avec les billes ayant lieu a température ambiante (*cf* p. 55) et donc pas à la température observée sur le terrain. Cette valeur ne caractérise donc que le pourcentage d'hémocytes aptes à la phagocytose, valeur qui semble être peu affectée par la température d'incubation (Marie-Agnès Travers, pers. comm.), mais ne permet pas d'évaluer la cinétique de phagocytose très probablement température dépendante. La capacité de phagocytose ne pourrait donc être évaluée qu'en tenant compte de la concentration en hémocytes, du pourcentage de phagocytose et de la dynamique de la phagocytose. Il est donc difficile de conclure quand à la relation entre la température et l'activité de phagocytose prise en compte dans le modèle.

La relation entre température et nombre total d'hémocytes peut être confirmée par des observations de terrain. Par contre la prévalence et l'intensité de la maladie n'ont pas montré de variations significatives au cours de la période d'investigations sur le terrain (*cf* Fig. 4.4 p. 64). Ceci montre donc que le lien entre le nombre total d'hémocytes et le développement de la maladie qui a été fait dans le modèle est difficile à confirmer par des observations *in situ*. Par ailleurs, l'absence de variations saisonnières de la maladie observée sur le terrain ne saurait être prédite par le modèle du fait de la forte influence de la température sur le système de défense contre le pathogène prise en compte dans le modèle.

En milieu naturel, il n'a pu être montré aucune corrélation entre la ressource trophique disponible et les paramètres hémocytaires (*cf* Tab. 4.1 p. 60). La prévalence de la maladie, stable au cours de l'année, n'a pas non plus pu être reliée à la disponibilité trophique. Néanmoins, le laps de temps entre la présence de nourriture dans le milieu et l'énergie utilisable pour l'organisme associé au processus de filtration et d'assimilation peuvent expliquer cette absence de relation. Il semble donc plus cohérent d'examiner ce problème en prenant en compte l'indice de condition.

6.3 Indice de condition

Comme nous l'avons vu dans le chapitre 3, l'indice de condition, apportant une information sur l'état énergétique de l'hôte, joue un rôle majeur dans le couplage entre le modèle bioénergétique de l'hôte (exposé en chapitre 2) et le système de défense contre le pathogène. Cette hypothèse relève du fait que l'on observe que les individus malades présentent un indice de condition plus faible que les individus sains (Paillard, 1992). Par ailleurs, l'augmentation de

la prévalence est souvent observée en fin de période hivernale (Paillard *et al.*, 1997; Paillard, 2004a), coïncidant avec le minimum annuel d'indice de condition et laissant à penser que le statut énergétique contrôle le développement de la maladie.

6.3.1   Indice de condition et concentration en hémocytes

Dans le modèle d'interaction environnement–hôte–pathogène dont les concepts de base on été développés dans la section 3.2, la concentration en hémocytes est calculée en fonction de l'indice de condition. Les données du suivi mensuel exposé au chapitre 4, permettent d'examiner la relation entre ces deux paramètres sur le terrain. La Fig. 6.1 montre la relation entre ces deux paramètres observée sur l'île de Bailleron au cours de la période d'étude. Il existe une relation positive et significative entre ces deux paramètres. Néanmoins cette relation ne saurait expliquer que 3% de la variance de la concentration en hémocytes ($r^2 = 0.03$). Par ailleurs, cette relation prend en compte la variabilité saisonnière et donc l'effet de la température à la fois sur l'indice de condition et sur le nombre total d'hémocytes. La relation entre les deux paramètres, indépendamment des variations saisonnières, a été examinée dans le Tab. 4.2 (p. 63). La relation est aussi significative, mais l'indice de condition n'explique alors plus que 0.9% de la variance de la concentration totale en hémocytes. En prenant en compte ces observations en milieu naturel, il semble difficile de valider cette hypothèse de construction du modèle.
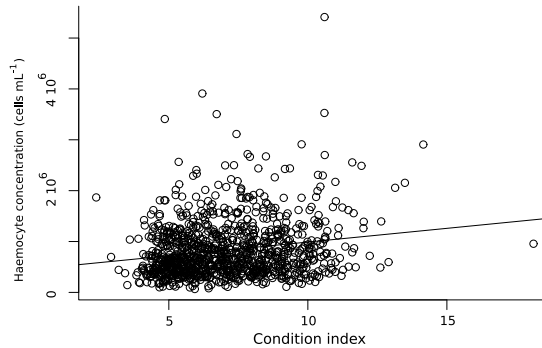
FIG. 6.1: Relation entre la concentration en hémocytes ($cellules.mL^{-1}$) et l'indice de condition sur l'ensemble du suivi. Modèle linéaire : $y = 5.4\,10^4 x + 4.5\,10^5$; R^2=0.03 ; p–value= $1\,10^{-9}$.

6.3.2 Relation entre l'indice de condition et les symptômes

Les données présentées dans le chapitre 4 permettent aussi d'examiner la relation entre l'indice de condition et la présence des symptômes. La Fig. 6.2 (A) montre l'évolution de l'indice de condition des individus symptomatiques et asymptomatiques au cours de la période d'étude. Sur ce graphique, on peut noter qu'il n'existe pas de tendance divergente entre les deux groupes. Pour chacun des prélèvements les différence d'indice de condition entre les individus sains et malades ont été testées (Test de Kruskal–Wallis), il n'a pas été possible de mettre en évidence de différence significative (p–value > 0.05).

La Fig. 6.2 (B) montre les indices de conditions d'individus sains et malades lors de la période hivernale (du 20/10/04 au 12/02/05) pendant laquelle l'indice de condition reste stable (voir Fig. 6.2 A). On notera qu'il n'y a pas de différence apparente entre les individus sains et malades, indiquant que des individus malades peuvent avoir des indices de conditions élevés.

Lors de la période d'investigation en milieu naturel, la prévalence et l'intensité des symptômes étaient faibles (*cf* p. 63) ; ce jeu de données montre donc qu'à des stades faibles de développement de la maladie il n'y a pas de relation entre l'indice de condition et le stade de maladie. Si l'on fait l'hypothèse que le statut énergétique contrôle le développement de la maladie alors on s'attend à ce que les individus présentant un indice de condition faible éliminent moins efficacement le pathogène. Dans ce cas, on peut s'attendre à observer que les individus présentant des intensités de symptômes faibles aient un indice de condition faible par rapport à leur congénères non infectés. Or la Fig. 6.2 (B) montre que des individus infectés peuvent présenter des valeurs élevés d'indice de condition, laissant a penser que la susceptibilité à la maladie est indépendante de l'indice de condition. Sur la base de ces observations il semble donc difficile de confirmer cette hypothèse forte de la construction du modèle. La relation entre l'indice de condition et la présence de symptômes observée par Paillard (1992) a été décrite pour des individus présentant un fort développement des symptômes, ce qui suggère que dans ce cas la maladie affecte le bilan énergétique de l'hôte et de ce fait l'indice de condition.

6.4 Conclusion

Il semble que certaines des hypothèses du modèle puissent être confirmées par les observations provenant du milieu naturel, notamment en ce qui concerne l'effet de la température sur la concentration totale en hémocytes, cependant si ce paramètre environnemental influence significativement la concentration en hémocytes il n'explique que 3,3% de sa variance totale au cours de

la période étudiée (*cf* 4.3 p. 66). Il en est de même pour la relation ente l'indice de condition et la concentration en hémocyte totale. Sur la base des résultats obtenus, il est difficile d'établir une relation claire entre la présence des symptômes et les paramètres hémocytaires, et il est donc difficile de conclure quant à leur rôle dans la susceptibilité à la maladie (*cf* chapitre 4).

Il semble aussi difficile d'associer des faibles valeurs d'indice de condition avec une quelconque susceptibilité à la maladie, hypothèse forte de la construction du modèle. Par contre il semble plutôt que l'on puisse relier le développement de la maladie avec une dégradation du bilan énergétique. Cet aspect sera donc étudié dans la partie suivante (Partie III).
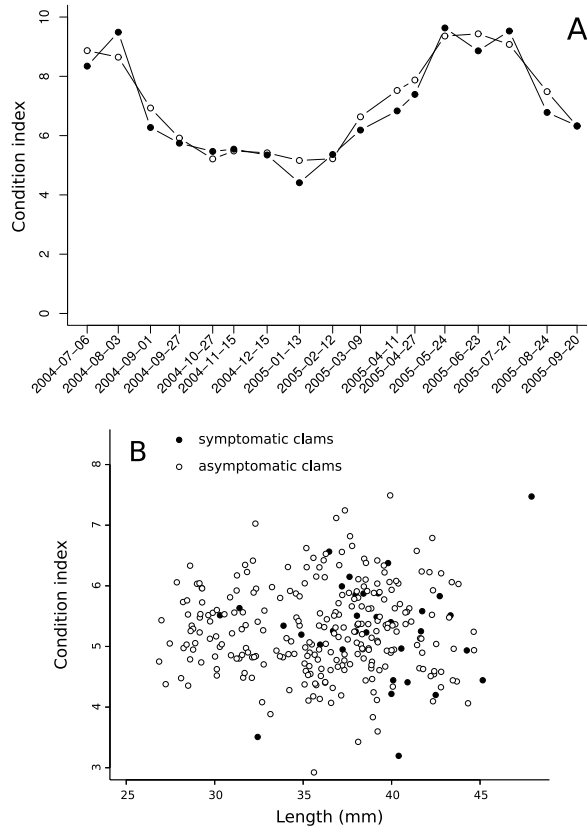
FIG. 6.2: A : Indice de condition moyen chez les individus sympto-
matiques (•) et asymptomatiques (○) au cours de la période d'étude.
Aucune différence significative n'a pu être mise en évidence entre les
individus sains et infectés pour chacune des dates de prélèvement (Test
Kruskal-Wallis ; p–value > 0.05). B : indice de condition chez les in-
dividus symptomatiques (•) et asymptomatiques (○) en fonction de la
taille au cours de la période hivernale (20/10/04 au 12/02/05). On note
la présence d'individus malades dans la partie haute du du nuage de
points.

Part III

BRD and host energy balance

Chapter 7

Impact of Brown Ring Disease on host energy budget

Jonathan FLYE-SAINTE-MARIE, Stéphane POUVREAU, Christine PAILLARD, Fred JEAN.

Abstract

Brown Ring Disease (BRD) is a bacterial disease caused by the pathogen, *Vibrio tapetis*. The disease induces formation of a brown deposit on inner shell of the Manila clam, *Ruditapes philippinarum*. Development of this disease is correlated with a decrease in the condition index of infected clams. Experiments were conduced in order to assess the effect of the development of BRD on two parameters affecting the energy balance of the clams: the clearance and the respiration rates. Experiments were performed in a physiological measurement system that allowed simultaneous measures of clearance and respiration rates. During both acclimation and measurements clams were fed with cultured *T-iso* and temperature was close to seasonal field temperature (10°C). Our results showed that severely diseased clams (conchiolin deposit stage, CDS $\geq$ 4) are subject to weight loss in comparison to uninfected ones, indicating that BRD induces a desequilibrium in the energy balance. We demonstrated a reduction of the clearance rate of severely diseased clams which led to a decrease in energy acquisition. Respiration rate showed asignificant decrease with BRD symptoms, but evidence in the literature allowed us to hypothesize that energy mobilised for an immune response and lesion repair increases overall organism maintenance costs. Both factors should thus contribute to the degradation of the energy balance of diseased clams. Because effects of BRD on naturally infected clams only appears significant for CDS $\geq$ 4, when brown ring assumes a significant place on the inner shell, we consider that the Manila clam is tolerant

of low disease levels.

Keywords: Clearance rate; filtration; respiration rate; Brown Ring Disease ; energy budget; *Ruditapes philippinarum*.

7.1 Introduction

Brown Ring Disease (BRD) in the Manila clam, *Ruditapes philippinarum*, was first observed in North Finistère (France) in 1987 (Paillard et al., 1989), and can be responsible for mass mortalities (see e.g. Paillard et al., 1989; Castro et al., 1992; Paillard, 1992, 2004b). This disease was shown to be caused by a *Vibrio* sp. (Paillard and Maes, 1990), which was named *Vibrio tapetis* (Borrego et al., 1996b). The infection disrupts the production of periostracal lamina and causes an anomalous deposition of periostracum on the inner shell of infected clams (Paillard and Maes, 1995a,b). Infected clams thus exhibit a characteristic brown deposit on the inner surface of the valves (Paillard et al., 1989) that gave the disease its name. Disease progression is estimated by the extent of the symptomatic deposit decribed by Paillard and Maes (1994). Infected clams show depressed defence-associated activities (Allam et al., 2000b; Paillard et al., 2004). The effects of BRD on Manila clams have been reviewed recently by Paillard (2004b).

Different studies of marine bivalve infections by pathogens and/or parasites have shown reduction in reproduction efficiency, condition and growth. The protozoan parasite *Perkinsus marinus* significantly reduces growth rate, condition index and gametogenesis of its host, *Crassostrea virginica* (Kennedy et al., 1995; Paytner, 1996; Dittman et al., 2001). A similar pattern has also been shown for *Perkinsus olseni* in the clam *Tapes decussatus* (see review in Villalba et al., 2004). The latter parasite also reduces the reproductive output of *R. philippinarum* (Ngo and Choi, 2004; Park et al., 2006a). The ascetosporan parasite *Haplosporidium nelsoni* also inhibits gametogenesis and reduces condition and glycogen reserves of its host, the oyster *C. virginica* (Barber et al., 1988a,b; Ford and Figueras, 1988). These results allowed the authors to conclude that infection induces an alteration of the host's energy budget. Nevertheless, few studies have been performed to document the influence of pathogens and/or parasites on components of the energy budget of bivalves such as food consumption and metabolism. The influence of the parasitism by the gastropod *Boonea impressa* on these parameters in the oyster *C. virginica* was documented by Ward and Langdon (1986) and Gale et al. (1991). The effects of *P. olseni* on food consumption and metabolism of *Tapes decussatus*

were documented in Casas (2002). Newell (1985) showed that the infection by the parasite *Haplosporidium nelsoni* reduced clearance rate but does not affect oxygen comsumption rate of the host *C. virginica*.

Experimental infections of Manila clams by *Vibrio tapetis* induced development of BRD, weight loss and depletion of glycogen reserves, suggesting an energetic cost of the disease (Plana, 1995; Plana et al., 1996). In the field, Goulletquer (1989b) also showed that winter mass mortalities of Manila clams were associated with low condition index and glycogen reserves. These mortalities were subsequently associated with BRD and Paillard (1992) demonstrated that BRD infected Manila clams exhibited low condition index. All these results lead to the conclusion that the development of BRD affects the energy balance of the Manila clam. The aim of this physiological study was to document the influence of the development of BRD on two components of the energy budget of naturally infected Manila clams: the clearance rate, a parameter involved in energy acquisition, and the respiration rate, reflecting the overall metabolism of the Manila clam.

7.2 Materials and methods

7.2.1 Biological material and acclimation procedure

Manila clams, *R. philippinarum*, were provided by the SATMAR hatchery and were grown in the Chausey Islands (Manche, France). Clams ranging from 37 mm to 50 mm were then transferred to Landéda (North Finistère, France) during autumn 2005. By early January 2006, BRD prevalence was 50%.

Samples were collected at low tide and transferred to IFREMER Argenton Shellfish Laboratory (North Finistère, France) on 13 January, and 2 and 28 February, 2006. As gametogenesis is initiated at 12°C in this species (Laruelle et al., 1994), clams from the three samples had empty gonads. Once in the laboratory, clams (37 to 50 mm length) were held in flow-through tanks in sieves containing field sediment. Tanks were supplied with thermoregulated, filtered (1 μm) seawater enriched in cultured microalgae *Isochrysis aff. galbana (T.iso)*. Salinity (35 ‰) and temperature (10°C) were kept constant during all experiments and were near to seasonal field conditions (field average temperature measured at Landéda during the experimental period was 9°C). Minimal acclimation time of one week before measurements was respected in order to limit influence of the stress due transfer from field to laboratory on our measurements. We limited acclimation time to a maximum of 4 weeks to avoid reparation processes or further development of BRD symptoms in laboratory conditions.

7.2.2   Physiological measurements

Physiological measurement system

Ecophysiological measurements were performed in the IFREMER Argenton Shellfish Laboratory, which is equipped with an experimental apparatus allowing the simultaneous monitoring of clearance rate (CR, $L\,h^{-1}$) and respiration rate (RR, $mg\,O_2\,h^{-1}$) in individual flow-through chambers, for seven individuals at a time (Savina and Pouvreau, 2004).

The apparatus consists of eight flow-through transparent chambers each having a volume of $1.2\,L$, (Fig.7.1 B) filled with $370\,g$ of sand. Sand was sieved on 1 mm mesh to avoid recirculation of small particles in the system and baked 4 h at 450°C to limit bacterial metabolism in the chambers. The first chamber (C0) was used as a control, the seven others (C1-C7) contained animals. Upstream water was thermoregulated, filtered (1 μm), and enriched with cultivated algae at a controlled concentration by means of a peristaltic pump. The flow rate through the chambers was controlled using manual flow meters (FM0 to FM7). Temperature, oxygen concentration and fluorescence were monitored alternately in the outflowing water of each chamber using an oxygen–meter (O$_2$; WTW sensor) and a fluorometer (F; Seapoint sensor). Data mesured by these sensors were collected by the controller and sent to a computer via a local area network. The controller controlled the valves that shunted water to either the measurement probes or to waste. The system allowed sampling of out-flowing water for particle counts.

Experimental conditions

A total of 15 experiments was performed between 15 January and 28 March 2006. For all experiments, conditions were similar. Temperature varied between 9.6 and 10.4°C and cultured algae concentration (*Isochrysis aff. galbana*; *T–iso*) in inflowing water was set to $50\,cells\,\mu L^{-1}$. Preliminary experiments (unpublished data) showed that this alga concentration was below the pseudofaeces production threshold for *R. philippinarum*. No pseudofaeces production was observed in any experiment thus ingestion rate was proportional to filtration rate.

Measurement procedure

For each experiment, individuals were placed in one of the eight individual chambers. A time interval of at least 2 h between the transfer of clams to the
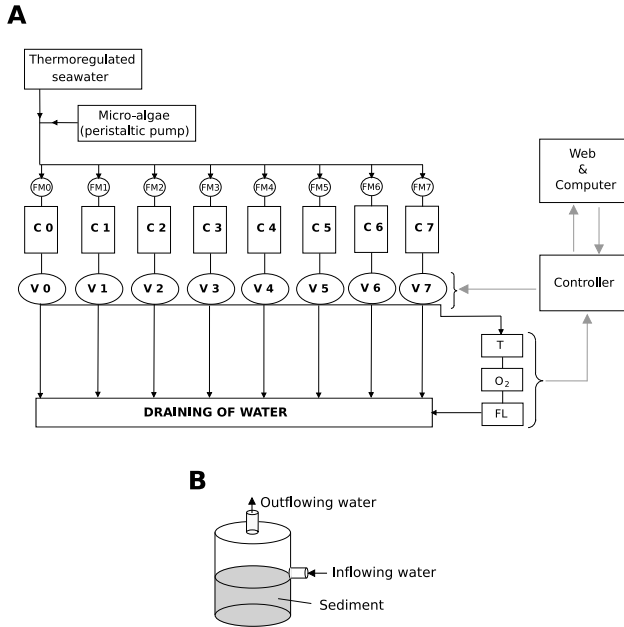
FIG. 7.1: The ecophysiological measurement system. A: General view (C: chamber, FM: manual flow meter, V: valve, T: temperature sensor, O_2: oxygen sensor, FL: fluorometer); B: individual chamber.

chambers and the beginning of any measurements allowed the clams to return to a normal activity. This time was chosen after preliminary experiments which showed that clams were consistently active 2 h after being transferred to the chambers. The first chamber was used as a control and had sediment but no clams. Flow rate in the chambers was constant and equal to $6.7 \, \text{L} \, \text{h}^{-1}$. This value was chosen after preliminary tests and allowed measurement of the respiration rate, while preventing the clam from removing too much algae. Experimental chambers were successively measured continuously for 5 min. Prior to each experimental chamber measurement, the control chamber was continuously measured for 3 min. Between each measurement a 5–min interval with no measurement allowed water from the next chamber to reach the sensors. This resulted in a record every 2 h and 20 min for each animal.

Every day, a new alga culture was used. Because the concentration of the culture varied, the flow rate of the peristaltic pump was adjusted to provide an algal concentration of $50 \, \text{cells} \, \mu\text{L}^{-1}$. Every day, excurrent water samples were collected for cell counting (Coulter counter, multisizer), which allowed

an intercalibration between fluorescence and cell concentration.

Characterization and classification of the BRD symptom requires observation of the inner surface of the clam shell (Paillard and Maes, 1994). Although this can be done in living clams, it is stressful (Ford and Paillard, 2007). As a consequence, diagnosis of BRD had to be done after the physiological measurements. Rhythmic variations in activity are well documented in bivalves (e.g. Bougrier et al., 1998; Kim et al., 2003; Ortmann and Greishaber, 2003; Rodland et al., 2006), including the Manila clam (Kim et al., 1999, 2001, 2004). They must be taken into account in order to obtain reliable individual measurements of clearance rate and respiration rate. A preliminary experiment was performed to determine the minimum experimental time needed to integrate these variations of activity. It was performed over 5 days under the experimental conditions cited above. After each respiration rate and clearance rate measurement, the average values were calculated from the beginning of the experiment. For both respiration and clearance rate, in all measured individuals, the average stabilized after 48 h. Thus 48 h was assumed to be the minimum experimental time needed to obtain measures that would reliably integrate variations in the activity of Manila clams.

7.2.3   Ecophysiological data processing

Average clearance rate

For each record, average values of the fluorescence of the effluent water from the control and from the experimental chamber were calculated. For each new cell culture, water-sample cell concentrations were measured using the Coulter Counter Multisizer 3 to allow the calculation of a regression equation between fluorescence and cell concentration. Using this equation, average fluorescence values were converted to cell concentration (cells L^{-1}). Then, for each record, the clearance rate (CR, $L\,h^{-1}$) was calculated following the equation (Hildreth and Crisp, 1976):

$$CR = \frac{C_c - C_a}{C_a} \times FR \qquad (7.1)$$

where C_c is the cell concentration (cells L^{-1}) in the effluent water from the control chamber, C_a is the cell concentration (cells L^{-1}) in the effluent water from the measured animal chamber and FR is the flow rate ($L\,h^{-1}$) through the chambers. The average of all records (c.a. 21 records per animal) was then calculated for each animal.

Average respiration rate

For each record, average values of the oxygen concentration of the effluent water from the control and from the experimental chamber were calculated. Then, the oxygen consumption rate (RR, $\mathrm{mg\,O_2\,h^{-1}}$) was calculated following the equation:

$$RR = (O_c - O_a) \times FR \tag{7.2}$$

where O_c is the oxygen ($\mathrm{mg\,O_2\,L^{-1}}$) in the effluent water from the control chamber, O_a is the oxygen ($\mathrm{mg\,O_2\,L^{-1}}$) in the effluent water from the measured animal chamber and FR is the flow rate ($\mathrm{L\,h^{-1}}$) through the chamber. Then the average of all records (c.a. 21 records per animal) was then calculated for each animal.

Maximum clearance rate

Our measurement procedure allowed us to examine instantaneous measurements of clearance rate (e.g. each of the 21 records). Maximum clearance rate was defined as the average of the three highest values obtained in the 21 records. Maximum clearance rate provides information about the filtration capacity of the clams, and permits discrimination between the impact of BRD on behaviour and that on physiological capacities.

Filtration and respiration–time activity

Filtration–time activity (FTA) and respiration–time activity (RTA) are defined as the proportion of time spent in the activity of filtration and respiration respectively (Bougrier et al., 1998; Huvet, 2000). Following Savina and Pouvreau (2004), FTA and RTA were calculated for each individual as the ratio between the number of records showing a measurable filtration or respiration activity and the total number of records. These values provide information about the behaviour of the clams.

Standardisation of clearance and respiration rates

In order to compare values obtained for different size individuals, clearance and respiration rates were corrected for weight differences between individuals following the formula of Bayne et al. (1987):

$$Y_s = (\frac{W_s}{W_m})^b \times Y_m \tag{7.3}$$

Were Y_s is the physiological rate for an individual of standard shell dry weight W_s , Y_m is the measured physiological rate for an individual of shell dry weight W_m and b the weight exponent for the physiological rate function. Clearance and respiration rates were standardised for a clam with a shell dry weight of 11 g (corresponding to a length of 43.9 mm). Considering that filtration and respiration processes scale with somatic tissue weight and that BRD may induce a loss of reserves rather than somatic tissue, shell dry weight was used as a proxy of somatic weight for correction of physiological rates for size. Reviews concerning weight exponents calculated for several bivalves (Pouvreau et al., 1999; Savina and Pouvreau, 2004, for clearance and respiration, respectively) showed that average weight exponents are generally around 2/3 for clearance and 3/4 for respiration. These values were thus chosen for standardisation of clearance and respiration rates respectively.

7.2.4 Biological sample treatment

Condition index

After each experiment, clams were individually numbered, flesh was removed from the shell, freeze-dried to constant mass (48h) and weighed. Shells were measured along the maximum length axis, dried and weighed. Condition index (CI) was calculated following

$$CI = \frac{Flesh\ Dry\ Weight}{Shell\ Dry\ Weight} \times 100 \qquad (7.4)$$

Characterisation and classification of BRD syndrome

Disease stage was classified according to the description of Paillard and Maes (1994). According to these authors, conchiolin deposit stage (CDS) range from microscopic brown spots on the inner face of the shell in the earliest stage (CDS 1) to a complete thick brown ring in the most advanced stage (CDS 7).

Statistical analysis

Statistical analysis were performed using the R software (R Development Core Team, 2006). ANOVA was used to test the effect of BRD development stage (CDS) on measured physiological rates after checking homoscedasticity (Barttlet test). Since FTA and RTA are ratios, data were arcsin–transformed and the same procedure used.

7.3 Results

7.3.1 Effect of BRD stage on condition index

Development of BRD symptoms was associated with a weight loss of the clams. Condition index decreased as the severity of BRD symptoms increased (Fig. 7.2). There were significant differences of condition index among CDS levels (ANOVA, f-value=12.89, p-value= $1.7\,10^{-11}$). In clams with CDS > 4, condition index was 27 to 35 % less than that of asymptotic (CDS = 0) clams (HSD Tukey, p-value < 0.05, see Fig. 7.2); however there were no significant differences between clams in CDS=0 and in those in CDS=1–4.

FIG. 7.2: Relationship of mean condition index (mean $\pm$ SE) with conchiolin deposit stage (CDS). p is the HSD Tukey p-value for the comparison with CDS=0. n = number of individuals in each CDS class.

7.3.2 Effect of BRD stage on respiration rate

Respiration rate decreased with the extent of BRD development (Fig. 7.3) and was significantly lower for clams with CDS $\geq$ 5 in comparison to asymptomatic (CDS=0) ones (ANOVA, f-value=4.86, p-value= $1.1\,10^{-4}$; HSD Tukey, p-value < 0.05, see Fig. 7.3). No clear effect of BRD was found for respiration–time activity.

7.3.3 Effect of BRD stage on clearance rate

Average clearance rate was negatively affected by the development of the brown ring symptom (Fig. 7.4). The clearance rate of clams with CDS $\geq$
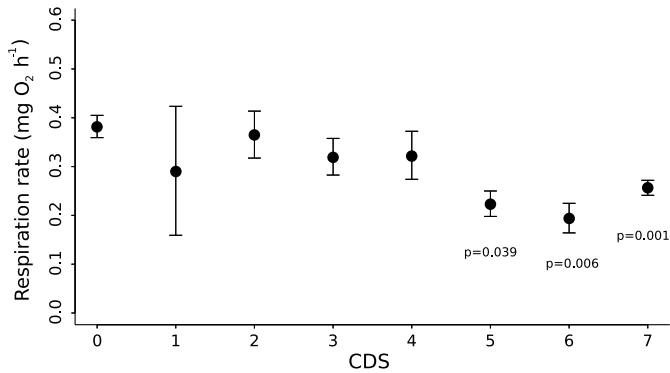
FIG. 7.3: Relationship of mean respiration rate (mean $\pm$ SE) with conchiolin deposit stage (CDS). p is the HSD Tukey *p*-value for the comparison with CDS=0. The number of individuals in each CDS class is indicated in Fig. 7.2.

4 was significantly lower than that of asymptomatic (CDS=0) clams (ANOVA, *f*-value=9.01, *p*-value= $2.0\,10^{-8}$; HSD Tukey, *p*-value < 0.05, see Fig. 7.4). The clearance rate of the former was 45% to 62% lower compared to latter.

Maximum clearance decreased with the development of BRD symptoms (Fig. 7.5), and was significantly lower in clams with CDS ≥ 4 compared to asymptomatic ones (CDS = 0) (ANOVA, *f*-value=8.35, *p*-value= $7.4\,10^{-8}$; HSD Tukey, *p*-value < 0.05, see Fig. 7.5). Maximum clearance rate in the former decreased between 41% and 56% in comparison to latter, thus suggesting that filtration capacity is affected by the development of BRD.

Filtration–time activity was also negatively affected by the development of BRD (Fig. 7.6). In individuals with CDS ≥ 4, FTA was significantly lower than for asymptomatic individuals (ANOVA, *f*-value=6.40, *p*-value= $3.8\,10^{-6}$; HSD Tukey, *p*-value < 0.05, see. Fig. 7.6) except for individuals with CDS = 6 (HSD Tukey, *p*-value > 0.05, see. Fig. 7.6) presumably because of the low number of individuals (n=6). On average, individuals with CDS < 4 spent between 80 and 95% in filtration activity, whereas severely diseased ones (CDS ≥ 4) spent between 67 and 59%.
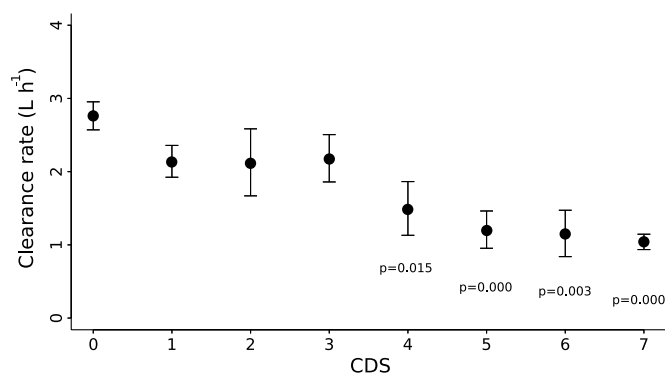
FIG. 7.4: Relationship of mean clearance rate (mean $\pm$ SE) with conchiolin deposit stage (CDS). p is the HSD Tukey *p*-value for the comparison with CDS=0. The number of individuals in each CDS class is indicated in Fig. 7.2.

7.4   Discussion

Effect of BRD development on the Manila clam energy budget   Clams with high CDS (> 4) exhibited a decrease of 27% to 35% in their condition index, indicating significant weight loss associated with the disease. These results are in accordance with Goulletquer (1989b), who showed that winter mortalities in Manila clams along the French Atlantic coast in the 1980s were associated with a decrease in the condition index and in the glycogen reserves, wich constitute the main energy reserves for bivalves (see reviews by Gabbot, 1976, 1983; Lucas, 1993). These winter mortalities were subsequently attributed to BRD (Paillard, 1992). Our results also confirm the observations of Plana (1995) and Plana et al. (1996), who showed that Manila clams experimentally infected by *Vibrio tapetis* showed a significant decrease in dry weight and glycogen reserves in comparison to uninfected individuals. In marine bivalves, weight loss associated with microparasite infection is a general pattern. *Haplosporidium nelsoni* and *Perkinus marinus* infections have been shown to reduce condition of the Eastern oyster *Crassostrea virginica* (see e.g. Barber et al., 1988a; Paytner, 1996). *P. olseni* was also shown to reduce condition in the clams *Tapes decussatus* (see. review in Villalba et al., 2004) and *Ruditapes philippinarum* (Park et al., 1999). Our results show that BRD, as is the case with other pathological conditions, affects the energy budget of the Manila clam.
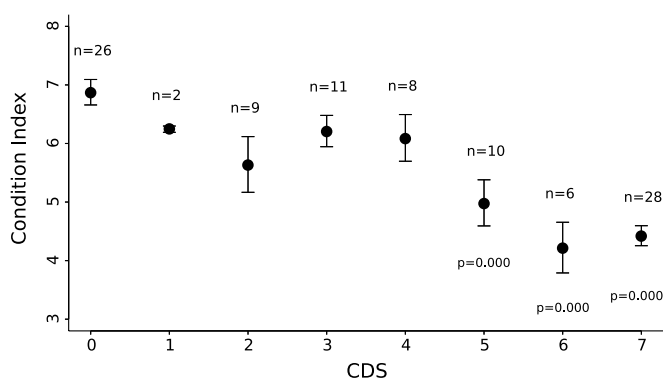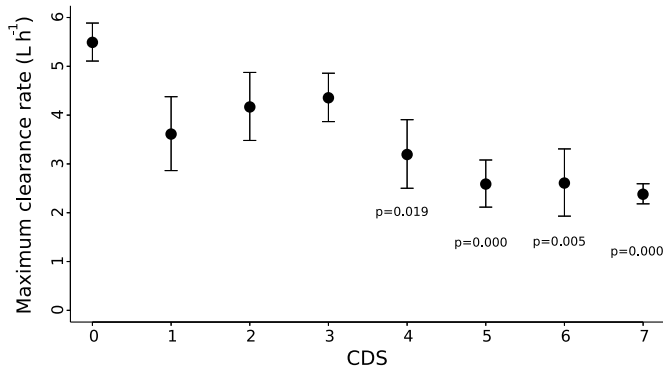
FIG. 7.5: Relationship of mean maximum clearance rate (mean $\pm$ SE) with conchiolin deposit stage (CDS). p is the HSD Tukey *p*-value for the comparison with CDS=0. The number of individuals in each CDS class is indicated in Fig. 7.2.

Effects of BRD development on filtration activity   A first source of alteration of the energy budget of infected Manila clams is the decrease of the average clearance rate. Clams exhibiting elevated CDS (≥ 4) showed a 45% to 62% decrease in their clearance rate, thus decreasing the energy input. Maximum clearance rates are significantly affected by the development of BRD also, which tends to show that filtration capacity is affected by BRD. Different explanations can be hypothesized to explain this decrease in the filtration capacity.

1. *Vibrio tapetis*, the etiologic agent of BRD, could induce gills lesions that would affect filtration ability. Such gills lesion were found in Manila clams populations experiencing winter mortalities in British Columbia by (Bower, 1992), but these mortalities were not linked to BRD. Moreover gills lesions have never been associated with the development of this disease (Paillard, unpublished observations).

2. Another explanation is that gill activity could be inhibited by a factor secreted by *Vibrio tapetis*. McHenery and Birkbeck (1986) showed that suspensions of marine vibrios (*V. anguillarum* and *V. fisheri*) inhibited filtration by adult *Mytilus edulis*. These authors hypothesized the involvement of an inhibitory surface or secreted factor, which inhibited gill ciliary activity, to explain this phenomenon. Secretion of toxins has been shown for different pathogenic *Vibrio* species. Labreuche et al.
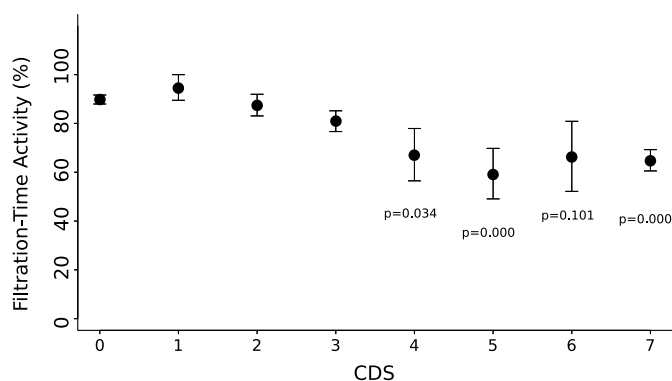
FIG. 7.6: Relationship of filtration–time activity (FTA; mean $\pm$ SE) with conchiolin deposit stage (CDS). p is the HSD Tukey *p*-value for the comparison with CDS=0. The number of individuals in each CDS class is indicated in Fig. 7.2.

(2006) showed that *Vibrio aesturianus* extracellular products (ECP) induced an inhibition in phagocytic and adhesive capabilities of *Crassostrea gigas* haemocytes. These authors concluded that an important part of the pathogenicity of this bacteria is attributable to *Vibrio aesturianus* extracellular products. *Vibrio tapetis* ECP have been shown to induce vacuolization, rounding, shrinking, detaching, and finally, destruction of fish cultured cells (Borrego et al., 1996a) and to inhibit adhesion properties of *R. philippinarum* haemocytes (Choquet, 2004). The existence of deleterious ECP effects by *V. tapetis* supports the hypothesis that filtration activity could be inhibited by one or more factors produced by this bacterium.

3. Goulletquer et al. (1989a) showed that the siphons of clams with heavy brown ring deposit tend to remain retracted and to maintain them at a 45° angle rather than vertically. This interference could thus decrease the pumping efficiency. Furthermore, these authors showed that thickness of the brown deposit induces a lack of tightness of pallial cavity, which could contribute to the degradation of the filter–pump efficiency. Thus a mechanical interference could be hypothesized to explain decreased filtration capacity.

Considering that the effects of BRD on filtration become significant only at CDS ≥ 4, when the brown deposit assumes a significant place on the inner

shell surface (Paillard and Maes, 1994) and that the relationship between *V. tapetis* densities and CDS is higly variable, as high *V. tapetis* concentrations can be found in clams with low CDS (Paillard, unpublished data) the latter hypothesis appears most consistent with available data. In the field, Manila clams live mainly in the intertidal zone and filtration is not possible during low tide. Moreover, food concentration may vary with the tidal cycle and over short time scales (Smaal and Haas, 1997; Smaal and Zurburg, 1997). Consequently, for such an intertidal bivalve, food is available during a limited period only; thus, decreased filtration capacity should lead to a pronounced loss of efficiency in the exploitation of available trophic resources.

Our results also show that filtration behaviour is affected by the development of BRD because filtration–time activity is reduced in clams with CDS $\geq$ 4. Ward and Langdon (1986) showed that physical irritation of the mantle by the parasitic gastropod *Boonea impressa* induces frequent valve adductions in *Crassostrea virginica* resulting in a decreased clearance rate. The presence of a thick conchiolin deposit along the shell margin may similarly cause an irritation that reduces time spent in filtration activity. Finally, burrowing activity has been shown to be affected in strongly diseased clams (Goulletquer et al., 1989a; Paillard, 1992). We can thus hypothesize that the development of BRD induces an inhibition of the overall activity of diseased clams.

This study shows that decrease in the average clearance rate of Manila clams with CDS $\geq$ 4 can be attributed both to a decrease in the filtration capacity and a change in the filtration behaviour. Plana and Le Pennec (1991) and Plana (1995) showed that BRD induces a degeneration of the digestive diverticula and concluded that digestion efficiency may be negatively affected by development of BRD. Such a decrease in the average clearance rate combined with a possible loss in digestion efficiency translate into reduced energy input that explains part of the observed weight loss linked to BRD development.

Effects of BRD development on overall metabolism   Respiration rate decreased with the development of BRD symptoms. Highly diseased clams (CDS $\geq$ 5) had lower respiration rates than asymptomatic ones. As feeeding rate is depressed at the same CDS levels, this decrease in oxygen consumption could be interpreted as a compensatory reduction of metabolic rate. Nevertheless, feeding processes may be associated with an important energy expenditure (Bayne, 2004) because digestion and absorption may amount to 15-20% of the total energy expenditure (Widdows and Hawkins, 1989); moreover feeding in bivalves is dependent on the secretion of mucus (Beninger and Venoit, 1999). Thus, part of the respiration measured during our experiments may be

attributable to the feeding processes. This may explain this decrease of respiration rate at CDS$\geq$5, when filtration was reduced.

Furthermore, Plana et al. (1996) and Plana (1995) presented evidence suggesting that starved Manila clams experimentally infected by *V. tapetis* lost weight at a greater rate than did uninfected control clams. This differential weight loss and energy depletion could not be explained by a difference in energy acquisition since both groups were starved. Rather, these results suggest an extra energy expenditure linked to the infection and thus other explanations for the effect of BRD on the clam's energy budget should be considered:

1. Energy is required for the growth of the *Vibrio tapetis* population which is normally restricted to the extrapallial fluids. This bacteria, was shown to have a high growth rate ($0.84 \, \text{h}^{-1}$) when cultured in Manila clam extrapallial fluids (Haberkorn, 2005). Taking into account this growth rate, the average bacterial burden in extrapallial fluids at CDS=7 ($2.25 \, 10^5$ cells ml^{-1}; measured by ELISA test; Paillard, unpublished data) and a generic value of yield efficiency for microrganisms ($0.024 \, \text{g DW}$ produced per KJ consumed; calculated from Prochazka et al., 1970), the energy consumption of the *V. tapetis* population for its growth was estimated as less than 1% of the metabolised energy (respiration) of the clam. This value may be overestimated because growth rate value was obtained at 18°C, temperature which is near to the thermal growth optimum of *V. tapetis* (Haberkorn, 2005). This rough estimate allows us to conclude that the host energy loss due to the *V. tapetis* population growth is very low and can not explain the weight loss and reserve depletion observed by Plana et al. (1996) and Plana (1995). Choi et al. (1989) showed that, for heavily infected oysters *Crassotrea virginica*, the protozoan parasite *P. marinus* consumes more energy than the oyster has available after meeting its own metabolic needs. This difference can be explained by the fact that, in the case of BRD, the parasite's biomass relative to the host's biomass is much lower.

2. Lesions have been observed in the digestive gland and the mantle of highly infected clams (Paillard, 1992; Plana and Le Pennec, 1991; Plana, 1995; Paillard, 2004b); thus, an energy demand could be associated with cell repair functions and clearance of damaged tissues. However, such processes are difficult to assess, although there is evidence for their energetic cost (Freitak et al., 2003; Romanyukha et al., 2006). An energetic cost may also be associated with production of the symptomatic conchiolin deposit. Conchiolin being mainly composed of proteins (Goulletquer et al., 1989a), its production may also be energetically costly.

Nevertheless, the dynamic of this production remains poorly known and can't be precisely estimated.

3. The energy mobilised for the development of immunological response to the pathogen (see reviews in Paillard, 2004b,a) may deplete reserves. The metabolic cost of immunity is difficult to assess during an immune challenge (Schmid-Hempel, 2003) and very few studies exist that show evidence of the energetic trade-off among immunity and other competing physiological and behavioral functions in molluscs. Activation cost of the response of immune system has been convincingly demonstrated in a wide range of animals and uses up a tangible part of an organism's energy budget (see review by Schmid-Hempel, 2003). In mammals (Lochmiller and Deerenberg, 2000) the metabolic costs of mounting an immune response range from about 10% up to 30% of the resting metabolic rate; in birds, an increase in basal metabolic activity of 9% has been measured, correlated with a 3% weight loss (Kerimov et al., 2001). Butterfly pupae raised their standard metabolic rate 8% when both humoral and cellular immune responses leading to melanization are induced (Freitak et al., 2003). Development of BRD may induce an energetically costly response of the clam's immune system in the context of the trade-off concept, coupled to finite energy inputs and reserves that must be allocated to a wide variety of competing biological functions. Furthermore, shell reparation by calcification of the conchiolin deposit has been documented (Paillard and Maes, 1994). An energy demand could thus be associated with shell repair functions. Palmer (1992) emphasized that the main energetic cost of production of shell in marine molluscs can be attributed to shell organic matrix. Goulletquer and Wolowicz (1989) showed that the shell matrix accounts for 2–3% of the total shell weight in the Manila clam. Consequently, the energetic cost of shell repair is probably not very high.

All these energetic costs are included in the organism's overall maintenance costs and should lead to variations in the basal metabolism. Further measurements of respiration rate on starving animals are needed to document the influence of BRD development on the basal metabolism of *R. philippinarum*.

Conclusions   In conclusion, the present study shows that in naturally infected clams, the observed effects of BRD become significant only for CDS ≥ 4, when the conchiolin deposit assumes a significant place on the inner shell surface. This emphasize that the energetic cost of BRD is dependent on the inten-
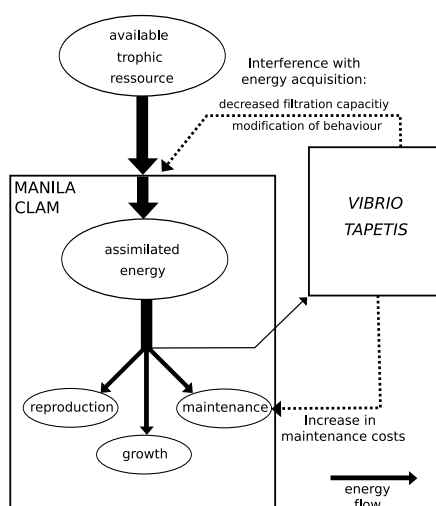
FIG. 7.7: Energetics of Manila clam / *Vibrio tapetis* interactions. Although a small amount of energy is required for *V. tapetis* population growth, the energy balance of the Manila clams is altered by the development of BRD through two main ways: (1) interference with energy acquisition by a decrease in the filtration capacity and a modification of the filtration behaviour and (2) increased maintenance costs.

sity of the symptoms. Alteration of the energy balance of the Manila clams by the presence of *V. tapetis* can be summarized by the scheme in Fig. 7.7. One primary way in which the energy balance is affected is the decrease in the energy inputs through a degradation of the filtration capacity and a modification of the filtration behaviour. A second way may be an increase in maintenance costs, due to the defence processes induced against the pathogen. Further investigations are needed to determine the relative contribution of these two factors on the overall degradation of the host energy budget.

Aknowledgements

Chapter 8

Energetic cost of Brown Ring Disease in the Manila clam, a modelling study

Abstract

Brown Ring Disease (BRD) in the Manila clam, *R. philippinarum*, is a bacterial disease caused by the pathogen *Vibrio tapetis*. This disease induces the formation of a characteristic brown conchiolin deposit on the inner shell and is associated with a decrease in condition index indicating that the development of the disease affects the energy balance of the clam. A previous study showed that the energy budget of the host was affected by a decrease in filtration activity, and hypothesized that a second way to degrade the energy balance was the increase in maintenance costs associated to the cost of immune response and lesion repair.

A starvation experiment confirmed that the energy balance was affected by BRD, independently of the effects on filtration activity, indicating an increase in the maintenance costs. An energy budget model of the Manila clam, based on DEB theory, was developed and allowed to properly predict length growth and weight loss at constant environmental condition. *Vibrio* development and its effects on the energy budget of the host was theoretically introduced in the model. Coupling modelling and experimental observations allowed to provide a quantitative and dynamic estimation of the increase in maintenance costs associated with the development of BRD. The estimation which is given here, indicates that during an infection the maintenance cost can almost double compared to the uninfected situation

Further development of the model, especially focussed on *Vibrio* dynamics and its effects on filtration activity will allow to provide a more extensive description of the energetic cost of BRD in the Manila clam.

8.1 Introduction

Brown Ring Disease in the Manila clam, *R. philippinarum*, is a bacterial disease caused by the pathogen *Vibrio tapetis* (Paillard and Maes, 1990; Borrego et al., 1996b). This clam species was introduced in western Europe at the beginning of the 70s (Flassch and Leborgne, 1992) for aquaculture purpose; venerid culture became subsequently increasingly important along the French Atlantic coast. BRD appeared in cultured clam beds of the Northwest cost of France in 1987 and caused mass clam mortalities (Paillard, 1992; Paillard et al., 1994). Disease progression has been recently reviewed in Paillard (2004b). The pathogenic agent, *V. tapetis*, penetrates and develops within the peripheral extrapallial compartment (*i.e.* peripheral space between mantle and shell). The infection disrupts the normal production of periostracal lamina and causes an abnormal deposit of periostracum on the inner shell (Paillard and Maes, 1995a,b). Therfore, diseased clams exhibit a characteristic brown deposit on the peripheral inner shell surface (Paillard et al., 1989) that gave the disease its name. Monitoring disease progression is based on the extent of the symptoms following a classification scale described by Paillard and Maes (1994). Defence processes against the bacterium occur in the extrapallial fluids in part at least through phagocytosis by hemocytes (Allam and Paillard, 1998; Allam et al., 2000a, 2001).

Infection by pathogens and/or parasites in bivalves has often been associated with evidences of modification of the energy budget of the host: reduction in reproduction efficiency, condition and growth. Several studies showed that infections by protozoan parasites of the genera *Perkinsus* reduce gametogenesis or reproductive output, condition index and growth rate in various host species: the oyster, *Crassostrea virginica* (Kennedy et al., 1995; Paytner, 1996; Dittman et al., 2001), the European clam, *Tapes decussatus* (see review in Villalba et al., 2004) and the Manila clam, *Ruditapes philippinarum* (Ngo and Choi, 2004; Park et al., 2006a). A similar pattern has also been shown for the infection by the ascetosporan *Haplosporidium nelsoni* which reduces gametogenesis, condition and glycogen reserves of the oyster *C. virginica* (Barber et al., 1988a,b; Ford and Figueras, 1988). BRD has also been associated with a decrease in flesh weight, condition and glycogen reserves (Paillard, 1992; Plana, 1995; Plana et al., 1996; Flye-Sainte-Marie et al., 2007b). All these observations indicate that infections affect the energy balance of the host; nevertheless, no studies provided a quantitative approach for these processes.

An experimental approach based on measurements of clearance and respiration rates detailed the impact of BRD on the energy budget of the Manila clam (Flye-Sainte-Marie et al., 2007b, see chapter 7). This study showed that

clams presenting heavy symptoms presented a significant weight loss, indicating that BRD can be associated with a modification of the energy budget of the host. This study emphasized that one way of alteration of the energy balance is an inhibition of the filtration activity leading to a decrease in the energy input. Surprisingly, clams presenting heavy symptoms had also significantly lower respiration rates (Flye-Sainte-Marie et al., 2007b). Respiration results from various processes in the organism (assimilation, maintenance, growth. . .) (see e.g. Kooijman, 2000), thus this paper hypothesize that the decreased respiration rate can be explained by the decrease in filtration activity rather than a decrease in the organism maintenance costs. This hypothesis is supported by the observations of Plana (1995) and Plana et al. (1996) that indicated that starved Manila clams infected by *V. tapetis* presented a higher weight loss than uninfected ones. This result suggests that the energy budget of infected clams is affected independently of feeding activity. Flye-Sainte-Marie et al. (2007b) thus hypothesised that BRD development was associated with an increase in maintenance costs due to immune response and lesions repair.

Dynamic Energy Budget (DEB) theory (Kooijman, 1986, 2000) provides a mechanistic framework for the study of mass and energy budgets in living systems. This theory describes quantitatively energy flow through living organisms and its allocation to growth, development, reproduction and maintenance. This theoretical approach have been applied to model growth and reproduction under influence of environmental factors in various bivalve species (Ross and Nisbet, 1990; Van Haren and Kooijman, 1993; Ren and Ross, 2001, 2005; Bacher and Gangnery, 2006; Pouvreau et al., 2006; Cardoso, 2007). The explicit rules of allocation of energy to maintenance provide a powerful tool to study the impact of disease on the energy budget of the host.

By coupling experimental starvation data of infected and uninfected clams and modelling approach, the aim of present study is to propose an approach allowing a quantitative estimation of the energetic cost of BRD.

8.2 Methods

8.2.1 Experimental data: starvation experiment

Biological material and infection procedure

Manila clams, *Ruditapes philippinarum*, ranging from 33 mm to 42 mm length (36.4 mm $\pm$ 1.7) came from a natural population in Baie de Lanveur, Bay of Brest (Finistère, France). Clams were transferred the 11 May 2007 to the Laboratoire des Sciences de l'Environnement Marin (LEMAR, IUEM, Plouzané,

North Finistère, France). Clams were held in 90 L tank equipped with a pump and an airing system allowing homogenisation and oxygenation of the water. Clams were acclimated to experimental conditions (15.7 °C ± 0.3; 0.5 μm filtered seawater; salinity 33.5 ‰) for 13 days before beginning the experiments.

Experimental infections were performed at 24 May 2007. Brown Ring Disease was experimentally induced in individual clams by injection of $5\,10^7$ cells of *Vibrio tapetis* (strain CECT 4600) into the pallial cavity as described by Paillard and Maes (1990). Prior to injection, virulence of the bacterial strain was checked following the Choquet et al. (2003) protocol. Individuals were separated in four groups: a control group (170 individuals) injected with sterile sea–water, two groups of 170 individuals each injected with *V. tapetis*, and a group of 40 individuals dissected for estimation of initial weight.

Starvation experiment

Each group (control + 2 infected groups) were held in a 90 L tank equipped with a pump and an aeration system allowing homogeneisation and aeration of the water. Goulletquer (1989a) showed that the retention efficiency was null for 1 μm particles in *R. philipinarum*, thus tanks were filled with 0.5 μm filtered seawater (salinity 33.5 ‰) to avoid any available potential trophic particle in the water. The tanks were held in a thermoregulated room (13°C) and water in the tanks was heated to 15.7°C, temperature was controlled using a thermostat. An autonomous temperature data logger (EBI-125A, Ebro, Germany) recorded the water temperature in the tanks every 20 min to control thermoregulation. The average measured temperature in the tanks was 15.7 ± 0.3 °C. Half of the water was renewed three times a week.

The experiment lasted for 3 month. Every month (2007-June-25, 2007-July-20 and 2007-August-21), 30 clams from each tank were dissected. Wet weight was measured, flesh was freeze-dried to constant mass (48h) and dry weight was measured. Shells were sized following the maximum length axis. Disease progression was monitored on the shells. Disease stage was classified according to the description of Paillard and Maes (1994). According to these authors, conchiolin deposit stage (CDS) range from microscopic brown spots on the inner face of the shell in the earliest stage (CDS 1) to a complete thick brown ring in the most advanced stage (CDS 7).

Based on the assumption that average flesh weight is proportional to cubed length (L^3), all dry flesh weights were corrected for size differences and standardized for a length of 37 mm.

To present the results of this experiment, individuals were classified into three groups: asymptomatic individuals, individuals presenting light symp-

toms ($1 \leq \text{CDS} \leq 3$) and clams presenting heavy symptoms ($\text{CDS} \geq 4$). In each group, mean and confidence intervals of standardized dry flesh weight were estimated using ordinary bootstrap (Efron and Tibshirani, 1993; Davison and Hinkley, 1997) with 999 replicates; 95% percentiles were used to determine width of the confidence intervals. Differences in mean lengths were tested using a classical student t test, after a Fisher test of homoscedasticity. All statistical analysis were performed using the R statistical software (R Development Core Team, 2006).

8.2.2 Model formulation

Structure of the model and basic concepts

The structure of the model is illustrated in Fig. 8.1, the host module is based on DEB theory (Kooijman, 2000), the interaction with the pathogen is adapted from Flye-Sainte-Marie et al. (2007b, see Fig. 7.7, p. 109).

According to Kooijman (2000), the energy budget of an organism can be fully described by the dynamics of three state variables: (1) the of structure (M_V), which corresponds to the somatic tissue excluding reserves; (2) the mass of reserves (M_E) and (3) the mass of the "reproduction buffer", which corresponds to reserves allocated to reproduction. The flux of energy from food goes into reserves. Flux of energy from reserves is allocated to somatic maintenance plus growth and to maturity (maturation, maturity maintenance and reproduction) with a constant ratio according to the "kappa–rule". DEB theory gives priority to maintenance, which means that somatic and maturity maintenance costs are first "paid" from the flux of energy from reserves, the remaining energy is then allocated to growth and maturity (or reproduction buffer). If maintenance costs cannot be "paid" from the flux of energy coming from reserves the maintenance is primarily paid from reproduction buffer and if the reproduction buffer is empty maintenances costs are "paid" from structural volume.

Interaction between the energy budget of the Manila clam and *V. tapetis* are derived from Flye-Sainte-Marie et al. (2007b). Since experimental data about *V. tapetis* dynamics within the extrapallial fluids are not available this part of the model is essentially theoretical. The justification for this theoretical approach is that the aim of this study is not to provide realistic dynamics of *Vibrio* within an infected clam, but to provide realistic dynamical modifications of the energy budget of the infected host. We suppose that after infection, *V. tapetis* grows within the extrapallial fluids and secretes a product. According to DEB theory, immunity work is taken into account in maturity maintenance

costs. Thus the product induces an increase in maintenance costs (which corresponds to the activation of the immune response) and this increase in maturity maintenance costs increases the death rate of the *Vibrio*. The product has also two other effects: (1) a toxicity effect which increases somatic maintenance costs (lesions) and (2) and a decrease of the filtration activity, these two points were discussed in Flye-Sainte-Marie et al. (2007b).
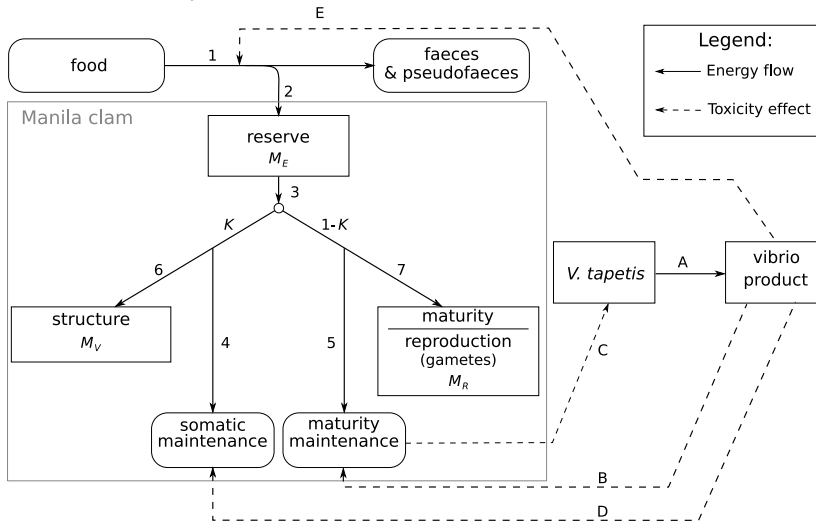
FIG. 8.1: Conceptual scheme of the Manila clam/*V. tapetis* interactions. Manila clam energy budget: 1: feeding, 2: assimilation, 3: use of reserves, 4: Somatic maintenance, 5: maturity maintenance, 6: somatic growth, 7: maturity and reproduction. *V. tapetis* and interaction with the host: A: secretion of *Vibrio* product, B: effect (toxicity) of *Vibrio* product on maturity maintenance (immune response), C: effect of maturity maintenance on *Vibrio* death rate, D: effect (toxicity) of *Vibrio* product on somatic maintenance (lesions), E: effect of *Vibrio* product on filtration activity.

Dynamics of the Manila clam budget

Notation of the symbols for the energy budget of the Manila clam is from Kooijman (2000) and Kooijman et al. (submitted). According to Kooijman (2000) biomass can be partitioned into structure (M_V), reserve (M_E) and reproduction buffer (M_R). The DEB model presented in this study is an application of the formulation extensively described in Kooijman (2000). This formulation

symbol	unit	description
Variables for the Manila clam		
X	$\mathrm{mol\,cm^{-3}}$	food density
M_V	mol	structural mass
M_E	mol	reserve mass
M_R	mol	reproduction mass
M_H	mol	cumulative investment in maturity
$\dot{J}_X$	$\mathrm{mol\,d^{-1}}$	Ingestion rate
$\dot{r}_B$	$\mathrm{d^{-1}}$	von Bertalanffy growth rate
$\dot{J}_{EM}$	$\mathrm{mol\,d^{-1}}$	somatic maintenance mass flux
$\dot{J}_{EJ}$	$\mathrm{mol\,d^{-1}}$	maturity maintenance mass flux
Scaled variables for the Manila clam		
L	cm	volumetric structural length
$U_H = M_H/\{\dot{J}_{EAm}\}$	$\mathrm{d\,cm^2}$	scaled maturity
$U_R = M_R/\{\dot{J}_{EAm}\}$	$\mathrm{d\,cm^2}$	scaled reproduction mass
$U_E = M_E/\{\dot{J}_{EAm}\}$	$\mathrm{d\,cm^2}$	scaled reserve mass
$f = X/(K + X)$	–	scaled functional response
$e = \dot{v} U_E L^{-3}$	–	scaled reserve density
Parameters for the Manila clam		
$\delta_{\mathcal{M}}$	–	shape coefficient
$\{\dot{J}_{EAm}\}$	$\mathrm{mol\,d^{-1}cm^{-2}}$	surface area-specific max assimilation rate
$\dot{v}$	$\mathrm{cm\,d^{-1}}$	energy conductance
$\dot{k}_J$	$\mathrm{d^{-1}}$	specific maturity maintenance
κ	-	allocation fraction
κ_R	-	reproduction efficiency
U_H^b	$\mathrm{d\,cm^2}$	Scaled maturity at birth
U_H^p	$\mathrm{d\,cm^2}$	Scaled maturity at puberty
$T_A, T_H, T_{AH}, T_L, T_{AL}$	K	Arrhenius temperatures
Compound parameters for the Manila clam		
K	$\mathrm{mol\,cm^{-3}}$	half-saturation constant
$\{\dot{J}_{XAm}\}$	$\mathrm{mol\,d^{-1}cm^{-2}}$	maximum specific ingestion rate
$L_m = \frac{\dot{v}}{\dot{k}_M g}$	cm	maximum structural length
$\dot{k}_M$	$\mathrm{d^{-1}}$	somatic maintenance rate coefficient
g	–	energy investment ratio
Variables, parameters and quantities for the Vibrio		
$[B], [B_m]$	$\mathrm{mol.m^{-3}}$	*Vibrio* density, max. *Vibrio* density
$[B_K]$	$\mathrm{mol.m^{-3}}$	half saturation constant of immune response
f_B	-	functional response for haemocytes
$[Q]$	$\mathrm{mol\,cm^{-1}}$	conc of *Vibrio* product
$\dot{r}_m^B$	$\mathrm{d^{-1}}$	specific growth rate of *Vibrio*
$\dot{k}_Q$	$\mathrm{d^{-1}}$	specific decay rate of *Vibrio* product
j_Q	$\mathrm{mol\,mol^{-1}\,d^{-1}}$	specific production rate
$\{\dot{J}_{BAm}\}$	$\mathrm{mol\,cm^{-2}\,d^{-1}}$	maximum surf. spec. *Vibrio* elimination rate
$[Q_b^0], [Q_b]$	$\mathrm{mol\,cm^{-3}}$	toxicity parameters for filtering
$[Q_M^0], [Q_M]$	$\mathrm{mol\,cm^{-3}}$	toxicity parameters for somatic maintenance
$[Q_J^0], [Q_J]$	$\mathrm{mol\,cm^{-3}}$	toxicity parameters for maturity maintenance

TAB. 8.1: Variables, scaled variables, parameters, compound parameters and quantities for the Manila clam and *Vibrio*. Where similar units occur in the specification of a quantity, they relate to different categories (such as structure *versus* environment, or structure *versus* reserve), and can, therefore, not be reduced.

includes maturity (M_H) as a state variable and is quantified as the cumulative investment of reserve in maturity. Birth, defined in the DEB theory concept as the first feeding of the organism, occurs at the amount of maturity M_H^b (maturity at birth); and puberty, defined as the first investment of reserve in reproduction buffer, occurs at the amount of maturity M_H^p (maturity at puberty). Maturity itself represents information and has no mass or energy. Equations of the standard DEB model described by Kooijman (2000) were rewritten to work with the following state variables (Kooijman et al., submitted):

- volumetric length L (cm) that can be converted to observed length (L^{Obs}) with the relation $L = L^{Obs}/\delta_{\mathcal{M}}$, with $\delta_{\mathcal{M}}$ the shape coefficient (dimensionless).

and scaled state variables, corresponding to the variables divided by the maximum surface specific assimilation rate ($\{\dot{J}_{EAm}\}$, mol d^{-1} cm^{-2}) :

- scaled reserve U_E (d cm^2).

- scaled maturity U_H (d cm^2)

- scaled reproduction buffer U_R (d cm^2)

Thus scaled reserve and scaled reproduction buffer can be converted to mass (g) by multiplying by $\{\dot{J}_{EAm}\}\,\bar{\mu}_E$ ($= \{\dot{p}_{Am}\}\,\bar{\mu}_E/w_E$) with $\bar{\mu}_E$, the chemical potential of reserves (g mol^{-1}), $\{\dot{p}_{Am}\}$, the maximum surface specific assimilation rate (J d^{-1}cm-2) and $\bar{\mu}_E/w_E$, the energy content of reserve (J g^{-1}). Variables, scaled variables, parameters and compound parameters used in this study are summarized in Tab. 8.1.

Food uptake is assumed to follow a Holling type II functional response depending on food density X (mol cm^{-3}) and to be proportional to structural body surface area (Kooijman, 2000). Thus the ingestion rate $\dot{J}_{XA}$ (mol d^{-1}) can be written as:

$$\dot{J}_{XA} \;=\; \{\dot{J}_{XAm}\}\, f\, L^2 \quad \text{with } f = \frac{X}{K + X} \qquad (8.1)$$

where $\{\dot{J}_{XAm}\}$ is the maximum surface specific ingestion rate (mol d^{-1} cm^2), f is the scaled functional response (dimensionless) and K the half saturation constant (mol cm^{-3}).

Change of state variables in time of this formulation for the DEB model were extensively described by Kooijman et al. (submitted). According to these authors, length change can be written as:

$$\frac{d}{dt}L = \dot{r}_B(eL_m - L) \tag{8.2}$$

$$\text{with } \dot{r}_B = \frac{\dot{k}_M g}{3(e + g)}; \quad L_m = \frac{\dot{v}}{\dot{k}_M g} \quad \text{and } e = \dot{v}U_E L^{-3}$$

where $\dot{r}_B$ (d^{-1}) is the von Bertalanffy growth rate, L_m (cm) is the maximum length of the species and e (dimensionless) is the scaled reserve density.

Since before birth the organism does not feed, and birth occurs at a particular amount of maturity (M_H^b) or at a particular amount of scaled maturity (U_H^b), change in scaled reserve can be written as:

$$\frac{d}{dt}U_E = fL^2 - S_C \quad \text{for } U_H > U_H^b \quad \text{else } \frac{d}{dt}U_E = -S_C \tag{8.3}$$

$$\text{with } S_C = L^2 \frac{ge}{g + e}\left(1 + \frac{L}{gL_m}\right)$$

where S_C (cm^2) is the "flux" of utilisation of scaled reserves.

According to Kooijman et al. (submitted) maturity is quantified as the cumulative investment of reserves into maturity. Investment of reserves into maturity stops at puberty, when a particular amount of maturity (M_H^p) or a particular amount of scaled maturity (U_H^p) is reached. After puberty energy from reserves is allocated to reproduction buffer rather than maturity (Kooijman, 2000), thus maturity is constant after puberty and equals to M_H^p. Thus change in scaled maturity and scaled reproduction buffer over time can be written as:

$$\frac{d}{dt}U_H = (1 - \kappa)S_C - \dot{k}_J U_H \quad \text{for } U_H < U_H^p \tag{8.4}$$

$$\frac{d}{dt}U_R = (1 - \kappa)S_C - \dot{k}_J U_H^p \quad \text{for } U_H = U_H^p \quad \text{else } \frac{d}{dt}U_R = 0 \tag{8.5}$$

Factors triggering spawning events in the Manila clam are not well known (see e.g. Flye-Sainte-Marie et al., 2007a), thus, for simplification purposes spawning events are supposed to occur at a specific day in the year, during this spawning event the total content of the reproduction buffer is released.

Somatic and maturity maintenance ($\dot{J}_{EM}$ and $\dot{J}_{EJ}$ respectively, mol d^{-1}) costs can be quantified as:

$$\dot{J}_{EM} = \kappa \frac{L^3}{L_m}\{\dot{J}_{EAm}\}$$

$$\dot{J}_{EJ} = \dot{k}_J U_H \{\dot{J}_{EAm}\}$$

DEB theory gives priority to maintenance (Kooijman, 2000). Thus, if maintenance costs cannot be paid from the flux coming from reserves it is primarily supplemented from the reproduction buffer. If this is also not sufficient, it is further supplemented from structure. In this case we assume that the overhead cost in paying maintenance from structure rather than reserve equals to the overhead cost of producing structure from reserve. In this case the change in structural length over time ($\frac{d}{dt}L$) becomes negative.

Dynamics of *Vibrio tapetis*

Since data are not available for the dynamics of *V. tapetis* in an infected clam, this part is essentially theoretical.

Suppose that at time $t = t_B$ an individual *Vibrio* successfully enters in the extrapallial compartment of a clam. The mass of *Vibrio* inside the host is denoted by M_B, so $M_B(t_B) = M_{B0}$ and the *Vibrio* density in the extrapallial fluids $[B]$ (mass of bacteria by volume of extrapallial fluids, so to structural volume). Based on the assumption that *Vibrio* growth is limited by the volume of the extrapallial compartment (or the nutrients present in that volume), a logistic growth equation is applied for the *Vibrio* population growth. We assume that the energy costs for the population dynamics of *Vibrio* are negligibly small, since their number remain small (typically $< 10^5$ cells ml^{-1} in the extrapallial fluids, Paillard, unpublished data). The presence of the *Vibrio* induces an immune response (Paillard, 2004b, for a review). DEB theory assumes that cost of immunity is included in maturity maintenance costs (Kooijman, 2000). Thus maturity maintenance might be affected by the presence of the *Vibrio*. We assumed that immune response is proportional to the increase in maturity maintenance costs induced by the pathogen and that it follows a Holling type II functional response. So the change in the *Vibrio* concentration can be written as:

$$\frac{d}{dt}[B] = \left(\dot{r}_m^B \left\{ 1 - \frac{[B]}{[B_m]} \right\} - \dot{r} \right)[B] - f_B(\dot{k}_J(0) - \dot{k}_J(Q))U_H\{\dot{J}_{BAm}\} \quad (8.6)$$

$$\text{with } f_B = \frac{[B]}{[B_K] + [B]}$$

where $\dot{r}_m^B$ (d^{-1}) is the maximum growth rate of the *Vibrio* population, $[B_m]$ (mol cm^{-3}) the maximum *Vibrio* concentration, $\dot{r} = \frac{d}{dt}\ln L^3$ (d^{-1}) is the dilution by growth rate, $\dot{k}_J(0)$ (d^{-1}) the maturity maintenance rate coefficient without *Vibrio*, $\dot{k}_J(Q)$ (d^{-1}) the maturity maintenance rate coefficient modified by *Vibrio* presence (see section "Effect of *Vibrio* on the host" p. 121), f_B (dimensionless) the functional response of immune response on *Vibrio*, and $\{\dot{J}_{BAm}\}$ (mol cm^{-2} d^{-1}) the maximum surface specific *Vibrio* elimination rate.

Suppose further that *Vibrio* excretes a compound Q that has the potential to change one or more parameters values of the host, following the DEBtox rules

for effects of chemical compounds on the budget of organisms (Kooijman and Bedaux, 1996). Note that this product is theoretical and aims at linking the effect of the *Vibrio* to the *Vibrio* population. The specific production rate is taken to be constant, as well as the specific decay rate. So the change in the *Vibrio* product concentration $[Q]$ (mol cm^{-3}) is:

$$\frac{d}{dt}[Q] \;\; = \;\; j_Q[B] - (\dot{k}_Q + \dot{r})[Q] \tag{8.7}$$

where j_Q is the mass-specific production rate (moles of product per mole of *Vibrio* per time) and $\dot{k}_Q$ the specific decay rate of the *Vibrio* product.

We assume that all interactions between the *Vibrio* and the Manila clam energy balance are linked to the vibrio product.

Variables and parameters for the *Vibrio* dynamics and its effects are summarized in Tab. 8.1.

Effects of *Vibrio* on the Manila clam energy balance

Effects of the development of BRD on the energy balance on the Manila clam were studied in Flye-Sainte-Marie et al. (2007b). This study emphasized that the energy balance of the Manila clam was affected in two main ways: a reduction of the filtration activity and an increase in the maintenance costs, presumably associated to immune response and lesion repair.

The effect of the *Vibrio* on filtration activity was modelled as an increase in the half saturation constant (K) of the scaled functional response (f). For a given food level (X) and an increase of K value has the effect of reducing the scaled functional response and thus the ingestion rate. The effect of the *Vibrio* on the immune system has been modelled has an increase of the maturity maintenance rate coefficient $(\dot{k}_J)$. *Vibrio* infection also induces lesions (see Paillard, 2004b). Since lesions are perturbations or destruction of structural body tissue, their repair should be attributed to the structural maintenance cost. Thus costs for lesions repair were modelled as an increase in the somatic maintenance rate coefficient $(\dot{k}_M)$. These effects were assumed to be linked to the *Vibrio* product according to the DEBtox rules for effects of chemical compounds on the budget of organisms (Kooijman and Bedaux, 1996). These effects were thus quantified as:

$$
\begin{aligned}
K(Q) &= K(0)/(1 - \max(0, [Q] - [Q_b^0])/[Q_b]) \\
\dot{k}_M(Q) &= \dot{k}_M(0)(1 + \max(0, [Q] - [Q_M^0])/[Q_M]) \\
\dot{k}_J(Q) &= \dot{k}_J(0)(1 + \max(0, [Q] - [Q_J^0])/[Q_J])
\end{aligned}
$$

where $[Q_b^0]$, $[Q_M^0]$ and $[Q_J^0]$ are the no-effect concentrations, when $[Q]$ is under these concentration the product has no effect. $[Q_b]$, $[Q_M]$ and $[Q_J]$ are tolerance concentrations; the larger their values, the smaller the effects. The values $K(0)$, $\dot{k}_M(0)$ and $\dot{k}_J(0)$ correspond to the uninfected situation. The motivation of these linear relationships is that the real functions might be more complicated, but we use a linear approximation for small effects; small changes in parameter values, however, not necessarily translate into small effects on the budget.

Effect of temperature on physiological rates

Physiological rates depends on body temperature. This dependency can be described by the Arrhenius relation within a species-specific tolerance range of temperatures. According to Kooijman (2000) this dependence can be described by the following relation:

$$\dot{k}(T) = \dot{k}_1 \exp\left(\frac{T_A}{T_1} - \frac{T_A}{T}\right)\left(1 + \exp\left\{\frac{T_{AL}}{T} - \frac{T_{AL}}{T_L}\right\} + \exp\left\{\frac{T_{AH}}{T_H} - \frac{T_{AH}}{T}\right\}\right)$$

where $\dot{k}(T)$ is the value of the physiological rate T, $\dot{k}_1$ is the physiological rate at temperature T_1, T_A is the Arrhenius temperature, T_H and T_L are the upper and lower boundaries of the tolerance range, and T_{AH} and T_{AL} are the Arrhenius temperature for the rate of decrease at both boundaries. All temperatures are expressed in Kelvin (K).

   All physiological rates of the budget of the Manila clam were corrected using this relation. Growth rate of the *Vibrio* population was corrected by taking into account only its Arrhenius temperature (T_A^B).

Parameter estimates

The parameters values of the host module of the model were estimated from data available in literature following methods described in van der Veer et al. (2006) and in Kooijman et al. (submitted). The estimation of these parameters is extensively detailed in chapter 9.

   The Arrhenius temperature for the *Vibrio* (T_A^B) was estimated from experimental growth experiments from Haberkorn (2005) using the procedure described in chapter 9 (section 9.2.1, p. 134). Since experimental data on *V. tapetis* dynamics during the infection process were not available, most of the parameters related to *Vibrio* dynamics and its interaction with the budget of the Manila clam were freely fitted with the following constraints: (1) to provide a realistic maximum bacteria density, and (2) to adjust the total weight loss to the observations.

Parameters for the Manila clam

$\kappa = 0.89$	$\kappa_R = 0.95$	$g = 1.384$
$\dot{v} = 0.0292$ cm d^{-1}	$\dot{k}_J = 0.0091$ d^{-1}	$\dot{k}_M = 0.0091$ d^{-1}
$U_H^b = 4.76\,10^{-7}$ d cm^2	$U_H^p = 0.1274$ d cm^2	$\delta_{\mathcal{M}} = 0.29$
$T_A = 6071$ K	$T_H = 300$ K	$T_L = 275$ K
$T_{AH} = 30424$ K	$T_{AL} = 299859$ K	

Parameters for the Vibrio and Vibrio products

$T_A^B = 6843$ K	$\dot{r}_m^B = 4.65$ d^{-1}	$[B_m] = 1\,10^{-5}$ C-mol cm^{-2}
$j_Q = 0.11$ d^{-1}	$\dot{k}_Q = 0.066$ d^{-1}	
$[B_K] = 1.10^{-7}$ C-mol cm^{-3}	$\{\dot{J}_{BAm}\} = 4.7\,10^{-4}$ C-mol cm^{-2} d^{-1}	
$[Q_M^0] = 1\,10^{-6}$ C-mol cm^{-3}	$[Q_M] = 1\,10^{-5}$ C-mol cm^{-3}	
$[Q_J^0] = 0$ C-mol cm^{-3}	$[Q_J] = 3.7\,10^{-7}$ C-mol cm^{-3}	

TAB. 8.2: Parameter estimates for the Manila clam, the *Vibrio* and the inter-action with the Manila clam budget used in the application presented in this study. All rates are given at 15°C. The meaning of the symbols is explained in Table 8.1.

The parameter values that we used in this study are listed in Table 8.2. Note that not all the parameter values given in Tab. 8.1 needed to be estimated for the applications presented in this study.

8.3 Results

8.3.1 Starvation experiment

Individuals are classified into three groups: asymptomatic individuals, individuals presenting light symptoms ($1 \leq$ CDS ≤ 3) and clams presenting heavy symptoms (CDS ≥ 4). There was no significant difference in the number of individuals in each group between the three sampling dates ($\chi^2 = 1.88$, df = 4, p-value = 0.75) and mortality was low ($< 10\%$) during the experiment. This allowed to hypothesize that there was negligible transfer of individuals between groups during the experiment.

At each sampling date there were no significant differences in total flesh dry weight between asymptomatic clams and clams presenting light symptoms. Fig. 8.2 shows the evolution of total flesh dry weight in asymptomatic clams and clams presenting heavy symptoms during the experiment. In asymptomatic clams weight loss was almost linear. Dry weights in heavily infected individuals were significantly lower than in asymptomatic one two and three month after the beginning of the experiment (randomized-*t*, tests *p*–values <

0.05). No difference between mean standardized dry flesh weight of asymptomatic and clams presenting light symptoms could be detected (randomized-t tests; p-values > 0.05) at any time.

Growth during the experiment was negligible; no difference in mean length could be detected between beginning and end of the starvation experiment, for any group of clams (t test; all p-values > 0.05)
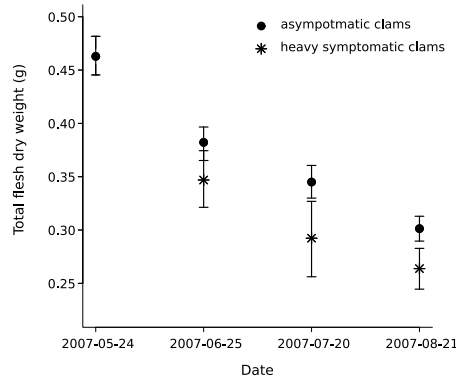
FIG. 8.2: Evolution of total flesh dry weight (mean $\pm$ 95% bootstrap percentile interval) during the starvation experiment in asymptomatic clams ($\bullet$) and in clams presenting heavy symptoms ($*$, CDS $\geqslant 4$)

8.3.2   Model simulations

Validation of growth

Length growth at constant food density and temperature was validated by comparing the model simulation to observed data from Rodde et al. (1976). A comparison of model output and experimental data are shown in Fig. 8.3 and shows that the model prediction is very close to the observed data.

Impact of BRD development on maintenance costs

The interaction model between the energy budget of the Manila clam and the *Vibrio* was used to estimate the energetic costs of disease development in the highly diseased clams of the starvation experiment. For this purpose, two simulations were performed. The first simulation only represents the energy budget of an uninfected clam under starvation conditions. For the second simulation, the *Vibrio* infection and its effects are introduced. This simulation is
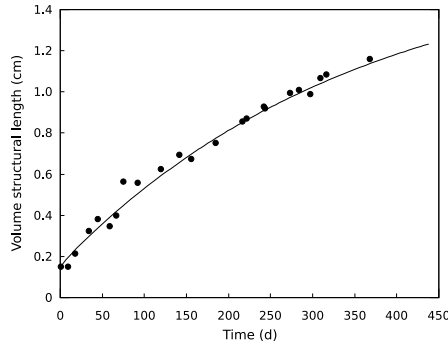
FIG. 8.3: Validation of the growth at constant food density and temperature (22°C). For this simulation scaled functional response on food was constant ($f = 0.72$) . Continuous curve: simulation, points: experimental data from Rodde et al. (1976).

supposed to reproduce the energy budget of an highly diseased Manila clam during starvation.

Initial conditions (*i.e.* state variables at the beginning of the simulation) were estimated from the initial mean length and initial mean total flesh dry mass. Initial structural length (L_{t0}) was estimated as $L_{t0} = \delta_\mathcal{M} L_{t0}^{Obs}$ and allowed to estimate initial structural weight (with $d_V = 0.216 \, \text{g cm}^3$ the structural volume to dry weight coefficient, see estimate in Tab. 9.3 p. 139). The difference between the structural weight and the mean observed weight allows to estimate the initial weight of reserve plus reproduction buffer. Since at the sampling period (April) the clams are in the main growing period of the year on French Atlantic coasts (see e.g. Flye-Sainte-Marie et al., 2007a) the weight of reserves were assumed to be 60% of the maximum energy density (see Tab. 9.3 p. 139 for the estimates). This allowed to estimate the initial weight of the reproduction buffer. Initial weight of reserves and reproduction buffer were then scaled (with $\bar{\mu}_E$ and $\{\dot{p}_{Am}\}$, see chapter 9, Tab. 9.3 p. 139). For both simulations, since Manila clam were in condition of starvation, the scaled functional response (f) was set to 0. Temperature for the simulation was constant and equal to 15.7°C (288.7 K). Initial *Vibrio* product concentration $[Q^{t0}]$ was set to 0. The simulation was performed over 100 days. For the infected clams, the infection was induced at the beginning of the simulation and the initial concentration of *Vibrio* was supposed to be $[B_0] = 3 \, 10^{-9}$ C-mole cm^{-3}; this value was computed from average *Vibrio* concentration observed in extrapallial fluids of clams with low symptom development (CDS=1) and recalculated

in C-moles cm^{-3} using data on carbon content of bacteria from Ohman and Snyder (1991). Since 37 mm-individuals typically reproduce, the initial scaled maturity was taken to be equal to scaled maturity at puberty. Initial conditions are summarized in Tab. 8.3.

symbol	value	unit	description
L_{t0}	1.073	cm	Initial volumetric length
U_E^{T0}	20	d cm^2	Initial scaled reserves
U_R^{T0}	32	d cm^2	Initial scaled reproduction buffer
$U_H^{T0} = U_H^p$	0.1274	d cm^2	Initial scaled maturity
$[Q^{t0}]$	0	C-mol cm^3	Initial *Vibrio* product concentration

TAB. 8.3: Initial values of the state variables for the simulation of the impact of the disease development during starvation condition.

Evolution of the state variables of the model during the simulations for the uninfected and the infected clam are shown in Fig. 8.4.

In the uninfected clam (continuous curve in Fig. 8.4) structural length remains constant over the whole simulation period (Fig. 8.4 A), indicating that there is no (or very low) allocation to somatic growth. Scaled reserve exponentially decrease during the simulation and are almost null after 100 days (Fig. 8.4 B). Scaled reproduction buffer is almost constant for ≈ 10 days, indicating that allocation of reserve to reproduction balance the maintenance costs; but after this period, maintenance costs cannot be balanced by the flux coming from reserves, and maintenance costs are paid from reproduction buffer which is almost empty after 100 days (Fig. 8.4 C).

In the infected clam (doted curves in Fig. 8.4), simulated *Vibrio* concentration rapidly increase after the infection and reaches its maximum after few days (Fig. 8.4 D). Increase in *Vibrio* product concentration (Fig. 8.4 E) increases maturity maintenance cost (immune response) and the *Vibrio* is eliminated after ≈ 35 days. In starvation conditions the *Vibrio* infection has small effects on the use of reserves (Fig. 8.4 B). The increased maintenance costs are mainly paid from the scaled reproduction buffer after a few days; the reproduction buffer is empty after ≈ 80 days. (Fig. 8.4 B) and maintenance is then paid from structure, this explains why simulated length decreases after ≈ 80 days (Fig. 8.4 A).

From the simulated evolution of length, scaled reserves and scaled reproduction buffer it was possible to estimate the evolution of total dry mass using the coefficients cited above. The evolution for the uninfected and infected clams is shown in Fig. 8.5. In uninfected clams the model simulates a linear
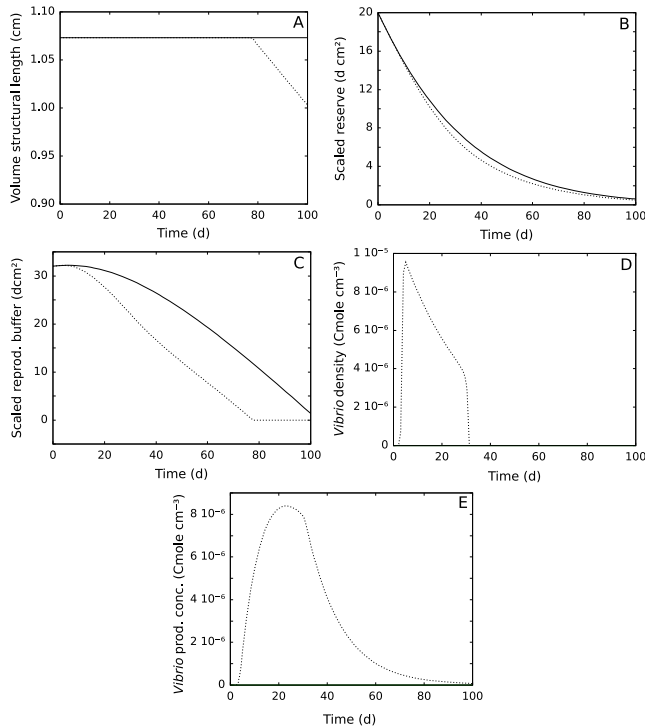
FIG. 8.4: Evolution of state variables during the simulation for uninfected (continuous curve) and infected (doted curve) clams in starvation conditions (f=0). A: evolution of structural length, B: evolution of scaled reserves, C: evolution of scaled reproduction buffer, D: evolution of *Vibrio* concentration, E: evolution of *Vibrio* product concentration.

decrease of total flesh dry weight during starvation and simulation is close to the observed points and stays within the bootstrap percentile intervals of the observations. Parameters for the *Vibrio* and the interaction with the Manila clam budget were estimated in order to provide a good representation of the weight loss during starvation until day 60. Nevertheless, after ≈ 80 days, when maintenance is paid from structure, the model simulates an acceleration of the total flesh weight loss, whereas data suggest a deceleration of the weight loss.

From the simulations it was also possible to estimate the total energy allocated to maintenance. The aim of the work was to estimate the increase of maintenance costs associated with BRD development. Thus the results are here presented as the total maintenance costs which correspond to the sum of
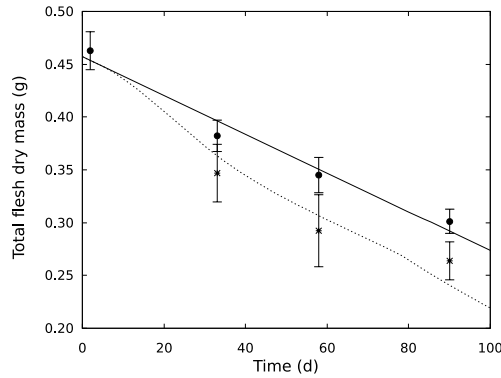
FIG. 8.5: Simulation of the evolution of total flesh dry mass for un-infected (continuous curve) and infected (doted curve) clams in starvation conditions (f=0). Experimental data: average total flesh dry weight (mean $\pm$ 95% confidence interval) during the starvation experiment in asymptomatic clams ($\bullet$) and in clams presenting heavy symptoms ($*$, CDS$\geqslant$4)

the energy flow invested in somatic and maturity maintenance (Fig. 8.6). For the uninfected clam the total flow invested in maintenance remains constant all along the simulation (Fig. 8.6). In the infected clam the maintenance cost rapidly increases after the infection due to the increase in vibrio product concentrations (see. Fig. 8.4 E). The total maintenance reaches a maximum value of ≈ 57 J d^{-1} after ≈ 25 days. The decrease simulated after ≈ 80 days is associated with the decrease in somatic maintenance due to reduction of structural length (shrinking). The maximum value of the energy flow to maintenance associated to BRD development (≈ 57 J d^{-1}) is comparable to the maximum assimilation flux can be estimated to $\dot{p}_A = 77.8$ J d^{-1} for an individual of this size and at the temperature of the experiment.

8.4   Discussion

Starvation experiment

The starvation experimental data indicated that individuals presenting a high development of symptoms had a significant higher weight loss than asymptomatic ones after two months of starvation. This observation confirms the observations of Plana (1995) and Plana et al. (1996), and indicates that an en-
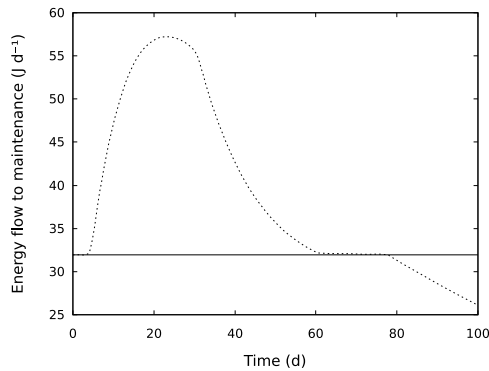
FIG. 8.6: Total energy allocated to maintenance (somatic and maturity maintenance for uninfected (continuous curve) and infected (doted curve) clams.

ergy loss can be associated with the development of BRD independently of the decrease in filtration activity shown by Flye-Sainte-Marie et al. (2007b). As discussed in this article this energy loss might be associated to an increase in the maintenance cost due to the energy needed for the immune response and for lesion repair. The energy needed for *Vibrio* population growth might be negligible (Flye-Sainte-Marie et al., 2007b).

No significant difference in weight could be found between the group of asymptomatic clams and the group of clams presenting moderate symptoms development: energy loss associated with low BRD development levels is negligible. This suggests that BRD development has poor effects on physiology at low disease intensity. This observation is consistent with most of the observations presented in this document. The low disease intensity observed during the survey in the Gulf of Morbihan (chapter 4) could not be associated with significant variations in any measured hemocyte parameter or in the condition index. It was also not possible to show any significant difference in clearance rate, respiration rate or condition index in clams presenting low symptom development (CDS < 4) (Flye-Sainte-Marie et al., 2007b). Thus the stage CDS = 4 can be considered as a critical stage above which physiology is strongly modified but under which effects of disease are negligible.

The proportion of clams in each group (asymptomatic, low symptoms and heavy symptoms) did not significantly varied after 30 days and low mortality was observed during the experiment. This tends to indicate that there was negligible transfer of individuals between the three groups during the experiment.

This can support the hypothesis that each group corresponds to a "batch" of clams that can be followed over time on the base of symptoms intensity.

Budget of the uninfected Manila clam

The simulation of length performed at constant food density and at constant temperature (see Fig. 8.3) was very close to the observed data from Rodde et al. (1976) which were not used for parameters estimation (see chapter 9). The prediction of weight loss during starvation was also close to the observations. For the simulated uninfected clam, the length is constant over the whole simulation period, which is consistent with the observations since no growth was observed during the experiment. This indicates that parameter estimates for the energy budget of Manila clam are reliable and emphasize that the prediction of the energy budget of Manila clam at constant environmental conditions by the DEB model developed in this study are reliable.

The model should also be validated with varying food density and temperature, but this implicates the estimation of food acquisition related parameters which was not necessary for the application presented in this study.

Impact of disease on the maintenance cost

The main objective of present study was to propose an approach to estimate quantitatively the impact of the development of the disease on the maintenance cost of the Manila clam by coupling simple observation (weight) and modelling. The strategy was to quantify the increase in total maintenance cost that can explain the observed weight loss in infected individuals. Since bacterial infections are dynamic processes, the associated increase in maintenance costs had to be treated dynamically. For this purpose, it was necessary to be able to follow a batch of infected clams and a batch of uninfected clams over time in the starvation experiment, this was possible on the basis of the observation of symptoms. The batch of asymptomatic clams is supposed to represent the uninfected case, as the batch of clams with heavy symptoms is supposed to represent the infected case.

The dynamics of the *Vibrio* within the clam were treated here theoretically since no experimental data were available, *Vibrio* dynamics only aim to modify dynamically the maintenance cost of the Manila clam. This justifies that the parameters were only estimated in order to represent the observed weight loss. Thus parameter values have to be considered carefully and simulated dynamics of the *Vibrio* may not be realistic. The *Vibrio* population is here eliminated by the host after $\approx$ 30 days, which is difficult to check since accurate detection

and quantification of the *V. tapetis* burden in clams is difficult (Drummond et al., 2006b). Further development in the *V. tapetis* detection techniques and experiments is needed to obtain data allowing a more realistic modelling of the *Vibrio* dynamics.

In spite of this difficulty it was possible to provide a realistic dynamic increase in the maintenance costs since the simulated trajectory of dry weight in the infected case was near to the observed weight of the clams with heavy symptoms. The simulation only deviated from the observation at the end of the simulation when maintenance was paid from structure. In this case, for simplification purposes, the assumption that the overhead costs in paying maintenance from structure was equal to the overhead costs in making structure from reserve was done. It is possible that this assumption is wrong and that the overhead costs in paying maintenance from structure are lower. Data from Whyte et al. (1990) during a long-term starvation experiment performed over 405 days in the oyster *Crassostrea gigas* indicated that the rate of total weight decrease was higher between 0 and 30 days than between 60 to 405 days. These data could suggest a regulation of the maintenance cost in conditions of extreme starvation, such a regulations is not taken into account in the model. Further investigations are needed to detail this particular extreme situation.

The dynamic quantification of energy flow to total (maturity and somatic) maintenance indicated that the cost of development of the disease was highest 30 days after infection. The maximum reaches the value of 57 J d^{-1}, which is almost two times the total energy flow to maintenance cost in uninfected clams (32 J d^{-1}). Thus BRD induces an important modification of the energy budget in the Manila clam. The maximum value can be compared to the maximum assimilation flux for an individual of this size and at the temperature of the experiment ($\dot{p}_A = 77.8$ J d^{-1}). Theoretically, only a well fed individual could compensate the maximum maintenance from assimilation. This increased maintenance cost, coupled with the decrease of filtration activity may explain the overall cost of BRD development.

8.5 Conclusions

Experimental data presented in this study indicate that an energetic cost can be associated to high intensity of BRD development, independently of the decrease in filtration activity previously described. This observation confirms the hypothesis presented in chapter 7 suggesting that the energy budget of the Manila clam is both affected by a decrease in the filtration activity and an increase in the maintenance costs.

The DEB model presented in this study allows to predict properly both length growth and weight loss at constant environmental condition. In spite of the lack of data about *Vibrio* dynamics this study shows that on the basis of simple measurements of weight loss during starvation it is possible, by coupling modelling and observation, to provide a quantitative and dynamic estimation of the increase in maintenance associated with the development of BRD. The estimation given here indicated that during an infection the maintenance cost can almost double compared to the uninfected situation.

Further development of the model, especially focussed on the *Vibrio* dynamics and its effects on filtration activity will allow to provide a more extensive description of the energetic cost of BRD in the Manila clam.

Chapter 9

Estimation of DEB parameters for the Manila clam

Abstract

By describing mass and energy flow through organisms from assimilation of food to the utilisation for growth, reproduction, development and maintenance, DEB theory provides a theoretical frame for studying living mass and energy balance in biological systems. Although estimation of parameters is necessary to apply the theory, most variables and parameters cannot be measured in a direct way. Based on methodologies previously described (Kooijman, 2000; van der Veer et al., 2006; Kooijman et al., submitted), the aim of this chapter is to describe more extensively the methods used to estimate the DEB parameters values for the Manila clam used in the previous chapter (Chap. 8).

The estimates were compared to values in literature estimated for various bivalve species (Kooijman, 2000; van der Veer et al., 2006). The estimates for the Manila clam, mainly based on the method described in Kooijman et al. (submitted) appear consistent with the values given by Kooijman (2000) and van der Veer et al. (2006), suggesting that inter-species comparison of DEB parameters help to check consistency of the estimates for one species.

9.1   Introduction

DEB theory provides a theoretical frame to study energy and mass budgets in biological systems (Kooijman, 2000). This theory describes mass and energy flows through organisms; from assimilation of food to the utilisation for growth, reproduction, development and maintenance. One interesting aspect of this theory is its generic aspect: the theoretical frame can be applied to various species and differences between species are characterised by differences in parameters values (Kooijman, 2000). Thus, estimation of parameters is an important aspect in the aim of applying this theory. Nevertheless, the variables and parameters that are taken into account in this theory are generally

not measurable in a direct way (van der Meer, 2006). Methods for evaluation of parameters are described in (Kooijman, 2000). Applications of these methods for various bivalves species have been presented in van der Veer et al. (2006). More recently, a method was described to estimate sets of parameters from sets of measurable quantities (Kooijman et al., submitted).

The aim of the work presented here was to provide a more extensive description of the method used to estimate the DEB parameters values for the Manila clam, *Ruditapes philippinarum*, used in the previous chapter (Chap. 8). Some parameters were estimated following Kooijman (2000) and van der Veer et al. (2006), but most of the parameters were estimated following Kooijman et al. (submitted), this chapter thus provides a practical application for this last method. Finally, the parameter values estimated for the Manila clam were compared with previously estimated values for other bivalve species given in Kooijman (2000) and van der Veer et al. (2006).

9.2 Estimation of DEB parameters: methods and results

9.2.1 Effect of temperature on physiological rates

All physiological rates depend on body temperature. Since DEB theory assumes that all physiological rates of an organism follow the same rule (Kooijman, 2000), parameters of the equation relating physiological rates to temperature given in Kooijman (2000) were estimated using a composite data set including filtration, respiration and growth rate data (Goulletquer et al., 1989b; Solidoro et al., 2000). All data were standardized to a value of 1 for a reference temperature (T_1) of 288 K (15°C) and pooled prior to the estimation of the parameters of the equation. Values of the parameters are shown in Tab. 9.3, Fig. 9.1 shows the adjustment of this equation to the experimental data.

9.2.2 Shape coefficient ($\delta_{\mathcal{M}}$)

The shape coefficient ($\delta_{\mathcal{M}} = V^{1/3}/L^{Obs}$) determines how a length measurement (L^{Obs}) relates to a structural body volume (V). Based on the assumption that wet flesh density equals 1 g cm^{-3}, the shape coefficient was estimated using length – body wet mass relationships from Gulf of Morbihan (unpublished data) during the post spawning period (November). Since the measured total body flesh weight can also contain reserves and reserves allocated to reproduction, the shape curve is estimated as the adjustment just beneath the observed data points as shown in Fig. 9.2. The estimate for the $\delta_{\mathcal{M}}$ value is shown in
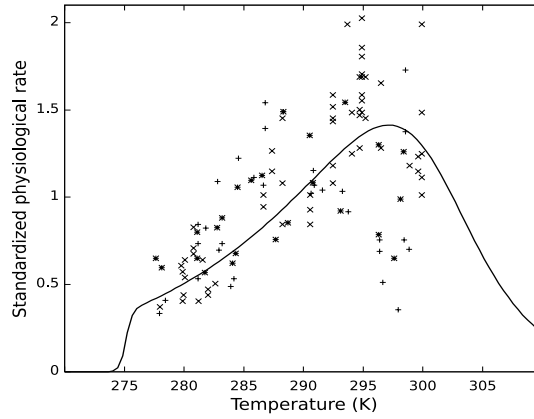
FIG. 9.1: Effect of temperature on physiological rates. Continuous curve shows the model. +: filtration data (from Goulletquer et al., 1989b; Solidoro et al., 2000), ×: growth data (from Solidoro et al., 2000), ∗: respiration data (from Goulletquer et al., 1989b).

Tab. 9.3. The relation between wet weight and dry weight available in this data set allowed to estimate the dry mass per structural volume coefficient (d_V), the estimate is given in Tab. 9.3.

9.2.3 Estimation of parameters using software package DEBtool

This section describes an application of the method for the estimation of DEB parameters presented in Kooijman et al. (submitted). These authors present the auxiliary theory that allows to extract DEB parameters values (principally constant within on species) from easy to measure quantities (that depend on environmental/experimental conditions). DEB theory intimately interlinks most of its underlying processes, which need to be studied in coherence. These relationships allow, knowing simultaneously few quantities in some specific conditions (temperature and food availability), to extract some parameters values. The software package DEBtool performs these computations.

The observed quantities necessary for this application are shown in Tab. 9.1. Some of these had to be recalculated to perform the computations:

- Length measurement (L_b^{Obs}, L_p^{Obs} and L_∞^{Obs}) was converted to structural volumetric length measurement ($L = \delta_\mathcal{M} L^{Obs}$). The shape coefficient $\delta_\mathcal{M}$ was used for L_p and L_∞ and $\delta_\mathcal{M}^{D-larvae}$ was used for L_b.

TAB. 9.1: Observed quantities necessary for the estimation of DEB parameters using the DEBtool software package

symbol	value	unit	description	source
Observed quantities required				
L_b^{Obs}	0.0095	cm	Length at first feeding ("birth", D–larvae)	Helm and Pelizzato (1990) Jones and Sanford (1993)
a_b	2	d	Age at first feeding (20–23 $^\circ C$)	Helm and Pelizzato (1990) Jones and Sanford (1993)
L_p^{Obs}	1-2	cm	Length at first gametogenesis (4–25 $^\circ C$)	Laruelle (1999), pers. obs.
$\dot{r}_{B\,20^\circ C}$	0.0029	d^{-1}	Von Bertalanffy growth rate (20°C)	from Melià et al. (2004)
L_∞	5.46	cm	Ultimate length	from Melià et al. (2004)
R_∞	2739	eggs d^{-1}	Ultimate reproduction rate	from Helm and Pelizzato (1990)
Additional values required				
L_m^{Obs}	8.0	cm	Manila clam maximum length (L_∞ at $f = 1$)	Pers. obs. (see Chap. 1 p. 4)
$\delta_{\mathcal{M}}^{D-larvae}$	0.5	–	Shape coefficient for bivalve D–larvae	Pouvreau (pers. comm.)
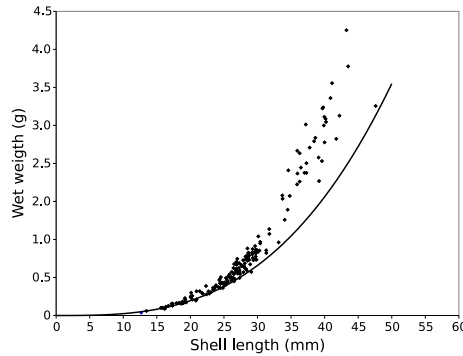
FIG. 9.2: Length–wet weight relationship of *R. philippinarum* in a November sample in Gulf of Morbihan, observed wet weight (points, unpublished data) include structure, reserves and reserves allocated to reproduction. Continuous curve represents the relation between length and structural body volume, this explains why the curve should be below wet weight observations.

- Von Bertalanffy growth rate was recalculated for temperature the reference temperature of 15°C (288 K).

- Scaled functional response on food (f) value for the observed Von Bertalanffy growth rate ($\dot{r}_B$) and ultimate length L_∞ were were estimated using the relation $L_\infty = f\,L_m$ (Kooijman, 2000).

Age at first feeding (a_b) is a difficult value to measure in bivalves since development is quick. This value was thus reduced to obtain a set of parameters consistent with previous estimations for bivalves given in (van der Veer et al., 2006). A default value for κ_R (fraction of energy fixed into eggs, dimensionless) of 0.95 was taken following Kooijman et al. (submitted). The recalculated values are given in Tab. 9.2. Using these values, the step 3 described in Kooijman et al. (submitted) was then applied using the get_pars_r routine of the software package DEBtool. The estimated values of the parameters are shown in Tab. 9.3; this estimation method assumes that $\dot{k}_J$ and $\dot{k}_M$ are equal.

9.2.4   Maximum surface–specific assimilation rate ($\{\dot{p}_{Am}\}$)

Maximum surface–specific assimilation rate $\{\dot{p}_{Am}\}$ is required to convert scaled reserves and reproduction buffer content ($\mathrm{d\,cm^2}$) to mass and subsequently to

TAB. 9.2: Quantities used for the estimation of DEB parameters using the DEBtool software package

Symbol	f	L_b	L_p	L_∞	a_b	$\dot{r}_B$	R_∞	κ_R
Value	0.68	0.0045	0.29	1.58	0.6	0.00203	27397	0.95
Units	–	cm	cm	cm	d	d^{-1}	eggs d^{-1}	–

compare the model outputs to observed data. Maximum surface–specific assimilation rate can easily be calculated using the relation $\{\dot{p}_{Am}\} = \dot{v}\,[E_m]$ with $[E_m]$ (J cm^{-3}) being the maximum energy density (Kooijman, 2000).

Maximum energy density $[E_m]$ was first estimated as the difference in energy content at the end of winter and at the end of the growing season according to van der Veer et al. (2006), using data from Goulletquer (1989a). The value of $[E_m] = 1800$ J cm^{-3} was obtained. $[E_m]$ corresponds to the reserve density at the equilibrium of a satiety fed individual (f=1) (Kooijman, 2000), but such a situation rarely occurs in nature which implies that the observed reserve density ($[E]$) is generally inferior to $[E_m]$. Thus this value represents a minimum estimate of the maximum energy density (van der Veer et al., 2006). $[E_m]$ values for various bivalves species given in van der Veer et al. (2006) ranged from 2085 cm^{-3} (for *Macoma balthica*) to 2295 cm^{-3} (for *Crassostrea gigas*) thus the value of 2200 J cm^{-3} may provide a more realistic estimate for $[E_m]$ in the Manila clam.

9.3   Consistency of the estimates

9.3.1   Arrhenius temperature

Estimation of Arrhenius temperature (T_A, K) for various bivalves species from literature is given in Tab. 9.4. The estimates gives values ranging from 5530 to 13000 K. Our estimation for the Manila clam (6071 K) is consistent with these values. No data about any physiological rate near the lower temperature boundary could be found in literature (see Fig. 9.1), thus the estimates of T_L and T_{AL} are approximative and more data are needed to better estimate these values.

TAB. 9.3: List of the DEB parameters estimated for *R. philippinarum*.

Symbol	Value	Unit	Description
Temperature equation parameters			
T_A	6071	K	Arrhenius temperature
T_1	288 (15)	K (°C)	Reference temperature (arbitrary)
T_H	300	K	Higher boundary of the thermic tolerance range
T_{AH}	30424	K	Arrhenius temperature for the decrease rate at high temp.
T_L	275	K	Lower boundary of the thermic tolerance range
T_{AL}	299859	K	Arrhenius temperature for the decrease rate at low temp.
Parameters estimated from DEB*tool software*			
κ	0.89	–	Fraction of the catabolic power spent on maintenance plus growth
g	1.384	–	Energy investment ratio
$\dot{k}_J$	0.0091	d^{-1}	Maturity maintenance rate coefficient
$\dot{k}_M$	0.0091	d^{-1}	Maintenance rate coefficient
$\dot{v}$	0.0292	$cm\,d^{-1}$	Energy conductance
U_H^b	$4.76\,10^{-7}$	$d\,cm^2$	Scaled maturity at birth
U_H^p	0.1274	$d\,cm^2$	Scaled maturity at puberty
Other parameters			
$\delta_{\mathcal{M}}$	0.29	–	Shape coefficient
κ_R	0.95	–	Fraction of reproduction energy fixed in eggs (Kooijman et al., submitted)
$[E_m]$	2200	$J\,cm^{-3}$	Maximum energy density (from van der Veer et al., 2006)
$\{\dot{p}_{Am}\}$	64.2	$J\,cm^{-2}\,d^{-1}$	Surface–area specific maximum assimilation rate
w_E/μ_E	$17.5\,10^3$	$J\,g^{-1}$	Energy content of reserves (from Deslous-Paoli and Héral, 1988)
d_V	0.216	$g\,cm^{-3}$	Structural volume to dry weight coefficient

9.3.2 DEBtool software parameters estimation

In most ecophysiological growth models, most of the parameters are estimated from experimental data obtained in an independent way. Each estimate comes with an uncertainty, more or less difficult to quantify. By applying such a method, each independent parameter value has a biological meaning. Nevertheless, the resulting set of parameters may contain some combination of parameters that is not biologically consistent. DEB theory interlinks most of the underlying processes. Based on this property, the DEBtool software allows to estimate several parameters at the same time from measured quantities. Using this method, each of the estimated parameter value depends on the other estimated values. Thus, this method provides a solution for the problem of estimating independently each parameter value to build a biologically consistent set of parameters.

TAB. 9.4: Comparison of DEB parameters estimated for *R. philippinarum* with other bivalve species (estimates from Kooijman, 2000 and van der Veer et al., 2006). Estimations are given for a temperature of 20°C (293 K).

	Parameter					
	T_A	$\dot{v}$	k_M	g	$\{\dot{p}_{Am}\}$	
Species	(K)	(cm d^{-1})	(d^{-1})	(–)	(J cm^{-2} d^{-1})	Source
Ruditapes philippinarum	6071	0.042	0.013	1.384	91.9	This study
Macoma balthica	5800	0.016	0.013	1.139	32.9	van der Veer et al. (2006)
Mya arenaria	5800	0.061	0.013	1.162	133.0	van der Veer et al. (2006)
	13 000					Kooijman (2000)
Cerastoderma edule	5800	0.032	0.013	1.123	68.6	van der Veer et al. (2006)
Mytilus edulis	5800	0.067	0.013	1.239	147.6	van der Veer et al. (2006)
	8460					Kooijman (2000)
	7600					Kooijman (2000)
Perna canaliculus	5530					Kooijman (2000)
Crassostrea gigas	5800	0.183	0.013	1.840	420.0	van der Veer et al. (2006)
Cardium edule	8400					Kooijman (2000)
Cardium glaucum	8400					Kooijman (2000)

Energy conductance ($\dot{v}$) and maintenance rate coefficient ($\dot{k}_M$) and energy investment ratio (g) The values of energy conductance and maintenance rate coefficient ($\dot{k}_M$) as estimated for the Manila clams and recalculated for 20°C are given in Tab. 9.4. They are compared to the values given in van der Veer et al. (2006) for various other bivalves species. The estimation of energy conductance for the Manila clam range between the estimates of van der Veer et al. (2006), and is close to the estimate of average energy conductance for animals given in Kooijman (2000) ($\dot{v} = 0.0433$ cm d^{-1} at 20°C). The maintenance rate

coefficient is equal to van der Veer et al. (2006) estimations. Another way to test the consistency of energy conductance and maintenance rate coefficient is given in Kooijman et al. (submitted): DEB theory predicts a linear relationship between the inverse von Bertalanffy growth rate ($\dot{r}^{-1}$) and ultimate length (L_∞), the origin of this line being equal to $3\dot{k}_M^{-1}$ and the slope being equal to $3\dot{v}^{-1}$. Fig. 9.3 shows the plot of the inverse of observed von Bertalanffy growth rates ($\dot{r}^{-1}$) as a function of ultimate length L_∞ and the prediction of the relation using the estimates of maintenance rate coefficient ($\dot{k}_M$) and energy conductance ($\dot{v}$) for the Manila clam. Though the scattering of experimental data, the predicted relationship is near the observations. Thus, the estimation of energy conductance and maintenance rate coefficients seem consistent.
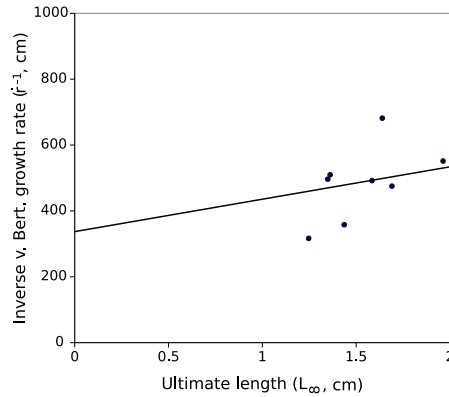
FIG. 9.3: Inverse of observed von Bertalanffy growth rate ($\dot{r}^{-1}$) as a function of ultimate length L_∞. Von Bertalanffy growth rates were corrected for temperature and are given for 15°C. Data from Yamamoto and Iwata (1956), Rodde et al. (1976), Robert et al. (1993), Melià et al. (2004) and personal data from Gulf of Morbihan. The continuous line shows the prediction of the relation using the estimates of maintenance rate coefficient ($\dot{k}_M$) and energy conductance ($\dot{v}$) for the Manila clam.

Surface–area specific maximum assimilation rate ($\{\dot{p}_{Am}\}$) Surface–area specific maximum assimilation rate is an extensive parameter which depends on size. This parameter is proportional to maximum structural length (L_m) of the species (Kooijman et al., submitted). Thus, the values given in Tab. 9.4 cannot be directly compared between species. This property imply a linear relationship between ultimate length (L_m) and surface–area specific maximum
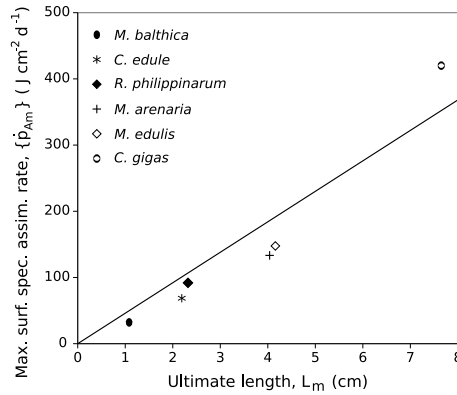
FIG. 9.4: Relationship between ultimate length (L_∞, cm) and maximum surface-specific assimilation rate ($\{\dot{p}_{Am}\}$, $J\,cm^{-2}\,d^{-1}$) estimated for *R. philippinarum* (this study) and various other bivalve species (van der Veer et al., 2006)

assimilation rate ($\{\dot{p}_{Am}\}$) as shown in Fig. 9.4. This figure indicates that the estimated value of $\{\dot{p}_{Am}\}$ for the Manila clam is close to the expected relationship based on estimates for various other bivalve species. The extensive property of the parameters also allows to recalculate these parameters for a given maximum length (see. Kooijman et al., submitted). The values given in van der Veer et al. (2006) were recalculated for $L_m = 2.32\ cm$ (maximum volumetric length of *R. philippinarum*) and range from 70.6 $J\,cm^{-2}\,d^{-1}$ for *Macoma balthica* to 127.4 $J\,cm^{-2}\,d^{-1}$ for *Crassostrea gigas*. The estimate for the Manila clams (Tab. 9.4) is between these two value suggesting that our estimate is consistent with previous estimates.

9.4   Conclusion

Although methodology for estimation of most parameters values was different from the methods used in van der Veer et al. (2006), the estimated parameters values for the Manila clam appear to be consistent with these estimations for various bivalves species. This indicates both that cross–checking parameters values by different methods may be a powerful strategy to ensure the parameters estimates and that comparison of parameter values between species may also allow to check the consistency of the estimates.

Part IV

Synthesis

Chapter 10

Synthesis

10.1 Comparison of energy budget modelling approaches

Modelling is an useful tool and one of the main objectives of this kind of approach is to summarize the information available about the system studied. This allows to pinpoint the elements susceptible to control the system and subsequently to drive experimental research. This point is illustrated by this work: the first model, presented in part I allowed to emphasize the need for further knowledge about (1) the relation between hemocyte system and disease development and (2) the impact of the BRD development on the energy balance of the host. The DEB model presented in chapter 8 provides a tool to analyse the effect of BRD development on the energy balance of the host. A few points of these two approaches can be compared.

10.1.1 Formulation of a model: empirical *versus* mechanistic

It is obvious that the more complex a model is, the greater the chance to find a combination of parameters that allow to fit the model to the observed data. Depending on the objective of the study, one should however wonder about the significance of such a model's equations.

This can be illustrated by a simple example : the length–filtration rate relationship of a bivalve species. Suppose a data set of filtration rate for individuals of different sizes at constant algae concentration and temperature. If the objective is to estimate empirically the filtration rate (F, $\mathrm{L\,h^{-1}}$) from a size measurement (L, cm), a simple strategy is to fit a polynomial equation ($F = aL + bL^2 + cL^3 + dL^4 \cdots$). The higher the degree of the polynomial equation, the higher are the chances to fit the data set properly, but also the higher is the number of parameters, and the more complex the model will be. Variables (F and L) of the model have physical units ($\mathrm{L\,h^{-1}}$ and cm) respectively, but the parameters of the model (a, b, c, d ...) have no unit, thus these parameters cannot explain the nature of the relationship between the two variables of the model.

On such a data set, it is also possible to fit an allometric equation: $F = \alpha L^\beta$. This equation indicates that filtration rate increases exponentially with size. This model is more simple than the first since it has only two parameters. In most case, the fit does not give an integer value for β, then it is not possible to determine the physical dimension of L^β (it can be neither a length, a surface or a volume). If we don't know the unit of L^β, then it is not possible to determine the unit of α. These coefficients are often in publications given as dimensionless but it would be more correct to mention that physical dimensions are undetermined. Thus, as the first model this second model does not give a physical explanation for the relation between length and filtration rate.

Based on the observations that gill surfaces are involved in the process of filtration and on the assumption that growth is isomorphic, it is possible to show that filtration rate might be proportional to the surface of the individual, thus to L^2. Thus the relation between filtration rate and length can be written as: $F = \alpha L^2$. Since F is expressed as L h^{-1} and L^2 is a surface (cm^2) the physical unit of α is L h^{-1} cm^{-2} this parameter can be named "surface specific filtration rate". This model for the relation gives an explanation for the length–filtration rate relationship and is rather simple since it has only one parameter (α).

The two first filtration rate models are only empirical and should be used carefully. They would be appropriate for some particular applications but do not give a physical explanation for the relation. The last model can be considered as a mechanistic model since from an observation and an assumption it allows to give a physical explanation for the length–filtration rate relationship. If the aim of a model is to give an explanation for an observed pattern, then the second strategy should be used. This is typically one of the main points of DEB theory. The model presented in chapter 2 makes use of empirical relationships and should be taken carefully. This is one of the reasons that motivated the choice of developing a model based on DEB theory to study the impact of BRD development on the energy budget of the Manila clam.

10.1.2   What to do with respiration?

Many studies focussing on bivalve energetics take respiration into account. One of the first questions is how to measure it. A first problem is measurement accuracy. Measurement systems in bivalve ecophysiology can be divided into two categories: open and closed systems. An open system was used for the study presented in chapter 7. One of their main interests is that they allow long term measurements. The respiration rate is measured by the difference in oxygen concentration between incoming and outflowing water from the cham-

ber. Thus two measures are needed for the estimation of respiration and each one comes with some uncertainty, thus the reliability of the measurement is affected and rather difficult to estimate. More simple, the closed systems, consist of incubations in a closed chamber and respiration is measured through the decrease in oxygen concentration. However, in these systems, oxygen concentration varies and this can affect the metabolism of the bivalves and subsequently the measurement. Variation of bivalves activity have been extensively described and indicated that, in constant conditions, respiration rates are not constant over time (see e.g. Kim et al., 1999, 2001, 2003). If the objective is to get information about the overall metabolism then a reliable measurement as to integrate variations in activity of the bivalves. An approach to check this important point was presented in chapter 7. All these problems make respiration rather difficult to measure and it is almost impossible to estimate the uncertainty in the measurements.

Supposing that reliable respiration data could be obtained. Then a second question appears : how to interpret respiration? Respiration is usually taken to represent the total metabolic rate in an organism. This is a vague concept because respiration results from various processes of the organism: digestion/assimilation, growth and maintenance (Kooijman, 2000). The unequal contribution of these various processes makes respiration data difficult to interpret. The Scope For Growth (SFG) concept, which is widely applied in bivalve bioenergetic studies (see chapter 2), assumes that the respiration corresponds to an energy loss. Respiration results from the oxidation of biochemical compounds, but in living organisms the energy released during oxidation is used for biosynthesis (see e.g. Lucas, 1993). During such a process, energy loss corresponds to the difference between the energy released by oxidation of the biochemical compound and the energy consumed by biosynthesis reaction. The biosynthetized compounds are used for various processes. If they are used for maintenance it is possible to consider that the energy is lost, nevertheless if they are used for growth then the energy is not lost for the organism. For this reason, in opposition to the DEB theory, the SFG concept does not respect law of energy conservation.

10.2   Development of Brown Ring Disease

By crossing modelling and experimental approaches this work revealed new results and hypotheses at different levels of the Brown Ring Disease progression of: from the initiation of the disease to the impact on host physiology. One of the originality of the experimental work presented in this study is that most

data were collected on naturally infected clams whereas as most data about BRD in literature are based on experimental infections.

10.2.1 Impact of BRD development on the host

Initiation of the disease

One of the first steps in the development of any disease is the initial infection. Progress of BRD in the Manila clam was recently reviewed in Paillard (2004b). This author states that the initial infection process was the entry of the pathogen, *V. tapetis*, into the extrapallial compartment. Chapter 5 provide a simple hypothesis for this process which was unknown. In short, field observations indicate that, on a same site, prevalence increases with size, suggesting that the infection probability is related to size. This pattern has been widely described for parasite infections in filter–feeders and is attributed to (1) an increase of filtration rate with size, and thus an increase of the probability to encounter a parasite; and (2) a longer potential exposition in larger, and subsequently older, individuals (see e.g. Andrews and Hewatt, 1957; Guralnick et al., 2004; Villalba et al., 2005). Nevertheless, field observation also indicate that prevalence of the disease is linked to the grain–size of the sediment: prevalence increases with the proportion of large particles in the sediment. Furthermore shell damage can be associated with development of the symptoms suggesting that injury may be a potential portal of entry for *V. tapetis*. These observations allowed to hypothesize that the main factor contributing to the initial infection process is the mechanical rupture of the periostracal lamina or damage of the shell edge. These injuries are induced by large sediment particles carried into the shell cavity by siphons or trapped within the shell aperture. This hypothesis provides another explanation for the size-prevalence relationship: larger individuals have higher siphon surface area and longer shell aperture which may subsequently increase the probability of trapping a deleterious sediment particle.

This hypothesis also suggests that any handling susceptible to induce a periostracal injury of a shell damage may open a entry portal for the pathogen. This can have severe consequences for aquaculture and fisheries management since clam handling in aquaculture beds and dredging may favour BRD development. Better understanding of this critical point of the disease is thus important and this hypothesis should be checked by experimental work in future.

Impact of the disease on the host

After the entry of the pathogen, the second process of the development of BRD is an interaction with the host and subsequently with its defence system (Paillard, 2004b). The interaction between the pathogen and hemocyte system have been extensively studied, most of these studies were based on experimental infections (see e.g. Allam et al., 2000a, 2001, 2002c; Reid et al., 2003; Paillard et al., 2004; Allam and Ford, 2006; Allam et al., 2006). Experimental infections are performed by injection of *V. tapetis* strains in the pallial cavity. This may uncouple the bacterial burden and the development of the symptoms: in this case a high bacterial burden should be found associated with low symptoms development. This uncoupling may provide valuable knowledge about the interaction between the bacteria and the hemocyte system independently of the symptoms development. The field study presented in chapter 4 failed to find any link between the development of symptoms and any of the measured hemocyte parameters. This leads to the problem of transferring the experimental laboratory results to conclusions about the development of the disease in the field. However, note that the disease intensity, estimated on the basis of the developed symptoms, was very low in this field study. This, combined with the high degree of variability of hemocyte parameters, may explain the lack of observed relationships between BRD development and hemocyte parameters.

The absence of a detectable relation between BRD symptoms and hemocyte parameters emphasizes the idea that the pathogen poorly affects host physiology at low levels of disease development. This is consistent with the experimental results presented in chapters 7 and 8 that the energy balance of individuals presenting low symptom development (CDS $\leq$ 3) were not significantly affected by the disease. It is also consistent with the observations of Plana and Le Pennec (1991), Paillard (1992) and Plana (1995) that indicate alterations of the digestive gland and the mantle were only found in the more advanced stages of the disease. The low stages of the disease (CDS $\leq$ 3) also correspond to a minor extent of the brown deposit on the inner surface of the shell. Thus the association of *V. tapetis* and the Manila clam in the first stages can almost be considered as commensalism.

Low development of the symptoms can hardly been associated with any physiological perturbation. However when the extent of the brown deposit takes a significant place on the inner shell surface (CDS $\geq$ 4) the results presented in the chapter 7 and 8 indicate that the energy balance is strongly affected. The results presented in chapter 7 allowed to show that heavy symptom development (CDS $\geq$ 4) can be associated with weight loss, indicative for a degradation of the energy balance of the host. In these individuals, average

clearance rate, maximum clearance rate and time spent on filtration activity were significantly reduced. This emphasizes that a primary way by which the energy balance of highly diseased clam was affected is a decrease in the food uptake through both a decrease of the filtration capacity and a modification of the filtration behaviour. Respiration rate was also significantly reduced in highly diseased clams, this could be associated with the decrease in food intake. The observation that starved infected clams lost weight at a greater rate than uninfected (Plana, 1995; Plana et al., 1996, and chapter 8) suggested a second way of degradation of the energy balance: an increase of the maintenance costs due to immune response and lesion repair.

Chapter 8 details this second way of degradation of the energy balance. Experimental data showed that individuals presenting high symptom development had significantly lower total flesh weights than asymptomatic ones. Thus, an energetic cost can be associated to the development of BRD independently of the effects on food intake which can be attributed to an increase of the maintenance costs. In spite of the lack of data about *V. tapetis* dynamics within a clam, the energy budget model based on DEB theory presented in this chapter allowed to provided a quantification of this increase in maintenance costs due to the development of the disease. This quantification indicated that BRD can be associated with an important increase in the maintenance costs. We also showed that, associated to simple weight measurements, the use of DEB models may provide a powerful tool to study quantitatively the impact of diseases on the energy balance of bivalves. Further development of the model is needed to detail the relative contribution of the two ways of degradation of the energy balance described in this study in the overall degradation of the energy balance.

One of the aims of DEB theory is to provide a generic framework to study mass and energy balances in living systems which is one of the greatest interests of this theory. In the aim of better understanding the energetic linkages between hosts and pathogens the general framework of interactions given in chapter 8 could be applied to other host/pathogen systems.

10.2.2   Variability in the development of the disease

Inter-individual variability

The work presented in chapter 5 allowed to show that, in natural populations, BRD prevalence is related to size. Thus one of the sources of inter-individual variability in the disease development is presumably linked to the infection probability.

The model presented in chapter 3, indicates that phenotypic inter-individual variations in functions which play key roles in disease development may provide a potential explanation for inter-individual variability in disease development. Nevertheless, the field work presented in chapter 4 showed the high degree of variability of hemocyte parameters involved in immune response, and this variability could not be correlated to the occurrence of symptoms. One interesting result of this study is that measured environmental and internal factors and diseases only explain little of the overall variability of hemocyte parameters. Similar to the study of Ashton-Alcox and Ford (1998) most of the variability could be attributed to unexplained inter-individual variations. This may hide subtle effects related to disease development and repeated individual sampling, as performed in Ford and Paillard (2007), may provide valuable information for understanding the links between hemocyte parameters and disease development.

The hypothesis presented in chapter 5 may also give an explanation for the inter-individual variability in disease development. If *V. tapetis* entry within the extrapallial compartment is initiated by mechanical injury, initial harm may be highly variable among individuals and this might have consequences for the further development of disease. Further experiments should be performed in order to answer these questions.

Environmental variability

Temperature is discussed as a modulating environmental factor of BRD in Paillard et al. (1997), Paillard et al. (2004), Paillard (2004b) and Paillard (2004a). However the data of chapter 4 failed to establish a link between temperature and disease development in the field, indicating that the relationship more complicated than suggested by these authors. In order to better understand how the environment does control BRD development, different questions have to be addressed. The first problem is the environmental control disease initiation. Part of the answer to this problem is brought by the high correlation between sediment grain–size and prevalence shown in chapter 5, and the probability of infection may be related to the sediment quality. This hypothesis also suggests that the environment may indirectly control the probability of infection through the host physiology. At the beginning of the growth season, the newly calcified layer may be more susceptible to mechanical disruption, thus increasing the probability of infection. Variation in clams activity linked to temperature may also indirectly affect the probability of mechanical disruption. Nevertheless, another element controlling the probability of infection is the presence and abundance of the pathogen in the environment of the clam. As suggested

by Maes (1992), Paillard et al. (1997) and Paillard (2004a) temperature, that controls the growth of *V. tapetis*, may here play an important role. Other factors, such as hydrology or eutrophication could also control the presence and abundance of *V. tapetis* in the environment of Manila clams.

A second problem is to better understand how the environment does influence the development of the disease when a clam is infected. Further development of the model presented in chapter 8 may provide valuable informations on this aspect. The model presented in chapter 2 emphasized the difficulty in evaluating food availability and this work suggested that chlorophyll *a* in the water column is not a good estimator of trophic resource for this species. Manila clam is an infaunal bivalve and filters water at the water–sediment interface. Thus microphytobenthos and detritic matter should account for an important part of its food resource. Two studies, based on DEB models, allowed to reconstruct food availability from growth in bivalves (Van Haren and Kooijman, 1993; Cardoso et al., 2006). A similar approach, based on the informations about growth archived in the shell, could be applied on the Manila clam in order to solve this problem. Furthermore such an approach allows to work at an individual scale avoids some problems linked to interindividual variability. This approach may also allow the comparison of growth patterns in healthy and infected clams and subsequently to detail further the effect of the disease on the host in the field.

References

Adamo, S. A., 2004. How sould behavioural ecologists interpret measurements of immunity? Animal behaviour 68, 1443–1449.

Allam, B., 1998. Rôle de fluides extrapalléaux des bivalves dans la défense immunitaire; cas de la maladie de l'anneau brun chez la palourde d'élevage, *Ruditapes philippinarum*. Thèse de Doctorat, Université de Bretagne Occidentale, Brest.

Allam, B., Ashon-Alcox, K. A., Ford, S. E., 2001. Haemocyte parameters associated with resistance to brown ring disease in *Ruditapes* spp. clams. Developmental and Comparative Immunology 25, 365–375.

Allam, B., Ashton-Alcox, K. A., Ford, S. E., 2002a. Flow cytometric comparison of haemocytes from three species of bivalve molluscs. Fish Shellfish Immunol. 13 (2), 141–158.

Allam, B., Ashton-Alcox, K. A., Ford, S. E., 2002b. Flow cytometric measurement of hemocyte viability and phagocytic activity in the clam, *Ruditapes philippinarum*. J. Shellfish. Res. 21, 13–19.

Allam, B., Ford, S. E., 2006. Effects of the pathogenic *Vibrio tapetis* on defence factors of susceptible and non-susceptible bivalve species: I. Haemocyte changes following in vitro challenge. Fish Shellfish Immunol. 20, 374–383.

Allam, B., Paillard, C., 1998. Defense factors in clam extrapallial fluids. Dis. Aquat. Org. 33, 123–128.

Allam, B., Paillard, C., Auffret, M., 2000a. Alterations in haemolymph and extrapallial fluid parameters in the Manila clam, *Ruditapes philippinarum*, challenged with the pathogen *Vibrio tapetis*. J. Invertebr. Pathol. 76, 63–69.

Allam, B., Paillard, C., Auffret, M., Ford, S. E., 2006. Effects of the pathogenic *Vibrio tapetis* on defence factors of susceptible and non-susceptible bivalve species: II. Cellular and biochemical changes following in vivo challenge. Fish Shellfish Immunol. 20, 384–397.

Allam, B., Paillard, C., Ford, S. E., 2002c. Pathogenicity of *Vibrio tapetis*, the etiological agent of Brown Ring Disease (BRD) in clams. Dis. Aquat. Org. 48, 221–231.

Allam, B., Paillard, C., Howard, A., Le Pennec, M., 2000b. Isolation of the pathogen *Vibrio tapetis* and defense parameters in brown ring diseased Manila clams, *Ruditapes philippinarum*, culivated in England. Dis. Aquat. Org. 41, 105–113.

Anderson, R. S., Burreson, E. M., Paynter, K. T., 1995. Defense responses of hemocytes withdrawn from *Crassostrea virginica* infected with *Perkinsus marinus*. J. Invertebr. Pathol. 66 (1), 82–89.

Anderson, R. S., Paynter, K. T., Burreson, E. M., 1992. Increased reactive oxygen intermediate production by hemocytes withdrawn from *Crassostrea virginica* infected with *Perkinsus marinus*. The Biological Bulletin 183 (3), 476–481.

Anderson, R. S., Unger, M. A., Burreson, E. M., 1996. Enhancement of *Perkinsus marinus* disease progression in TBT-exposed oysters (*Crassostrea virginica*). Marine Environmental Research 42 (1), 177–180.

Andrews, J. D., Hewatt, W. G., 1957. Oyster mortality studies in Virginia. II. the fungus disease caused by *Dermocystidium marinum* in oysters of Chesapeake Bay. Ecol. Monogr. 27 (1), 1.264.

Ashton-Alcox, K. A., Ford, S. E., 1998. Variability in molluscan hemocytes: a flow cytometric study. Tissue & cell 30 (2), 195–204.

Auffret, M., Duchemin, M., Rousseau, S., Boutet, I., Tanguy, A., Moraga, D., Marhic, A., 2004. Monitoring of immunotoxic responses in oysters reared in areas contaminated by the" Erika" oil spill. Aquat. Living Resour. 17 (3), 297–302.

Auffret, M., Oubella, R., 1994. Cytometric parameters of bivalve molluscs: effect of environmental factors. In: Stolen, J.S., Fletcher, T.C. (Eds.), Modulators of Fish Immune Response. SOS publication, Fair Haven, NJ, USA , 23–32.

Auffret, M., Oubella, R., 1997. Hemocyte aggregation in the oyster *Crassostrea gigas*: *In vitro* measurement and experimental modulation by xenobiotics. Comp. Biochem. Physiol. A 118 (3), 705–712.

Auffret, M., Rousseau, S., Boutet, I., Tanguy, A., Baron, J., Moraga, D., Duchemin, M., 2006. A multiparametric approach for monitoring immunotoxic responses in mussels from contaminated sites in Western Mediterranea. Ecotox. Env. Safty 63, 393–405.

Bacher, C., Gangnery, A., 2006. Use of dynamic energy budget and individual based models to simulate the dynamics of cultivated oyster populations. J. Sea Res. 56, 140–155.

Barber, B. J., Ford, S. E., Haskin, H. H., 1988a. Effects of the parasite MSX (*Haplosporidium nelsoni*) on oyster (*Crassostrea virginica*) energy metabolism. I. Condition index and relative fecundity. J. Shellfish. Res. 7, 25–31.

Barber, B. J., Ford, S. E., Haskin, H. H., 1988b. Effects of the parasite MSX (*Haplosporidium nelsoni*) on oyster (*Crassostrea virginica*) energy metabolism. II: Tissue biochemical composition. Comp. Biochem. Physiol. A 91 (3), 603–608.

Barillé, L., Héral, M., Barillé-Boyer, A.-L., 1997. Modélisation de l'écophysiologie de l'huitre *Crassostrea gigas* dans un environnement estuarien. Aquat. Living Resour. 10, 31–48.

Barracco, M. A., Medeiros, I. D., Moreira, F. L. M., 1999. Some haemato-immunological parameters in the mussel *Perna perna*. Fish Shellfish Immunol. 9 (5), 387–404.

Bayne, B., 1998. The physiology of suspension feeding by bivalve molluscs: an introduction to the Plymouth "TROPHEE" workshop. J. Exp. Mar. Biol. Ecol. 219, 1–19.

Bayne, B. L., 2004. Phenotypic flexibility and physiological tradeoffs in the feeding and growth of marine bivalve molluscs. Integr. Comp. Biol. 44, 425–432.

Bayne, B. L., Hawkins, A. J. S., Navarro, E., 1987. Feeding and digestion by the mussel, *Mytilus edulis* L. (Bivalvia: Mollusca) in mixtures of silt and algal cell at low concentrations. J. Exp. Mar. Biol. Ecol. 111, 1–22.

Beninger, P. G., Venoit, A., 1999. The oyster proves the rule: Mechanism of pseudofeaces transport and rejection on the mantle of *Crassostrea virginica* and *C. gigas*. Mar. Ecol. Prog. Ser. 190, 179–188.

Blanchard, G., Guarini, J.-M., Orvain, F., P.-G., S., 2001. Dynamic behaviour of benthic microalgal biomass in intertidal mudflats. J. Exp. Mar. Biol. Ecol. 264, 85–110.

Blanchard, G. F., Guarini, J.-M., Bacher, C., Huet, V., 1998. Control of the short-term dynamics of intertidal microphytobenthos by the exondation-submersion cycle. C. R. Acad. Sci. Paris 321 (6), 501–508.

Bodoy, A., Maitre-Allain, T., Riva, A., 1980. Croissance comparée de la palourde européenne *(Ruditapes decussatus)* et de la palourde japonaise *(Ruditapes philippinarum)* dans un écosystème artificiel meditérannéen. Vie Marine 2, 39–51.

Borrego, J., Luque, A., Castro, D., Santamaria, J. A., Martinez-Manzanares, E., 1996a. Virulence factors of *Vibrio* P1, the causative angent of brown ring disease in the Manila clam, *Ruditapes philippinarum*. Aquat. Living Resour. 9, 125–136.

Borrego, J. J., Castro, D., Luque, A., Paillard, C., Maes, P., Gracia, M., Ventosa, A., 1996b. *Vibrio tapetis* sp. nov., the causative agent of the brown ring disease affecting cultured clams. Int. J. Syst. Bacteriol. B 46, 480–484.

Bougrier, S., Collet, B., Geairon, P., Geffard, O., Héral, M., Deslous-Paoli, J., 1998. Respiratory time activity of the Japonese oyster *Crassostrea gigas* (Thunberg). J. Exp. Mar. Biol. Ecol. 219, 205–216.

Bower, S. M., 1992. Winter mortalities and histopathology in Japanese littlenecks [*Tapes philippinarum* (A. Adams and Reeves, 1850)] in British Columbia due to freezing temperatures. J. Shellfish. Res. 2, 255–263.

Bradford, M. M., 1976. A rapid and sensitive method for the quantification of microgram quantities of protein utilizing the principle of protein-dye binding. Anal. Biochem. 72 (1), 248–254.

Butt, D., Aladaileh, S., O'Connor, W. A., Ratios, D. A., 2007. Effect of starvation on biological factors related to immunological defence in the Sydney rock oyster (*Saccostrea glomerata*). Aquaculture 264 (1-4), 82–91.

Calvez, I., 2003. Approche de la variabilité spatiale d'une population de palourdes *Ruditapes philippinarum* (Adams et Reeve), aux stades larvaires et post-larvaires. Thèse de Doctorat, Université de Bretagne Occidentale, Brest.

Carballal, M., Villalba, A., López, C., 1998. Seasonal variation and effects of age, food availability, size, gonadal development, and parasitism on the hemogram of *Mytilus galloprovincialis*. J. Invertebr. Pathol. 72 (3), 304–312.

Carballal, M. J., Lopez, C., Azevedo, C., Villalba, A., 1997. In vitro study of phagocytic ability of *Mytilus galloprovincialis* Lmk. haemocytes. Fish Shellfish Immunol. 7 (6), 403–416.

Cardoso, J. F. M. F., 2007. Growth and reproduction in bivalves, an energy budget approach. phd thesis, Groningen Universiteit, Groningen, The Netherlands.

Cardoso, J. F. M. F., Witte, J. . I., van der Veer, H. W., 2006. Intra- and interspecies comparison of energy flow in bivalve species in Dutch coastal waters by means of the Dynamic Energy Budget (DEB) theory. J. Sea Res. 56, 182–197.

Casas, S. M., 2002. Estudio de la perkinsosis en la almeja fina, *Tapes decusssatus* (Linnaeus 1758), de Galicia. Ph.D. Thesis, University of Santiago de Compostela, Spain.

Castro, D., Martinez-Manzanares, E., Luque, A., Fouz, B., Morinigo, M., Borrego, J. J., Toranzo, A. E., 1992. Characterization of strains related to brown ring disease outbreaks in southwestern spain. Dis. Aquat. Org. 14, 229–236.

Castro, D., Santamaria, J., Luque, A., Martinez-Manzanares, E., Borrego, J. J., 1996. Antigenic characterization of the etiological agent of the Brown Ring Disease affecting Manila clams. Systematic and Applied Microbiology 19 (2), 231–239.

Cesari, P., Pellizzato, M., 1990. Tapes philippinarum: biologia e sperimentazione. Ente di Svilupo Agricolo Veneto, Ch. Biologia di *Tapes philippinarum*, pp. 21–46.

Chen, J. H., Bayne, C. J., 1995. Bivalve mollusc hemocyte behaviors: Characterization of hemocyte aggregation and adhesion and their inhibition in the california mussel (*Mytilus californianus*). The Biological Bulletin 188 (3), 255–266.

Cheng, T. C., 1996. Hemocytes: forms and functions. In: Kennedy, V. S., Newell, R. I. E., Eble, F. (Eds.), The eastern oyster *Crassostrea virginica*. Maryland Sea Grant College, pp. 299–333.

Choi, K., Park, K., Lee, K., Matsuoka, K., 2002. Infection intensity, prevalence, and histopathology of *Perkinsus* sp. in the Manila clam, *Ruditapes philippinarum*, in Isahaya bay, Japan. J. Shellfish. Res. 21 (1), 119–126.

Choi, K.-S., Wilason, E. A., Lewis, D. H., Powell, E. N., Ray, S. M., 1989. The energetic cost of *Perkinsus marinus* parasitism in oysters: quantification of the thioglycollate method. J. Shellfish. Res. 8, 125–131.

Choquet, G., 2004. Caractérisation et pathogénie des isolats de *Vibrio tapetis*, bactérie responsable de la maladie de l'anneau brun chez les palourdes. Thèse de Doctorat, Université de Bretagne Occidentale, Brest.

Choquet, G., Soudant, P., Lambert, C., Nicolas, J.-L., Paillard, C., 2003. Reduction of adhesion properties of *Ruditapes philippinarum* hemocytes exposed to *Vibrio tapetis*. Disease of aquatic organisms 57, 109–116.

Chu, F.-L. E., 1998. Host defenses against *Perkinsus marinus*: a review of recent findings in the eastern oyster, *Crassostrea virginica*. J. Shellfish. Res. 18 (1), 321–322.

Chu, F.-L. E., 2000. Defence mechanism of marine bivalves. In: Fingerman, M., Nagabhushanam, R. (Eds.), Recent advances in Biotechnology. Volume 5 Immunobiology and pathology. Science publishers, Inc., pp. 1–42.

Chu, F.-L. E., La Peyre, J. F., 1991. Effect of salinity on *Perkinsus marinus* susceptibility and defense-related activities in eastern oysters, *Crassostrea virginica*. J. Shellfish. Res. 10, 294.

Chu, F.-L. E., La Peyre, J. F., 1993. *Perkinsus marinus* susceptibility and defense-related activities in eastern oysters *Crassostrea virginica*: temperature effects. Dis. Aquat. Org. 16 (3), 223–234.

Dame, R., 1996. Ecology of marine bivalves: an ecosystem approach. CRC Press, Boca Raton.

Davison, A., Hinkley, D., 1997. Bootstrap methods and their application. Cambridge University Press Cambridge.

Delaporte, M., Soudant, P., Lambert, C., Moal, J., Pouvreau, S., Samain, J.-F., 2006. Impact of food availability on the energy storage and defense related hemocyte of the Pacific oyster *Crassostrea gigas* during an experimental reproductive cycle. Aquaculture 254, 571–582.

Delaporte, M., Soudant, P., Moal, J., Lambert, C., Quéré, C., Miner, P., Choquet, G., Paillard, C., Samain, J.-F., 2003. Effect of a mono-specific algal diet on immune functions in two bivalves species, *Crassostrea virginica* and *Ruditapes philippinarum*. J. Exp. Biol. 206 (17), 3053–3064.

Deslous-Paoli, J.-M., Héral, M., 1988. Biochemical composition and energy value of *Crassostrea gigas* (Thunberg) cultured in the bay of Marennes-Oleron. Aquat. Living Resour. 1 (4), 239–249.

Devauchelle, N., 1990. Tapes philippinarum: biologia e sperimentazione. Ente di Svilupo Agricolo Veneto, Ch. Sexual developement and maturity of *Tapes philippinarum*, pp. 49–62.

Dittman, D. E., Ford, S. E., Padilla, D. K., 2001. Effects of *Perkinsus marinus* on reproduction and condition of the Eastern oyster, *Crassostrea virginica*, depend on timing. J. Shellfish. Res. 20, 1025–1034.

Drummond, L., Mulcahy, M., Culloty, S., 2006a. The reproductive biology of the Manila clam, *Ruditapes philippinarum*, from the North-West of Ireland. Aquaculture 254, 326–340.

Drummond, L. C., O'Reilly, P., Mulcahy, M. F., Culloty, S. C., 2006b. Comparison of techniques for diagnosis of Brown Ring Disease and detection of *Vibrio tapetis* in the Manila clam, *Venerupis* (*Ruditapes*) *philippinarum*. J. Shellfish. Res. 25 (3), 1043–1049.

Efron, B., Tibshirani, R., 1993. An introduction to the bootstrap. Chapman & Hall New York.

Fegley, S., MacDonald, B., Jacobsen, T., 1992. Short-term variation in the quantity and quality of seston available to benthic suspension feeders. Estuar. Coast. Shelf. Sci. 34, 393–412.

Fisher, W. S., 1986. Structure and function of oyster hemocytes. In: Brehelin, M. (Ed.), Immunity in invertebrates, cells, molecules and defense reactions. Springer, Berlin, pp. 25–35.

Fisher, W. S., 2004. Relationship of amaebocytes and terrestrial elements to adult shell deposition in eastern oysters. J. Shellfish. Res. 23, 353–367.

Fisher, W. S., Oliver, L. M., Edwards, P., 1996. Hematologic and serologic variability of eastern oysters from Apalachicola Bay, Florida. J. Shellfish. Res. 15, 555–564.

Flassch, J. P., Leborgne, Y., 1992. Introduction in Europe, from 1972 to 1980, of the Japanese Manila clam (*Tapes philippinarum*) and effects on aquaculture production and natural settlement. ICES Marine Symposium 194, 92–96.

Flye-Sainte-Marie, J., Jean, F., Paillard, C., Ford, S., Powell, E., Hofmann, E., Klinck, J., 2007a. Ecophysiological dynamic model of individual growth of *Ruditapes philippinarum*. Aquaculture 266, 130–143.

Flye-Sainte-Marie, J., Pouvreau, S., Paillard, C., Jean, F., 2007b. Impact of Brown Ring Disease on the energy budget of the Manila clam *Ruditapes philippinarum*. J. Exp. Mar. Biol. Ecol. 349 (2), 378–389.

Ford, S. E., Figueras, A. J., 1988. Effects of sublethal infection by the parasite *Haplosporidium nelsoni* (MSX) on gametogenesis, spawning, and sex ratios of oysters in Delaware Bay, USA. Dis. Aquat. Org. 4, 121–133.

Ford, S. E., Paillard, C., 2007. Repeated sampling of individual bivalve mollusks I: Intraindividual variability and consequences for haemolymph constituents of the Manila clam, *Ruditapes philippinarum*. Fish Shellfish Immunol. 23, 280–291.

Ford, S. E., Powell, E., Klinck, J., Hofmann, E., 1999. Modeling the MSX parasite in eastern oyster (*Crassostrea virginica*) populations. I. Model development, implementation, and verification. J. Shellfish Res 18, 475–500.

Fréchette, M., Alunno-Bruscia, M., Dumais, J.-F., Sirois, R., Daigle, G., 2005. Incompleteness and statistical uncertainty in competition stocking experiments. Aquaculture 246, 209–225.

Freitak, D., Ots, I., Vanatoa, A., Hõrak, P., 2003. Immune response is energetically costly in white cabbage butterfly pupae. Proc. R. Soc. B 270 (Biology Letters Suppl. 2), S220–S222.

Gabbot, P. A., 1976. Energy metabolism. In: Bayne, B. (Ed.), Marine Mussels, their Ecology and Physiology. Cambridge University Press, Cambridge, pp. 294–355.

Gabbot, P. A., 1983. Developmental and seasonal metabolic actvities in marine molluscs. In: Hochachka, P., K.M., W. (Eds.), The Mollusca, Vol 2. Environmental Biochemistry and Physiology. Academic Press, New York, pp. 165–217.

Gagné, F., Blaise, C., Pellerin, J., Fournier, M., Durand, M. J., Talbot, A., 2007. Relationships between intertidal clam population and health status of the soft-shell clam *Mya arenaria* in the St. Lawrence Estuary and Saguenay Fjord (Québec, Canada). Environment International , in press.

Gale, L. D., Manzi, J. J., Crosby, M. P., 1991. Energetic costs to the eastern oyster *Crassostrea virginica* due to recent parasitism by the ectoparasitic gastropod *Boonea impressa*. Mar. Ecol. Prog. Ser. 79, 89–98.

Gangnery, A., Chabirand, J.-M., Lagarde, F., Le Gall, P., Oheix, J., Bacher, C., Buestel, D., 2003. Growth model of the Pacifc oyster, *Crassostera gigas* cultured in Thau Lagoon (Méditerranée, France). Aquaculture 215, 267–290.

Garcia, F., 1993. Interpretation of shell marks for the estimation of growth of the European carpet clam *Ruditapes decussatus* L. of the Bay of Fos (Mediterranean Sea). Oceanol. Acta 16, 199–203.

Goulletquer, P., 1989a. Etude des facteurs environnementaux intervenant sur la production de le palourde japonaise d'élevage *Ruditapes philippinarum*. Thèse de Doctorat, Université de Bretagne Occidentale, Brest.

Goulletquer, P., 1989b. Mortalité hivernale chez la palourde japonaise *Ruditapes philippinarum* sur le littoral Atlantique : aspects biochimiques et ecophysiologiques. Haliotis 19, 215–226.

Goulletquer, P., Héral, M., Bechemin, C., Richard, P., 1989a. Abnormal calcification in the shell of the manila clams *Ruditapes philippinarum*: characterization and comparison of amino-acid content in different shell parts. Aquaculture 81, 169–183.

Goulletquer, P., Héral, M., Deslous-Paoli, J.-M., Prou, J., Garnier, J., Razet, D., Boromthanarat, W., 1989b. Ecophysiology and energy balance of the Japanese clam *Ruditapes philippinarum*. J. Exp. Mar. Biol. Ecol. 132, 85–108.

Goulletquer, P., Lombas, I., Prou, J., 1987. Influence du temps d'immersion sur l'activité reproducrice et sur la croissance de la palourde japonaise *Ruditapes philippinarum* et l'huitre japonaise *Crassostrea gigas*. Haliotis 16, 453–462.

Goulletquer, P., Wolowicz, M., 1989. The shell of *Cardium edule*, *Cardium glaucum* and *Ruditapes philippinarum* : Organic content, composition and energy value, as determined by different methods. J. Mar. Biol. Assoc. 132, 563–572.

Grant, J., Bacher, C., 1998. Comparative models of mussel bioenergetics and their validation at field culture sites. J. Exp. Mar. Biol. Ecol. 219, 21–44.

Guarini, J. M., Blanchard, G. F., Gros, P., 2000. Quantification of the microphytobenthic primary production in European intertidal mudflats - a modelling approach. Contin. Shelf Res. 20 (12-13), 1771–1788.

Guralnick, R., Hall, E., Perkins, S., 2004. A comparative approach to understanding causes and consequences of mollusc–digenean size relationships: A case study with allocreadiid trematodes and *Cyclocalyx* clams. J. Parasitol. 90 (6), 1253–1262.

Haberkorn, H., 2005. Description des paramètres de croissance, de cytotoxicité et des caractéristiques sérologiques et génétiques d'une souche de *Vibrio* sp. thermotolérante. Rapport de master, Université de Bretagne Occidentale, Quimper.

Hawkins, A., Duarte, P., Fang, J., Pascoe, P., Zhang, J., Zhu, M., 2002. A functional model of responsive-feeding and growth in bivalve shellfish, configured and validated for the scallop *Chlamys farreri* during culture in China. J. Exp. Mar. Biol. Ecol. 281, 13–40.

Hégaret, H., da Silva, P. M., Wikfors, G. H., Lambert, C., De Bettignies, T., Shumway, S. E., Soudant, P., 2007. Hemocyte responses of manila clams, *Ruditapes philippinarum*, with varying parasite, *Perkinsus olseni*, severity to toxic-algal exposures. Aquat. Toxicol. 84 (4), 469–479.

Hégaret, H., Wikfors, G. H., 2005a. Effects of natural and field-simulated blooms of the dinoflagellate *Prorocentrum minimum* upon hemocytes of eastern oysters, *Crassostrea virginica*, from two different populations. Harmful Algae 4 (2), 201–209.

Hégaret, H., Wikfors, G. H., 2005b. Time-dependent changes in hemocytes of eastern oysters, *Crassostrea virginica*, and northern bay scallops, *Argopecten irradians irradians*, exposed to a cultured strain of *Prorocentrum minimum*. Harmful Algae 4 (2), 187–199.

Helm, M. M., Pelizzato, M., 1990. Tapes philippinarum: biologia e sperimentazione. Ente di Svilupo Agricolo Veneto, Ch. Hatchery, Breeding and Rearing of the *Tapes philippinarum* species, pp. 117–140.

Hildreth, D., Crisp, D., 1976. A corrected formula for calculation of filtration rate of bivalve molluscs in an experimental flowing system. J. Mar. Biol. Assoc. UK 56 (11), 111–120.

Hofmann, E., Ford, S., Powell, E., Klinck, J., 2001. Modeling studies of the effect of climate variability on MSX disease in eastern oyster (*Crassostrea virginica*) populations. Hydrobiologia 460 (1), 195–212.

Hofmann, E. E., Klinck, J. M., Kraeuter, J. N., Powell, E. N., Grizzle, R. E., Buckner, S. C., Bricelj, M. V., 2006. A population model of the hard clam, *Mercenaria mercenaria*: development of the age- and length-frequency structure of the population. J. Shellfish. Res. 25, 417–444.

Hofmann, E. E., Powell, E. N., Klinck, J. M., Saunders, 1995. Modeling diseased oyster populations. I. modelling *Perkinsus marinus* infections in oysters. J. Shellfish. Res. 14, 121–151.

Hofmann, E. E., Powell, E. N., Klinck, J. M., Wilson, E. A., 1992. Modeling oyster populations III. Critical feeding periods, growth and reproduction. J. Shellfish. Res. 11, 399–416.

Humphreys, J., Caldow, R. W. G., McGrorty, S., West, A. D., Jensen, A. C., 2007. Population dynamics of naturalised Manila clams *Ruditapes philippinarum* in British coastal waters. Mar. Biol. 151, 2255–2270.

Huvet, A., 2000. Ressources génétiques et phylogéographie des huitres creuses *Crassostrea gigas* et *C. angulata*: variabilité, différenciation et adaptation des populations naturelles et introduites. Thèse de doctorat, Université de Tours, Tours.

Jensen, A. C., Humphreys, J., Caldow, R. W. G., Grisley, C., Dyrynda, P. E. J., 2004. Naturalization of the Manila clam (*Tapes philippinarum*), an alien species, and establishment of a clam fishery within Poole Harbour, Dorset. J. Mar. Biol. Assoc. 84 (05), 1069–1073.

Jones, G. G., Sanford, C. L., 1993. Manila Clams: Hatchery and Nursery Methods. Innovative Aquaculture Products Ltd.

Kasai, A., Horie, H., Sakamoto, W., 2004. Selection of food sources by *Ruditapes pilippinarum* and *Mactra veneriformis* (Bivalvia: Mollusca) determined from stable isotope analysis. Fisheries science 70, 11–20.

Kennedy, V. S., Newell, R. I. E., Krantz, G. E., Otto, S., 1995. Reproductive capacity of the eastern oyster *Crassostrea virginica* infected with the parasite *Perkinsus marinus*. Dis. Aquat. Org. 23, 135–144.

Kerimov, A. B., Ivankina, E. V., Ilyina, T. A., Horak, P., 2001. Immune challenge affects basal metabolic activity in wintering great tits. Proc. R. Soc. B 268 (1472), 1175–1181.

Kim, W., Huh, H., Je, J.-G., Han, K.-N., 2003. Evidence of two-clock control of endogenous rhythm in the Washington clam, *Saxidomus purpuratus*. Marine Biology 142, 305–309.

Kim, W., Huh, H. T., Huh, S. H., Lee, J. H., 2001. Effects of salinity on endogenous rhythm of the the Manila clam *Ruditapes philippinarum* (Bivalvia: Veneridae). Mar. Biol. 138, 157–162.

Kim, W., Huh, H.T. Lee, J.-H., Rumohr, H., Koh, C., 1999. Endogenous circatidal rhythm in the Manila clam *Ruditapes philippinarum* (Bivalvia: Veneridae). Marine Biology 134, 107–112.

Kim, W.-S., 1994. Population dynamics and energy budget of *Ruditapes philippinarum* (Adams and Reeve, 1850) (Bivalvia: Veneridae) in Garolim Bay, Yellow sea, Korea. Dissertation zur erlangug des doktorgrades, Christian-Alrechts-Universitat, Kiel.

Kim, W. S., Yoon, S.-J., Yang, D.-B., 2004. Effects of chlorpyrifos on the endogenous rhythm of the Manila clam, *Ruditapes philippinarum* (Bivalvia: Veneridae). Marine Pollution Bulletin 48, 164–192.

Kooijman, S., Bedaux, J. J. M., 1996. The Analysis of Aquatic Toxicity Data. VU University Press, Amsterdam, The Netherlands.

Kooijman, S. A. L. M., 1986. Energy budgets can explain body size relations. J. Theor. Biol. 121, 269–282.

Kooijman, S. A. L. M., 1995. The stoichiometry of animal energetics. Journal of thoritical biology 177, 139–149.

Kooijman, S. A. L. M., 2000. Dynamic Energy and Mass Budgets in Biological Systems. Second edition. Cambridge University Press.

Kooijman, S. A. L. M., Sousa, T., Pecquerie, L., van der Meer, J., Jager, T., submitted. The estimation of Dynamic Energy Budget parameters, a practical guide .

La Peyre, J. F., Chu, F.-L. E., Meyers, J. M., 1995. Haemocytic and humoral activities of eastern and pacific oysters following challenge by the protozoan *Perkinsus marinus*. Fish Shellfish Immunol. 5, 179–190.

Labreuche, Y., Soudant, P., Gonçalvez, M., Lambert, C., Nicolas, J.-L., 2006. Effects of extracellular products from the pathogenic *Vibrio aesturianus* strain 01/32 on the lethality and cellular immune responses of the oyster *Crassostrea gigas*. Developmental and Comparative Immunology 30, 367–379.

Laruelle, F., 1999. Phénologie et déterminisme de la reproduction chez *Ruditapes decussatus* (L.) and *Ruditapes philippinarum* (Adams and Reeve) en Bretagne. Thèse de Doctorat, Université de Bretagne Occidentale, Brest.

Laruelle, F., Guillou, J., Paulet, Y., 1994. Reproductive pattern of the clams, *Ruditapes decussatus* and *Ruditapes philippinarum*, on intertidal flats in Brittany. J. Mar. Biol. Assoc. 172, 69–96.

Lassalle, G., de Montaudouin, X., Soudant, P., Paillard, C., 2007. Parasite co-infection of two sympatric bivalves, the Manila clam (*Ruditapes philippinarum*) and the cockle (*Cerastoderma edule*) along a latitudinal gradient. Aquat. Living Resour. 20, 33–42.

Lawrence, D., Scott, G., 1982. The determination and use of condition index of oysters. Estuaries 5, 23–27.

Leite, R. B., Afonso, R., Cancela, M. L., 2004. *Perkinsus* sp. infestation in carpet-shell clams, *Ruditapes decussatus* (L), along the Portuguese coast. Results from a 2-year survey. Aquaculture 240, 39–53.

Lewis, D. E., Cerrato, R. M., 1997. Growth uncoupling and the relationship between shell growth and metabolism in the soft shell clam *Mya arenaria*. Mar. Ecol. Prog. Ser. 158, 177–189.

Li, S.-C., Wang, W.-X., 2001. Radiotracers studies on the feeding of two marine bivalves on the toxic and non toxic dinoflagellate *Alexandrium tamarense*. J. Exp. Mar. Biol. Ecol. 263, 65–75.

Liu, S., Jiang, X., Hu, X., Gong, J., Hwang, H., Mai, K., 2004. Effects of temperature on non-specific immune parameters in two scallop species: *Argopecten irradians* (Lamarck 1819) and *Chlamys farreri* (Jones & Preston 1904). Aquacult. Res. 35 (7), 678–682.

Lochmiller, R. L., Deerenberg, C., 2000. Trade-offs in evolutionary immunology: just what is the cost of immunity? Oikos 88, 87–98.

Lopez, C., Carballal, M. J., Azevedo, C., Villalba, A., 1997. Differential phagocytic ability of the circulating haemocyte types of the carpet shell clam *Ruditapes decussatus* (Mollusca: Bivalvia). Dis. Aquat. Org. 30 (3), 209–215.

Lucas, A., 1993. Bioénergétique des animaux aquatiques. Masson, Paris.

Lucas, A., Beninger, P., 1985. The use of physiological indices in marine bivalve aquaculture. Aquaculture 44, 187–200.

Maes, P., 1992. Pathologie bactérienne chez deux invertébrés marins d'intérêt commercial, *Ruditapes philippinarum* et *Paracentrotus lividus*. Thèse de Doctorat, Université de Bretagne Occidentale, Brest.

Mann, R., 1979. The effect of temperature on growth, physiology, and gametogenesis in the Manila clam *Tapes Philippinarum* (Adams & Reeve, 1850). J. Exp. Mar. Biol. Ecol. 38, 121–133.

Marie, D., Partensky, F., Vaulot, D., Brussaard, C., 1999. Enumeration of phytoplankton, bacteria and viruses in marine samples. Curr. Protocols Cytom 11, 1–15.

Marin, M. G., Moschino, V., Deppieri, M., Lucchetta, L., 2003. Variations in gross biochemical composition, energy value and condition index of *T. philippinarum* from the Lagoon of Venice. Aquaculture 219, 859–871.

Matozzo, V., Da Ros, L., Ballarin, L., Meneghetti, F., Marin, M. G., 2003. Functional responses of haemocytes in the clam *Tapes philippinarum* from the Lagoon of Venice: fishing impact and seasonal variations. Can. J. Fish. Aquat. Sci. 60 (8), 949–958.

Matozzo, V., Monari, M., Foschi, J., Serrazanetti, G. P., Cattani, O., Marin, M. G., 2007. Effects of salinity on the clam *Chamelea gallina*. Part I: alterations in immune responses. Mar. Biol. 151 (3), 1051–1058.

Maître-Allain, T., 1982. Influence du milieu sur la croissance de deux palourdes, *Ruditapes decussatus* et *Ruditapes philippinarum*, dans l'étang de Thau (Hérault). Vie Marine 4, 11–20.

McHenery, J. M., Birkbeck, T. H., 1986. Inhibition of filtration in *Mytilus edulis* L. by marine vibrios. J. Fish Dis. 9, 257–261.

Melià, P., De Leo, G. A., Gatto, M., 2004. Density and temperature-dependence of vital rates in the Manila clam *Tapes philippinarum*: a stochastic demographic model. Mar. Ecol. Prog. Ser. 272, 153–164.

Meneghetti, F., Moschino, V., Da Ros, L., 2004. Gametogenic cycle and variations in oocyte size of *Tapes philippinarum* from the lagoon of Venice. Aquaculture 240, 473–488.

Monari, M., Matozzo, V., Foschi, J., Cattani, O., Serrazanetti, G., Marin, M., 2007. Effects of high temperatures on functional responses of haemocytes in the clam *Chamelea gallina*. Fish Shellfish Immunol. 22 (1-2), 98–114.

Mortensen, S., Strand, O., 2000. Release and recapture of Manila clams (*Ruditapes pilippinarum*) introduced to Norway. Sarsia 85, 87–91.

Mount, A. S., Wheeler, A. P., Paradkar, R. P., Snider, D., 2004. Hemocyte-mediated shell mineralization in the eastern oyster. Science 304, 297–300.

Muñoz, P., Meseguer, J., Ángeles Esteban, M., 2006. Phenoloxidase activity in three commercial bivalve species. changes due to natural infestation with *Perkinsus atlanticus*. Fish Shellfish Immunol. 20, 12–19.

Nakamura, Y., 2001. Filtration rates of the manila clam, *Ruditapes philippinarum*: dependence on prey items including bacteria and picocyanobacteria. J. Exp. Mar. Biol. Ecol. 266, 181–192.

Newell, R. I. E., 1985. Physiological effects of the MSX parasite *Haplosporidium Nelsoni* (Haskin, Stauber and Mackin) on the american oyster, *Crassostrea virginica*. J. Shellfish. Res. 5 (2).

Ngo, T. T. T., Choi, K.-S., 2004. Seasonal change of *Perkinsus* and *Cercaria* infections in the Manila clam *Ruditapes philippinarum* from Jeju, Korea. Aquaculture 239, 57–68.

Novoa, B., Luque, A., Castro, D., Borrego, J., Figueras, A., 1998. Characterization and infectivity of four bacterial strains isolated from Brown Ring Disease-affected clams. J. Invertebr. Pathol. 71 (1), 34–41.

Ohman, M. D., Snyder, R. A., 1991. Growth kinetics of the omnivorous oligotrich cilate *Strombidium* sp. Limnol. Oceanogr. 36, 922–935.

Oliver, L. M., Fisher, W. S., 1999. Appraisal of prospective bivalve immunomarkers. Biomarkers 4, 71–82.

Oliver, L. M., Fisher, W. S., Winstead, J. T., Hemmer, B. L., Long, E. R., 2001. Relationships between tissue contaminants and defense-related characteristics of oysters (*Crassostrea virginica*) from five Florida bays. Aquat. Toxicol. 55 (3-4), 203–22.

Ordás, M. C., Ordas, A., Beloso, C., Figueras, A., 2000. Immune parameters in carpet shell clams naturally infected with *Perkinsus atlanticus*. Fish Shellfish Immunol. 10 (7), 597–609.

Ortmann, C., Greishaber, M. K., 2003. Energy metabolism and valve closure behaviour in the asian clam *Corbicula fluminea*. The Journal of Experimental Biology 206, 4167–4178.

Oubella, R., Maes, P., Allam, R., Paillard, C., Auffret, M., 1996. Selective induction of hemocytic response in *Ruditapes philippinarum* (Bivalvia) by different species of *Vibrio* (Bacteria). Aquat. Living Resour. 9, 137–143.

Oubella, R., Maes, P., Paillard, C., Auffret, M., 1993. Experimentally induced variation in hemocyte density for *Ruditapes philippinarum* and *R. decussatus* (Mollusca, Bivalvia). Dis. Aquat. Org. 15 (3), 193–197.

Oubella, R., Paillard, C., Maes, P., Auffret, M., 1994. Changes in hemolymph parameters in the manila clams *Ruditapes philippinarum* (Mollusca, Bivalvia) following bacterial challenge. J. Invertebr. Pathol. 64 (1), 33–38.

Paillard, C., 1992. Etiologie et caractérisation de la maladie de l'anneau brun chez la palourde d'élevage, *Ruditapes philippinarum*. Thèse de Doctorat, Université de Bretagne Occidentale, Brest.

Paillard, C., 2004a. Rôle de l'environnement dans les interactions hôtes-pathogènes; développement d'un modèle de vibriose chez les bivalves. Habilitation à diriger des recherches (HDR), Université de Bretagne Occidentale, Brest.

Paillard, C., 2004b. A short-review of brown ring disease, a vibriosis affecting clams, *Ruditapes philippinarum* and *Ruditapes decussatus*. Aquat. Living Resour. 17, 467–475.

Paillard, C., Allam, B., Oubella, R., 2004. Effect of temperature on defense parameters in Manila clams *Ruditapes philippinarum* challenged with *Vibrio tapetis*. Dis. Aquat. Org. 59, 249–262.

Paillard, C., Kjornes, K., Le Chevalier, P., Le Boulay, C., Bergh, O., Bovo, C., Skar, C., Mortensen, S., submitted. *Vibrio tapetis* isolated from introduced manila clams, *Ruditapes philippinarum*, affected by the brown ring disease in Norway. Dis. Aquat. Org. .

Paillard, C., Maes, P., 1990. Etiologie de la maladie de l'anneau brun chez *Tapes philippinarum*: pathogénicité d'un *Vibrio* sp. C. R. Acad. Sci. Paris 310, 15–20.

Paillard, C., Maes, P., 1994. Brown ring disease in the Manila clam *Ruditapes philippinarum*: establishment of a classification system. Dis. Aquat. Org. 19, 137–146.

Paillard, C., Maes, P., 1995a. Brown ring disease in the Manila clam, *Ruditapes philippinarum*. I. Ultrastructural alterations of the periostracal lamina. J. Invertebr. Pathol. 65, 91–100.

Paillard, C., Maes, P., 1995b. Brown ring disease in the Manila clam, *Ruditapes philippinarum*. II. Microscopy study of the brown ring syndrome. J. Invertebr. Pathol. 65, 101–110.

Paillard, C., Maes, P., Mazurie, J., Claude, S., Marhic, A., Le Pennec, M., 1997. Epidemiological survey of the brown ring disease in clams of Atlantic coast : role of temperature in variation of prevalence. Proceedings of the VIIIe Symposium of the internationnal Society for Veterinary Epidemiology and Economics, 31/32, 14.03.1–14.03.3.

Paillard, C., Maes, P., Oubella, R., 1994. Brown ring disease in clams. Ann. Rev. Fish Dis. 4, 219–240.

Paillard, C., Percelay, L., Le Pennec, M., Picard, D. L., 1989. Origine pathogène de l'"anneau brun" chez *Tapes philippinarum* (Mollusque, Bivalve). C. R. Acad. Sci. Paris 309, 235–241.

Palmer, A. R., 1992. Calcification in marine molluscs: how costly is it? Proc. Natl. Acad. Sci. USA 89, 1379–1382.

Paraso, M. C. Ford, S. E., Powell, E., , Hofmann, E., Klinck, J., 1999. Modeling the MSX parasite in eastern oyster (*Crassostrea virginica*) populations. II. Salinity effects. J. Shellfish Res 18, 501–516.

Park, K.-I., Choi, K.-S., 2001. Spatial distribution of the protozoan parasite *Perkinsus* sp. found in the manila clams, *Ruditapes philippinarum*, in Korea. Aquaculture 203, 9–22.

Park, K.-I., Choi, K.-S., 2004. Application of enzyme-linked immunosorbent assay for studying of reproduction in the Manila clam *Ruditapes philippinarum* (Mollusca: Bivalvia) I. Quantifying eggs. Aquaculture 241, 667–687.

Park, K.-I., Choi, K.-S., Choi, J.-W., 1999. Epizootiology of *Perkinsus* sp. found in the Manila clam, *Ruditapes philippinarum* in Komsoe Bay, Korea. J. Korean Fish. Soc. 32, 303–309.

Park, K.-I., Figueras, A., Choi, K.-S., 2006a. Application of enzyme-linked immunosorbent assay (ELISA) for the study of reproduction in the Manila clam *Ruditapes philippinarum* (Mollusca: Bivalvia) II. Impacts of *Perkinsus olseni* on clam reproduction. Aquaculture 251, 182–191.

Park, K.-I., Paillard, C., Le Chevalier, P., Choi, K.-S., 2006b. Report on the occurrence of brown ring disease (BRD) in Manila clam, *Ruditapes philippinarum*, on the west coast of Korea. Aquaculture 255, 610–613.

Paytner, K. T., 1996. The effects of *Perkinsus marinus* infection on physiological processes in the Eastern oyster, *Crassostrea virginica*. J. Shellfish. Res. 15, 119–125.

Pérez Camacho, A., Delgado, M., Fernandez-Reiriz, M., Labarta, U., 2003. Energy balance, gonad developement and biochemical composition in the clam *Ruditapes decussatus*. Mar. Ecol. Prog. Ser. 258, 133–145.

Pipe, R. K., Coles, J. A., 1995. Environmental contaminants influencing immune function in marine bivalve molluscs. Fish Shellfish Immunol. 5 (8), 581–595.

Pipe, R. K., Coles, J. A., Thomas, M. E., Fossato, V. U., Pulsford, A. L., 1995. Evidence for environmentally derived immunomodulation in mussels from the Venice lagoon. Aquat. Toxicol. 32 (1), 59–73.

Plana, S., 1995. Perturbations de la glande digestive et du métabolisme chez la palourde aquacole, *Ruditapes philippinarum*, affectée par la maladie de l'anneau brun. Thèse de Doctorat, Université de Bretagne Occidentale, Brest.

Plana, S., Le Pennec, M., 1991. Alteration of the digestive diverticule and nutritional consequences in the manila clam *Ruditapes philippinarum* infected by a *Vibrio*. Aquat. Living Resour. 4, 255–264.

Plana, S., Sinquin, G., Maes, P., Paillard, C., Le Pennec, M., 1996. Variation in biochemical composition of juvenile *Ruditapes philippinarum* infected by a *Vibrio* sp. Dis. Aquat. Org. 24, 205–213.

Ponurovsky, S. K., Yakolev, Y. M., 1992. The reproductive biology of the japanese littleneck, *Tapes philippinarum* (adames and reeves, 1850) (bivalvia : Veneridae). J. Shellfish. Res. 11, 265–277.

Pouvreau, S., Bacher, C., Héral, M., 2000. Ecophysiological model of growth and reproduction of the black pearl oyster, *Pinctada margaritifera*: potential applications for pearl farming in French Polynesia. Aquaculture 186, 117–144.

Pouvreau, S., Bourles, Y., Lefebvre, S., Gangnery, A., Alunno-Bruscia, A., 2006. Application of a dynamic energy budget model to the pacific oyster, *Crassostrea gigas*, reared under various environmental conditions. J. Sea Res. 56, 156–167.

Pouvreau, S., Jonquières, G., Buestel, D., 1999. Filtration by the pearl oyster, *Pinctada margaritifera*, under conditions of low seston load and small particle size in a tropical lagoon habitat. Aquaculture 176, 295–314.

Powell, E., Klinck, J., Ford, S. E., Hofmann, E., Jordan, S. J., 1999. Modeling the MSX parasite in eastern oyster (*Crassostrea virginica*) populations. II. regional appilcation and the problem of transmission. J. Shellfish Res 18, 517–537.

Powell, E. N., Hofmann, E. E., Klinck, J. M., Ray, S. M., 1992. Modelling oyster populations I. A commentray on filtration rate. Is faster always better ? J. Shellfish. Res. 2, 387–398.

Powell, E. N., Klinck, J. M., Hofmann, E. E., 1996. Modeling diseased oyster populations. II. triggering mechanisms for *Perkinsus marinus* epizootics. J. Shellfish. Res. 15, 141–165.

Powell, E. N., Klinck, J. M., Hofmann, E. E., Ray, S. M., 1994. Modeling oyster populations. IV. population crashes and management. U. S. Fish. Wildl. Serv. Fish. Bull. 92, 347–373.

Powell, E. N., Stanton, R. J., 1985. Estimation of biomass and energy flow of molluscs in palaeo-communities. Palaeontology 28, 1–34.

Prochazka, G. J., Payne, W. J., Mayberry, W. R., 1970. Calorific content of certain bacteria and fungi. Journal of Bacteriology 104, 646–649.

Pronnier, F., 1996. Le développement larvaire et l'alimentation de larves de bivalves d'écolserie. Thèse pour le diplôme d'etat de docteur vétérinaire, Ecole Nationales Vétérinaire de Nantes, Nantes, France.

Quayle, D., Bourne, N., 1972. The clam fiseries of Bbritish Columbia. Fish. Res. Bd. Can. Bull. 179, 42–48.

R Development Core Team, 2006. R: A Language and Environment for Statistical Computing. R Foundation for Statistical Computing, Vienna, Austria, ISBN 3-900051-07-0.
URL http://www.R-project.org

Ray, S. M., 1966. A review of the culture method for detecting *Dermocystidium marinum*, with suggested modifications and precautions. Proc. Natl. Shellfish. Assoc. 54, 55–69.

Reid, H. I., Soudant, P., Lambert, C., Paillard, C., Birkbeck, T. H., 2003. Salinity effects on immune parameters of *Ruditapes philippinarum* challenged with *Vibrio tapetis*. Dis. Aquat. Org. 56, 249–258.

Ren, J. S., Ross, A. H., 2001. A dynamic energy budjet model of the pacific oysters *Crassostrea gigas*. Ecological Modelling 142, 105–120.

Ren, J. S., Ross, A. H., 2005. Environmental influence on mussel growth: A dynamic energy budget model and its application to the greenshell mussel *Perna canaliculus*. Ecological Modelling 189, 347–362.

Riera, P., Richard, P., 1996. Isotopic determination of food sources of *Crassostrea gigas* along a trophic gradient in the estuarine bay of Marennes–Oléron. Estuar. Coast. Shelf. Sci. 42, 347–360.

Robert, R., Deltreil, J.-P., 1990. Elevage de la plaourde japonaise, *Ruditapes philippinarum* dans le bassion d'Aracachon. Bilan des dix dernières années et perspectives de développement. Rapport internes de la Direction des Ressources Vivantes de l'IFREMER. IFREMER.

Robert, R., Trut, G., Laborde, J. L., 1993. Growth, reproduction and gross biochemical composition of the Manila clam *Ruditapes philippinarum* in the Bay of Arcachon, France. Mar. Biol. 116, 291–299.

Rodde, K. M., Sunderlin, J. B., Roels, O. A., 1976. Experimental cultivation of *Tapes japonica* (Deshayes) (Bivalvia: Veneridae) in an artificial upwelling culture system. Aquaculture 9, 203–215.

Rodland, D. L., Schöne, B. R., Helama, S., Nielsen, J. K., Baier, S., 2006. A clockwork mollusc: Ultradian rhythms in bivalve activity revealed by digital photography. J. Exp. Mar. Biol. Ecol. 334, 316–323.

Romanyukha, A. A., Rudnev, S. G., Sidorov, I. A., 2006. Energy cost of infection burden: An approach to understanding the dynamics of host-pathogen interactions. J. Theor. Biol. 241, 1–13.

Ross, A. H., Nisbet, R. M., 1990. Dynamic models of growth and reproduction of the mussel mytilus edulis L. Functional Ecology 4 (6), 777–787.

Savina, M., Pouvreau, S., 2004. A comparative ecophysiological study of two infaunal filter-feeding bivalves: *Paphia rhomboides* and *Glycymeris glycymeris*. Aquaculture 239, 289–306.

Schmid-Hempel, P., 2003. Variation in immune defence as a question of evolutionary ecology. Proc. R. Soc. B 270, 357–366.

Shafee, M. S., Lucas, A., 1982. Variations saisonnières du bilan énergétique chez les individus d'une population de *Chlamys varia* (L.): Bivalvia, pectinidae. Oceanol. Acta 5, 331–338.

Smaal, A., Haas, H., 1997. Seston dynamics and food availability on mussel and cockle beds. Estuar. Coast. Shelf. Sci. 47, 247–259.

Smaal, A., Zurburg, W., 1997. The uptake and release of suspended and dissolved material by osyters and mussels in Marennes–Oléron Bay. Aquat. Living Resour. 10, 23–30.

Solidoro, C., Pastres, R., Melaku Canu, D., Pellizzato, M., Rossi, R., 2000. Modelling the growth of *Tapes philippinarum* in northern adriatic lagoons. Mar. Ecol. Prog. Ser. 199, 137–148.

Sorokin, Y., Giovanardi, O., 1995. Trophic characteristics of the Manila clam (*tapes philipinarum* adams and reeve). ICES J. Mar. Sci 52, 853–862.

Soudant, P., Paillard, C., Choquet, G., Lambert, C., Reid, H. I., Marhic, A., Donaghy, L., Birkbeck, T., 2004. Impact of season and rearing site on the physiological and immunological parameters of the Manila clam *Venerupis (=Tapes, =Ruditapes) philippinarum*. Aquaculture 229, 401–418.

Thompson, R. G., 1984. Production and reproductive effort in the blue mussel *Mytilus edulis*, the sea urchin *Strongylocentrotus droebachiensis* and the snow crab *Chionocetes opilio* from populations in Nova Scotia and Newfoundland. J. Fish. Res. Board Canada 36, 955–964.

Tiscar, P. G., Mosca, F., 2004. Defense mechanisms in farmed marine molluscs. Veterinary Research Communications 28, 57–62.

Toba, M., Natsume, Y., Yamakawa, H., 1993. Reproductive cycle of Manila clams collected from Funabashi waters, Tokyo bay. Nippon Suisan Gakkaishi 59 (1), 15–22.

Truscott, R., White, K., 1990. The influence of metal and temperature stress on the immune system of crabs. Functional Ecology 4 (3), 455–461.

van der Meer, J., 2006. An introduction to Dynamic Energy budget (DEB) models with special emphasis on parameter estimation. J. Sea Res. 56, 85–102.

van der Veer, H. W., Cardoso, J. F. M. F., van der Meer, J., 2006. The estimation of DEB parameters for various northeast atlantic bivalve species. J. Sea Res. 56, 107–124.

Van Haren, R. J. F., Kooijman, S. A. L. M., 1993. Application of dynamic energy budget model to *Mytilus edulis* (l.). Netherlands Journal of Sea Research 31, 119–133.

Villalba, A., Casas, S., Lopez, C., Carballal, M., 2005. Study of perkinsosis in the carpet shell clam *Tapes decussatus* in Galicia (NW Spain). II. Temporal pattern of disease dynamics and association with clam mortality. Dis. Aquat. Org. 65 (3), 257–267.

Villalba, A., Reece, K. S., Camino Ordás, M., Casas, S. M., Figueras, A., 2004. Perkinsosis in molluscs: A review. Aquat. Living Resour. 17, 411–432.

Ward, J. E., Langdon, C. J., 1986. Effects of the ectoparasite *Boonea* (=*Odostomia*) *impressa* (Say) (Gastropoda:pyramidellidae) on the growth rate, filtration rate, and valve movements of the host *Crassotrea virginica* (Gmelin). J. Exp. Mar. Biol. Ecol. 99, 163–180.

Weiss, E. L., Frock, H. N., 1976. Rapid analysis of particle size distributions by laser light scattering. Powder Technology 14 (2), 287–93.

Whyte, J. N. C., Englar, J. R., Carswell, B. L., 1990. Biochemical composition and energy reserves in *Crassostrea gigas* exposed to different levels of nutrition. Aquaculture 90 (2), 157–172.

Widdows, J., Hawkins, A. J. S., 1989. Partitioning of rate of heat dissipation by *Mytilus edulis* into maintenance, feeding and growth components. Physiol. Zool. 62, 764–784.

Yamamoto, K., Iwata, F., 1956. Studies on the bivalve, *Venerupis japonica*, in Akkeshi Lake II. growth rate and biological minimum size. Bull. Hokkaido Reg. Fish. Res. Lab. 14, 57–62.

Yap, W. G., 1977. Population biology of the Jappanese little–neck clam, *Tapes philippinarum* in Keneohe Bay, Hawaiian Islands. Pacific Science 31, 223–244.

Summary

Ecophysiology of Brown Ring Disease in the Manila clam *Ruditapes philippinarum*, experimental and modelling approaches

Brown Ring Disease (BRD) in the Manila clam, *Ruditapes philippinarum*, is a disease caused by the bacterium *Vibrio tapetis*. This pathology was first observed in Northern Brittany (France) in 1987. The pathogenic agent enters in the extrapallial cavity (*i.e.* the space between mantle and shell), disrupts the normal production of periostracal lamina and causes an anomalous deposition of periostracum on the inner shell of the clams. Infected clams exhibit a characteristic brown deposit on the peripheral inner surface of the valves that gave the disease its name. This disease can be associated with mass mortalities impacting clam aquaculture. The objective of this thesis, based on both modelling and experimental approaches, was to provide further insight on the linkages between the host physiology and the development of BRD, with a special emphasis on the host energy balance.

The first part of this thesis describes the development of an interaction model between the host, the pathogen and the environment. Chapter 2 describes the development of an energy balance model based on the "scope for growth" concept for the Manila clam. This model allowed to describe variations in growth, condition index and reproduction of the Manila clam under forcing of trophic resource and temperature. This work emphasized the difficulty in estimating food availability for such an infaunal bivalve and suggested that chlorophyll *a* in the water column was not a good estimator for the trophic resource for the Manila clam. Contribution of microphytobenthos and detritic matter may also be taken into account. This work also emphasized the difficulty in validating such a model when asynchronous spawning events occur in

173

the studied population.

The interaction model between the host, the pathogen and the environment presented in chapter 3 attempts to link the development of the disease to the energy balance of the host. The host's portion of the model is based on the model developed in chapter 2. The defence system against the pathogen is both controlled by the condition index of the host and the temperature. Individuals that differ phenotypically were simulated by varying parameters values implicated in functions susceptible to play a critical role in disease development. This phenotypic variability allowed to provide a potential explanation for the observed variability in disease development.

The second part of the manuscript deals with observations of BRD in the field. Chapter 4 shows the results of a field monitoring of hemocyte parameters of the Manila clam, environmental factors (temperature, trophic resource and salinity) and disease (BRD and perkinsosis) development. This study showed the high degree of variability of hemocyte parameters and demonstrated that temperature and clam length explain the greater part of the recorded variability. During this survey, BRD prevalence and intensity, evaluated on the basis of symptom development, were low and it was not possible to find any significant relationship between any of the measured parameters and BRD in the clams. On the basis of this results, chapter 6 discusses the model assumptions. These results do not confirm that BRD development can be explained by the energy balance of the host.

By using data sets from the study presented in chapter 4 and additional data sets, chapter 5 presents a simple hypothesis for the first step of infection. We show that: (1) prevalence is correlated to clam size, (2) prevalence is correlated to the abundance of large particles in the sediment and (3) that a shell breakage is a potential portal for pathogen entry. From these observations, this study hypothesizes that the main factor controlling the infection process may be a mechanical disruption of the periostracal lamina or shell edge by large sediment particles, thus opening a portal of entry for *V. tapetis*. This hypothesis suggests that (1) clam handling in aquaculture beds may favour BRD development and (2) variations in the initial injury of the periostracal lamina or shell edge could explain part of the observed variability in disease development.

The third part of the manuscript deals with the impact of BRD development on the energy budget of the Manila clam. Experimental results presented in chapter 7 indicate that severely infected clams are subject to a higher weight loss than uninfected ones, indicating that BRD affects the energy budget. Measurements showed that the clearance rate of severely diseased clams was sig-

nificantly decreased by both a decrease in filtration capacity and a reduction of the time spent on filtration activity. Thus one primary way of modification of the energy balance is a decrease in the food intake. Data in the literature suggested that a second way of could be an increase in the maintenance costs due to energy needed for immune response and repair of lesions induces by the disease.

DEB theory provides a mechanistic framework to study mass and energy balances in living systems and describes the energy flow through organisms from assimilation to allocation for growth, reproduction development and maintenance. A model based on this theory was developed in chapter 8 to discern the effect of disease development on maintenance. A starvation experiment presented showed that in highly infected clams weight loss was higher than in uninfected one. This allowed to confirm that the energy balance was modified by the disease independently of the effect on filtration activity. Subsequently we could show that the disease could be associated to an increase in maintenance costs. Coupling the DEB model simulations and starvation observations provides a quantitative and dynamic evaluation of the effect of BRD on maintenance costs and indicated that BRD development could be associated with an important increase in the maintenance cost. This demonstrates that DEB theory can provide a powerful tool to study the effect of disease/parasites on the energy budget of the host. Further development of the model is needed to describe the relative contribution of the two ways for degradation of the energy balance and to assess the effect of the environment on the whole system.

Samenvatting

De ekofysiologie van de bruine ring ziekte in de Aziatische tapijtschelp *Ruditapes philippinarum*, experimentele en modelmatige benaderingen

De Bruine Ring Ziekte (BRZ) in de Aziatische tapijtschep *Ruditapes philippinarum* wordt veroorzaakt door de bacterie *Vibrio tapetis*. De ziekte werd in Bretagne (Frankrijk) voor het eerst waargenomen in 1987. De ziekteverwekker dringt de buiten-palliale holte (dit is de ruimte tussen mantel en schelp) van de gastheer binnen en verstoort de normale productie van periostracale laagjes op de schelp en veroorzaakt een afwijkende afzetting van periostracum op de binnenkant van de schelp van besmette dieren. Infecteerde dieren tonen dus een characteristieke bruine afzetting op de binnenkant van de schelp, evenwijdig aan de rand van de kleppen, vandaar de naam van de ziekte. De ziekte kan in verband worden gebracht met massale sterfte die soms optreedt in de kweek van deze schelpdieren. Het doel van dit proefschrift was om langs experimentele en modelmatig weg kennis te vergaren over de verbanden tussen de fysiologie van de gastheer en de ontwikkeling van BRZ, en in het bijzonder over de effecten van de ziekte op de energie-huishousing.

Het eerste deel van dit proefschrift beschrijft een model voor de interactie tussen de gastheer, de ziekteverwekker en de omgeving. Hoofdstuk 2 beschrijft een model voor de energie-balans van de Aziatische tapijtschelp dat gebaseerd is op het "ruimte voor groei" concept. Dit model beschrijft de variaties in de groei, in de conditie en in de reproductie van de Aziatische tapijtschelp bij een gegeven regiem in voedselbeschikbaarheid en temperatuur. Uit dit werk kwam naar voren dat het erg moeilijk is voedselbeschikbaarheid in te schatten voor zo'n uitheems schelpdier en dat chlorophyll a in de water kolom geen goede maat is voor voedselschikbaarheid. Detritus en de micro-algen op de bodem

177

moeten ook meegenomen worden. Dit werk toont ook aan dat het buitengewoon moeilijk is het model te valideren als er asynchrone broedval optreedt in de bestudeerde populaties.

Hoofdstuk 3 beschrijft het effect van de ziekteverwekker op de energiebalans van de gastheer in relatie met de omgeving, zoals gemodelleerd in Hoofdstuk 2. De verdediging van de gastheer hangt af van zijn conditie en van de temperatuur. Verschillen in gedrag van individuen werden nagebootst door parameter-waarden te variëren die te maken hebben met de ontwikkeling van de ziekte. Deze variatie in parameter waarden geeft op zijn beurt een verklaring voor de waargenomen variabliliteit van het effect van de ziekte.

Het tweede deel van het proefschrift behandelt de waarnemingen aan de ziekte in het veld. Hoofdstuk 4 laat het verloop van bloedwaarden van de Aziatische tapijtschelp zien als funktie van omgevingsfactoren (temperatuur, voedselbeschikbaarheid en zoutgehalte) and ziekten (BRZ and *Perkinsus*). De bloedwaarden variëerden enorm, hetgeen vooral door temperatuur en schelpgrootte variaties verklaard kon worden. In dit overzicht bleek het onmogelijk enig verband te vinden tussen de gemeten parameters en de symptomen van BRZ in de tapijtschelpen.

Op basis van deze resultaten bespreekt Hoofdstuk 6 waarom deze experimentele data niet toelaten de ontwikkeling van BRZ in verband te brengen met de energie-balans van de gastheer. Gebruik makend van de data uit Hoodfstuk 4 en van aanvullende data, presenteert Hoofdstuk 5 een eenvoudig hypothese voor de eerste stap in de ontwikkeling van de ziekte. De data laten zien dat het voorkomen van de ziekte gecorreleerd is met (1) de grootte van de tapijtschelp, (2) het voorkomen van grote deeltjes in het sediment waarin de tapijtschelpen leven en (3) dat breuken in de schelp het voor de ziekteverwekker mogelijk maken binnen te dringen. Deze waarnemingen hebben tot de hypothese geleid dat de belangrijkste factor in de infectie de mechanische beschadiging van de periostracale laagjes is, of van de schelprand, veroorzaakt door de grote deeltjes in het sediment, die het aldus mogelijke maken dat de bacterie *V. tapetis* binnendringt. Deze hypothese suggereert dat (1) het manupuleren van de tapijtschelpen in de kweek de ontwikkeling van BRZ bevordert en (2) variaties in de verwondingen aan de periostracale laagjes of aan de schelprand aan het begin van de ziekte kunnen een deel van de waargenomen variabiliteit van het verloop van de ziekte verklaren.

Het derde deel van dit proefschrift behandelt het effect de BRZ op het energie-budget van de Aziatische tapijtschelp gedurende het verloop van de ziekte. De experimentele resulten die in hoofdstuk 7 worden gepresenteerd duiden erop dat ernstig zieke tapijtschelpen een snellere gewichtsafname laten zien dan gezonde tapijtschelpen. Dit wijst erop dat BRZ een effect heeft op

de energie-huishouding. Metingen van de filtratie snelheid van ernstig zieke tapijtschelpen laten zien dat zowel de filtratie capaciteit als de filtratie periode duidelijk afnemen. Dien ten gevolge heeft de energie-balans last van een duidelijke afname in de voedsel-opname. Deze studie formuleert ook de hypothese dat de ziekte de onderhoudskosten verhoogt, via de activatie van het immuun-systeem en het herstel van de gaten die de bacterien maken in de celmembranen.

DEB theorie levert een mechanistisch raamwerk om massa en energie-balansen in levende systemen te bestuderen en beschrijft de energie-stromen door organismen vanaf de assimilatie tot de besteding aan groei, reproductie en onderhoud. Een model dat op deze theorie gebaseerd is wordt in hoofdstuk 8 ontwikkeld om het effect van de ziekte op de energie-balans nader te precieseren. Een hongerings-experiment met geïnfecteerde en niet-geïnfecteerde tapijtschelpen wordt in Hoofdtuk 8 beschreven en de resultaten laten zien dat zwaar-geïnfecteerde dieren sneller gewicht verliezen dan niet-geïnfecteerde dieren. Dit bevestigt dat de energie-balans niet alleen door de filtratie activiteit is verstoord, maar dat ook de onderhoudskosten verhoogd zijn. Door de computer-simulaties van het DEB model te vergelijken men de waarnemingen tijdens hongering werd een getalsmatige evaluatie van het effect van BRZ op de belangrijke verhoging van de onderhoudskosten verkregen. Dit laat zien dat DEB theorie een krachtig gereedschap is in de studie van ziekten en parasieten op het energie-budget van de gastheer. Vervolg-onderzoek is nodig om de relatieve bijdragen van de verlaging van de voedelopname en een verhoging van de onderhoudskosten vast te stellen om zodoende de bijdrage van de omgeving op het systeem te kunnen beoordelen.

Acknowledgements

I first like to thank Fred JEAN, my French scientific supervisor, who follows my work since quit a long time now. Fred, un grand MERCI pour le temps que tu m'a accordé, pour ta patience mais surtout pour la confiance et le soutient que tu m'a apporté tout au long de la réalisation de ce travail. Merci pour ton amitité et tous les bons moment passé au cours de ces dernière années.

I want to thank Christine PAILLARD, supervisor of the french fold of this work. Christine, merci pour ton entousiasme de tous les jours et les bons moments passés au cours de la réalisation de ce travail.

I want to thank Bas KOOIJMAN, for the time spent working with me, for nice scientific discussions and advices and for walks in the dunes...

This work is also the results of collaboration with number of poeple. I want to thank all of them. Many thanks to Philippe SOUDANT and Christophe LAMBERT for their large investment in collecting field data presented in this work, and for their help. Great thanks to Nelly LE GOÏC for her help on the field and in the lab, especially for BRD diagnostic.

Thanks also to the american team : Eric POWEL, John KLINCK and Eileen HOFFMAN for their collaboration of the first model presented here.

I especially want to greatly thank Susan FORD, who followed my work during this PhD. Thanks you, Susan, for the time you invested in reviewing my article, for your corrections and advices. It was a great pleasure to work with you.

Many thanks to Stéphane POUVREAU who received me in his lab, for his help for ecophysiological measurements, and for nice exchanges about DEB

theory. I also want to thank all the "Argenton team" for thier technical help.

Thanks also to Laure PECQUERIE, for long and helping DEB phone calls.

Thanks to Marcel KOKEN who spent a lot of time reading and re-reading this manuscript.

I also want to thank all my friends of the LEMAR. Piero, Briva, Sorcha, Joelle, Pieru et Céline, merci de m'avoir supporté, je sait que ca n'a pas toujours été facile!

Thanks also to Céline and Ronan who accepted to come in Amsterdam to support me for the defence of this thesis.

I finally want to thank my parents for their trust and their support all along my studies.